UNIWERSYTET MIKOŁAJA KOPERNIKA W TORUNIU

Collegium Medicum
im. Ludwika Rydygiera w Bydgoszczy

Bydgoszcz 2025 r.

UNIWERSYTET
MIKOŁAJA KOPERNIKA
W TORUNIU

Collegium Medicum
im. Ludwika Rydygiera w Bydgoszczy

Paulina Śledzińska-Bebyn

Zastosowanie zaawansowanego obrazowania MRI w predykcji profilu molekularnego i charakterystyki glejaków

Rozprawa na stopień doktora nauk medycznych i nauk o zdrowiu

Promotor:

prof. dr hab. n. med. Zbigniew Serafin

Promotor pomocniczy

dr hab. n. o zdr. Jacek Furtak

Bydgoszcz rok 2025

Spis treści

Wykaz skrótów....4
Wykaz artykułów stanowiących cykl publikacji....6
Publikacja nr 1....6
Publikacja nr 2....6
Publikacja nr 3....7
Wprowadzenie....8
Przegląd piśmiennictwa....10
Cel badania, hipotezy badawcze....13
Cel badania....13
Hipotezy badawcze....13
Omówienie wyników poszczególnych prac....15
Publikacja nr 1....15
Publikacja nr 2....18
Publikacja nr 3....20
Podsumowanie wyników....22
Wnioski....23
Piśmiennictwo....26
Streszczenie....28
Summary....30
Załączniki....32
Kopie artykułów stanowiących cykl publikacji....33
Publikacja nr 1....34
Publikacja nr 2....54
Publikacja nr 3....66
Zgoda Komisji Bioetycznej....78
Oświadczenia współautorów....81

Wykaz skrótów

Skrót	Rozwinięcie angielskie	Rozwinięcie polskie
ADC	Apparent Diffusion Coefficient	Współczynnik dyfuzji
BTIP	BTIP	Protokół MRI do diagnostyki guzów mózgu, zgodny z międzynarodowymi wytycznymi
CDKN2A	Cyclin Dependent Kinase Inhibitor 2A	Inhibitor kinazy cyklinozależnej 2A
DSC	Dynamic Susceptibility Contrast	
DWI	Diffusion-Weighted Imaging	Obrazowanie dyfuzyjne
EGFR	Epidermal Growth Factor Receptor	Receptor naskórkowego czynnika wzrostu
FLAIR	Fluid-Attenuated Inversion Recovery	Obrazowanie FLAIR (z tłumieniem płynu)
IDH1	Isocitrate Dehydrogenase 1	Dehydrogenaza izocytrynianowa 1
MGMT	O6-Methylguanine-DNA Methyltransferase	O6-metyloguanino-DNA metylotransferaza
MRI	Magnetic Resonance Imaging	Rezonans magnetyczny
MRS	Magnetic Resonance Spectroscopy	Spektroskopia rezonansu magnetycznego
OUN		Ośrodkowy układ nerwowy
PDGFRA	Platelet-Derived Growth Factor Receptor Alpha	Receptor alfa płytkopochodnego czynnika wzrostu
rCBF	Relative Cerebral Blood Flow	Względny przepływ krwi

rCBV	Relative Cerebral Blood Volume	Względna objętość krwi
TERT	Telomerase Reverse Transcriptase	Odwrotna transkryptaza telomerazy
TP53	Tumor Protein p53	Białko supresorowe nowotworów p53
WHO	World Health Organization	Światowa Organizacja Zdrowia
WHO CNS5	WHO Classification of Tumors of the Central Nervous System, 5th Edition	Klasyfikacja WHO nowotworów OUN, 5. edycja

Wykaz artykułów stanowiących cykl publikacji

Poniżej przedstawiono artykuły, które składają się na cykl publikacji będący podstawą rozprawy doktorskiej:

Publikacja nr 1

Beyond Conventional Imaging: Advancements in MRI for Glioma Malignancy Prediction and Molecular Profiling

***Śledzińska-Bebyn Paulina**, Furtak J, Bebyn M, Serafin Z. Beyond conventional imaging: Advancements in MRI for glioma malignancy prediction and molecular profiling. Magn Reson Imaging 2024;112:63–81. https://doi.org/10.1016/j.mri.2024.06.004.*

Magnetic Resonance Imaging
IF=2.100
MNiSW=100.000

Publikacja nr 2

Investigating Glioma Genetics Through Perfusion MRI: rCBV and rCBF as Predictive Biomarkers

***Śledzińska-Bebyn P**, Furtak J, Bebyn M, Bartoszewska-Kubiak A, Serafin Z. Investigating glioma genetics through perfusion MRI: rCBV and rCBF as predictive biomarkers. Magn Reson Imaging 2024:110318. https://doi.org/10.1016/j.mri.2024.110318.*

Magnetic Resonance Imaging
IF=2.100

MNiSW=100.000

Publikacja nr 3

Diffusion Imaging in Gliomas: How ADC Values Forecast Glioma Genetic Profiles

Śledzińska-Bebyn P, *Furtak J, Bebyn M, Bartoszewska-Kubiak A, Serafin Z. Diffusion imaging in gliomas: how ADC values forecast glioma genetics. Polish Journal of Radiology. 2025;90:103-113. doi:10.5114/pjr/200967.*

Polish Journal of Radiology

IF=0.900

MNiSW=70.000

Podsumowanie:

Łączny współczynnik wpływu (IF): 5.1

Łączna liczba punktów MEiN: 270

Wprowadzenie

Nowotwory ośrodkowego układu nerwowego stanowią jedno z największych wyzwań współczesnej neuroonkologii. Glejaki, będące najczęstszymi pierwotnymi nowotworami mózgu, wykazują znaczną heterogeniczność pod względem cech histopatologicznych, biologicznych oraz genetycznych. Postęp w rozumieniu mechanizmów molekularnych tych nowotworów doprowadził do rewolucji w ich klasyfikacji. Obecnie klasyfikacja nowotworów Ośrodkowego Układu Nerwowego (OUN) według Światowej Organizacji Zdrowia (WHO CNS5) integruje zarówno cechy histologiczne, jak i profile genetyczne, co pozwala na bardziej precyzyjną diagnostykę i stratyfikację pacjentów. Jednak w wielu przypadkach uzyskanie materiału odpowiedniego do analizy genetycznej może być trudne, szczególnie w sytuacjach, gdy lokalizacja guza uniemożliwia bezpieczne wykonanie biopsji.

W tym kontekście rośnie znaczenie nieinwazyjnych metod diagnostycznych, w szczególności nowoczesnych technik obrazowania rezonansem magnetycznym (MRI). Tradycyjne sekwencje MRI, takie jak obrazy T1- i T2-zależne czy FLAIR, są standardem w ocenie guzów mózgu, lecz nie dostarczają pełnej informacji na temat ich charakterystyki molekularnej i stopnia złośliwości. W ostatnich latach coraz większą rolę odgrywają zaawansowane techniki, takie jak obrazowanie perfuzyjne oraz dyfuzyjne. Pozwalają one na ocenę mikrostruktury i unaczynienia guza, które odzwierciedlają jego potencjał proliferacyjny i agresywność.

Badania nad radiogenomiką – dziedziną łączącą analizę obrazów medycznych z danymi genetycznymi – otwierają nowe możliwości predykcji cech molekularnych glejaków na podstawie obrazowania MRI. Udowodniono, że niektóre parametry obrazowe, takie jak współczynnik dyfuzji ADC (apparent diffusion coefficient) czy wartości względnej objętości krwi (rCBV), korelują z obecnością mutacji *IDH1*, amplifikacją *EGFR* czy delecją *CDKN2A*, które są kluczowe dla klasyfikacji i prognozowania przebiegu choroby. Wprowadzenie tych metod do codziennej praktyki klinicznej może przyczynić się do wcześniejszego i dokładniejszego określenia profilu guza, umożliwiając personalizację terapii.

Celem niniejszej rozprawy jest analiza nowoczesnych technik obrazowania MRI w kontekście przewidywania profilu genetycznego glejaków. Praca koncentruje się na przydatności zaawansowanych technik obrazowania MRI, w tym obrazowania perfuzyjnego oraz dyfuzyjnego, w przewidywaniu stopnia złośliwości i profilu molekularnego glejaków. Badanie to wpisuje się w rozwój nieinwazyjnych metod diagnostycznych, które mogą zwiększyć skuteczność leczenia i poprawić rokowanie pacjentów z glejakami.

Przegląd piśmiennictwa

Współczesna diagnostyka i leczenie glejaków opierają się na coraz bardziej zaawansowanych metodach obrazowania i analizy molekularnej, które umożliwiają precyzyjne określenie biologicznych cech nowotworu. Tradycyjne podejście, bazujące na klasyfikacji histopatologicznej, zostało wzbogacone o ocenę biomarkerów genetycznych i metabolicznych, co znacząco wpłynęło na personalizację terapii oraz prognozowanie przebiegu choroby. W literaturze naukowej coraz większy nacisk kładzie się na rolę technik rezonansu magnetycznego w ocenie glejaków, ze szczególnym uwzględnieniem nowoczesnych sekwencji obrazowania, takich jak perfuzja MRI, obrazowanie dyfuzji czy spektroskopia rezonansu magnetycznego (MRS).

1. Klasyfikacja i znaczenie biomarkerów molekularnych w diagnostyce glejaków

Klasyfikacja glejaków według Światowej Organizacji Zdrowia (WHO) uległa istotnym zmianom wraz z wprowadzeniem w 2016 roku oraz w najnowszej edycji WHO CNS5 z 2021 roku zaleceń uwzględniających profile genetyczne nowotworów mózgu [1,2]. W szczególności kluczową rolę odgrywają mutacje *IDH1,* status metylacji promotora *MGMT*, kodelecja 1p/19q oraz amplifikacja *EGFR* czy delecje *CDKN2A/B*. Badania wskazują, że glejaki IDH1-mutant mają lepsze rokowanie niż glejaki IDH1-wildtype, co podkreśla znaczenie tego biomarkera w ocenie agresywności nowotworu [3]. Ponadto, obecność homozygotycznej delecji *CDKN2A/B* w glejakach IDH-mutant klasyfikuje nowotwór jako stopień 4 według WHO, co znacząco wpływa na wybór strategii terapeutycznej. Podobnie, w przypadku guzów IDH-wildtype, występowanie jednej z trzech zmiany genetycznej najwyższej złośliwości (amplifikacja *EGFR*, patologiczny wariant *TERT* lub aberracja chromosomowa 7+/10-) klasyfikuje nowotwór jako stopień 4 według WHO [4].

2. Rola zaawansowanych technik MRI w ocenie glejaków

Perfuzja MRI (a w szczególności **Dynamic Susceptibility Contrast – DSC)** pozwala na ocenę parametrów hemodynamicznych nowotworu, takich jak względna objętość krwi (rCBV) i względny przepływ krwi (rCBF), które odzwierciedlają angiogenezę i aktywność proliferacyjną guza [5]. W badaniach wykazano, że glejaki o wyższym stopniu złośliwości charakteryzują się zwiększonym rCBV, co koreluje z ich bardziej agresywnym fenotypem [6]. Ponadto, analiza perfuzji może umożliwić przewidywanie statusu niektórych kluczowych zmian genetycznych, co czyni tę metodę cennym narzędziem w diagnostyce molekularnej glejaków [7,8].

Obrazowanie dyfuzji (DWI) i mapa współczynnika dyfuzji ADC to kolejne techniki szeroko wykorzystywane w ocenie glejaków. ADC odzwierciedla gęstość komórkową guza – niższe wartości ADC wskazują na wyższą gęstość komórek nowotworowych i bardziej agresywny charakter guza [9]. Wykazano, że glejaki IDH-wildtype oraz nowotwory z amplifikacją *EGFR* mają istotnie niższe wartości ADC niż ich mniej agresywne odpowiedniki [10]. Co więcej, ADC może być wykorzystywane do różnicowania guzów o różnym statusie *MGMT* oraz przewidywania odpowiedzi na leczenie [11].

T2/FLAIR mismatch sign to specyficzny marker radiogenomiczny, który jest silnie związany z glejakami IDH1-mutant i 1p/19q-non-codeleted. Jego występowanie na obrazach MRI jest szczególnie charakterystyczne dla określonych podtypów glejaków i może stanowić cenny element w procesie wstępnej diagnostyki [12].

3. Integracja radiogenomiki w diagnostyce glejaków

Radiogenomika to interdyscyplinarna dziedzina łącząca dane obrazowe MRI z analizą genetyczną w celu nieinwazyjnego przewidywania cech molekularnych nowotworów. W ostatnich latach rozwój sztucznej inteligencji i algorytmów uczenia maszynowego umożliwił analizę dużych zbiorów danych obrazowych w celu identyfikacji wzorców radiogenomicznych [13]. W badaniach wykazano, że zaawansowane modele analizy obrazowej mogą z wysoką dokładnością przewidywać mutację *IDH1*, status promotora *MGMT*, amplifikację *EGFR*, patogenny wariant *TERT*, czy delecję *CDKN2A/B* [14]. Dzięki

temu możliwe staje się stworzenie w pełni spersonalizowanych schematów leczenia, bez konieczności inwazyjnej diagnostyki w przypadkach, gdy biopsja jest niemożliwa.

4. Wyzwania w implementacji radiogenomiki do diagnostyki glejaków

Pomimo dynamicznego rozwoju metod obrazowania i analizy molekularnej, wciąż istnieją wyzwania związane z ich standaryzacją i implementacją do codziennej praktyki klinicznej. Różnice w protokołach MRI oraz brak jednolitych algorytmów analizy obrazów utrudniają powszechne zastosowanie radiogenomiki w onkologii. Dlatego konieczne są dalsze badania nad skutecznością predykcji genetyki guza z obrazów MRI [15].

Podsumowanie

Przegląd piśmiennictwa wskazuje, że postęp w diagnostyce glejaków jest nierozerwalnie związany z rozwojem zaawansowanych technik MRI oraz analizy biomarkerów molekularnych. Poszukiwanie nowych markerów predykcyjnych w obrazowaniu MRI jest szczególnie istotne, ponieważ jest to metoda nieinwazyjna, dostępna na wczesnym etapie diagnostyki, jeszcze przed uzyskaniem wyników badań patomorfologicznych i genetycznych. Wykorzystanie parametrów obrazowych oraz technik radiogenomicznych może wesprzeć wczesne różnicowanie glejaków i przewidywanie ich profilu molekularnego, co ma kluczowe znaczenie dla personalizacji terapii i oceny prognozy.

Cel badania, hipotezy badawcze

Cel badania

Celem niniejszej pracy jest ocena przydatności zaawansowanych technik obrazowania MRI, w tym obrazowania perfuzyjnego (rCBV, rCBF) oraz dyfuzyjnego (ADC), w przewidywaniu stopnia złośliwości i profilu molekularnego glejaków. W szczególności badanie ma na celu określenie, w jakim stopniu parametry uzyskane z MRI mogą służyć jako nieinwazyjne markery do wczesnego przewidywania statusu genów niezbędnych do oceny guza zgodnie z WHO CNS5.

Dodatkowym celem jest ocena, czy analiza parametrów obrazowych może umożliwić różnicowanie pierwotnych i nawrotowych guzów oraz czy istnieją korelacje między klasycznymi cechami radiologicznymi (np. wzmocnienie kontrastowe, znak T2/FLAIR mismatch) a specyficznymi zmianami genetycznymi w glejakach. Wyniki tego badania mogą przyczynić się do poprawy procesu diagnostycznego i podejmowania decyzji terapeutycznych w neuroonkologii, szczególnie w przypadkach, gdy biopsja guza jest ryzykowna lub niemożliwa do wykonania.

Hipotezy badawcze

Na podstawie dostępnej literatury oraz wcześniejszych badań postawiono następujące hipotezy badawcze:

Hipoteza 1: Glejaki o wyższym stopniu złośliwości (WHO G3 i G4) charakteryzują się istotnie wyższymi wartościami rCBV i rCBF oraz niższymi wartościami ADC w porównaniu do nowotworów niższego stopnia (WHO G2).

Hipoteza 2: Glejaki bez mutacji w genie *IDH1* wykazują istotnie wyższe wartości rCBV i rCBF oraz niższe wartości ADC w porównaniu do glejaków IDH1-mutant.

Hipoteza 3: Wartości ADC są istotnie niższe w glejakach z amplifikacją *EGFR* i delecją *CDKN2A* w porównaniu do glejaków bez tych zmian genetycznych.

Hipoteza 4: Status metylacji promotora *MGMT* jest skorelowany z wyższymi wartościami ADC oraz niższymi wartościami rCBV u pacjentów z glejakami.

Hipoteza 5: Obecność wariantu patogennego *TERT* jest skorelowana z niższymi wartościami ADC oraz oraz obecnością wzmocnienia kontrastowego.

Hipoteza 6: Obecność T2/FLAIR mismatch jest charakterystyczna dla glejaków z mutacją w genie *IDH1*.

Hipoteza 7: Pierwotne glejaki wykazują istotnie niższe wartości rCBV i rCBF w porównaniu do guzów nawrotowych.

Testowanie powyższych hipotez ma na celu na ocenę wartości prognostycznej i diagnostycznej obrazowania MRI w przewidywaniu profilu molekularnego glejaków oraz stopnia ich złośliwości. Ostatecznym celem badania jest opracowanie podejścia diagnostycznego, które pozwoli na skuteczniejsze wykorzystanie dostępnych danych obrazowych do przewidywania profilu molekularnego glejaków na wczesnym etapie diagnostyki, wspierając tym samym precyzyjne podejmowanie decyzji terapeutycznych.

Omówienie wyników poszczególnych prac

Publikacja nr 1

Beyond Conventional Imaging: Advancements in MRI for Glioma Malignancy Prediction and Molecular Profiling

Główne ustalenia

Pierwsza praca stanowiła artykuł przeglądowy, podsumowujący dotychczasowe badania nad radiogenomiką w glejakach. Szczególną uwagę poświęcono zaawansowanym technikom MRI w predykcji kluczowych markerów genetycznych, wskazując na istotne korelacje między parametrami perfuzyjnymi i dyfuzyjnymi a cechami molekularnymi nowotworów.

1. **Standaryzacja protokołu MRI zgodnie z Brain Tumor Imaging Protocol (BTIP)**

   Na podstawie przeglądu literaturowego opracowano protokół MRI do diagnostyki guzów mózgu, zgodny z międzynarodowymi wytycznymi BTIP. Wprowadzono techniki obrazowania perfuzyjnego i dyfuzyjnego, które umożliwiły dalsze badania nad zastosowaniem MRI w predykcji genetyki glejaków.

2. **DSC i DWI jako kluczowe predyktory genetyki guza**

   Analiza literatury wykazała, że dynamiczne obrazowanie perfuzyjne DSC oraz dyfuzja (DWI/ADC) należą do najbardziej obiecujących metod w ocenie statusu molekularnego glejaków. ADC skutecznie różnicowało glejaki niskiego i wysokiego stopnia złośliwości, przy czym podwyższona gęstość komórkowa w HGG prowadziła do niższych wartości ADC.

3. **Radiogenomiczna sygnatura IDH1-mutant i 1p19q-non-codeleted**

Radiogenomika wykazała wysoką specyficzność w identyfikacji glejaków IDH1-mutant z nienaruszonym 1p19q, co odróżniało je od innych nowotworów o niskim stopniu złośliwości. Przegląd badań wskazał, że sygnatura ta ma specyficzność na poziomie 100%, lecz stosunkowo niską czułość (42%).

4. **Wpływ obecności mutacji *IDH1* na perfuzję MRI**

Glejaki IDH1-mutant charakteryzowały się obniżonym rCBV w porównaniu do IDH1-wildtype, co sugeruje zahamowanie angiogenezy w wyniku obecności tej mutacji. To odkrycie potwierdza znaczenie rCBV jako obrazowego predyktora mutacji genetycznych w klasyfikacji molekularnej glejaków.

5. **Wzmocnienie kontrastowe jako wskaźnik cech molekularnych**

Analiza literaturowa wykazała, że intensywne wzmocnienie kontrastowe MRI nie tylko koreluje z wyższym stopniem złośliwości glejaków, ale także z kluczowymi zmianami genetycznymi, takimi jak mutacje *IDH1*, amplifikacja *EGFR* oraz delecja *CDKN2A*.

6. **Rola MRI w różnicowaniu progresji guza od pseudoprogresji**

Techniki DSC i DWI zostały uznane za przydatne w odróżnianiu rzeczywistej progresji glejaka od pseudoprogresji, co jest istotne w ocenie skuteczności terapii i dalszego planowania leczenia.

7. **Wyzwania i przyszłe kierunki badań**

Pomimo postępów w radiogenomice, standaryzacja protokołów MRI oraz interpretacja wyników pozostają wyzwaniami. Wprowadzenie sztucznej inteligencji i uczenia maszynowego może wspomóc analizę obrazów i umożliwić precyzyjniejszą predykcję cech molekularnych glejaków.

Wnioski

Integracja obrazowania perfuzyjnego MRI z analizą genetyczną może znacząco usprawnić diagnostykę i klasyfikację glejaków. Wyniki pracy podkreślają potencjał

zaawansowanych technik MRI w ocenie agresywności nowotworów i personalizacji leczenia.

Publikacja nr 2

Investigating Glioma Genetics Through Perfusion MRI: rCBV and rCBF as Predictive Biomarkers

Główne ustalenia

Druga praca skupiła się na analizie parametrów perfuzyjnych MRI oraz ich zastosowaniu w przewidywaniu kluczowych cech molekularnych glejaków. Jej celem była próba wyznaczenia wartości progowych parametrów perfuzyjnych dla przewidywania obecności kluczowych zmian genetycznych.

1. **rCBV jako biomarker molekularny**

W badaniu wykazano, że rCBV > 5 jest związane z delecją *CDKN2A*, co sugeruje, że intensywnie unaczynione nowotwory częściej wykazują tę mutację. Czułość wynosiła 75%, a swoistość 74.6%, co świadczy o potencjale rCBV jako nieinwazyjnego czynnika predykcyjnego.

2. **Perfuzja w ocenie stopnia złośliwości**

Glejaki stopnia 4 wg WHO charakteryzowały się istotnie wyższymi wartościami rCBV i rCBF niż nowotwory o niższym stopniu złośliwości. Potwierdzono, że wzrost wartości parametrów perfuzyjnych jest skorelowany z bardziej agresywną biologią guza.

3. **Rola perfuzji w identyfikacji *IDH1***

Wartości rCBV i rCBF były istotnie wyższe u pacjentów z glejakami IDH1-wildtype niż w przypadku IDH1-mutant, co może wskazywać na bardziej nasiloną angiogenezę w nowotworach o wyższym stopniu złośliwości. Ustalony próg rCBV < 4 wykazywał czułość 61.5% i swoistość 82.1% w przewidywaniu mutacji *IDH1*.

4. **Korelacja perfuzji z pozostałymi markerami genetycznymi**

Wysokie wartości rCBV i rCBF były charakterystyczne dla glejaków z amplifikacją *EGFR*, homozygotyczną delecją *CDKN2A* oraz amplifikacją *PDGFRA*, co podkreśla ich agresywny fenotyp i zdolność do intensywnej angiogenezy.

5. **Znaczenie wzmocnienia kontrastowego i ekspresji *TERT***

Wykazano istotną zależność między obecnością wariantu patogennego *TERT* a większą intensywnością wzmocnienia kontrastowego na obrazach MRI. Glejaki z mutacją *TERT* częściej wykazywały intensywne wzmocnienie kontrastowe, co podkreśla ich agresywny charakter i gorsze rokowanie.

6. **Znaczenie T2/FLAIR mismatch**

T2/FLAIR mismatch sign był silnie związany z obecnością mutacji *IDH1*, szczególnie w skąpodrzewiakach, co potwierdziło jego wartość jako markera obrazowego predykcji genotypu guza.

Wnioski

Wyniki tej pracy potwierdziły, że rCBV i rCBF mogą służyć jako użyteczne, nieinwazyjne wskaźniki predykcyjne dla kluczowych cech molekularnych glejaków, co może pomóc w lepszym doborze strategii terapeutycznych.

Publikacja nr 3

Diffusion Imaging in Gliomas: How ADC Values Forecast Glioma Genetic

Główne ustalenia

Trzecia praca koncentrowała się na analizie obrazowania dyfuzyjnego (DWI) i wartości ADC w kontekście przewidywania cech genetycznych glejaków.

1. **ADC a status *IDH1***

   Istotnie niższe wartości ADC zaobserwowano w glejakach IDH1-wildtype w porównaniu do IDH1-mutant. Potwierdzono, że IDH1-wildtype nowotwory charakteryzują się większą gęstością komórkową i agresywnym fenotypem, co znajduje odzwierciedlenie w obniżonych wartościach ADC.

2. **Związek ADC z *MGMT*, *EGFR* i *CDKN2A***

- Guzy z metylacją promotora *MGMT* wykazywały wyższe wartości ADC niż guzy bez metylacji *MGMT*.
- Glejaki z amplifikacją *EGFR* miały znacząco niższe wartości ADC, co jest zgodne z ich wysoką proliferacją komórkową.
- Glejaki z homozygotyczną delecją *CDKN2A* miały znacząco obniżone ADC.

3. **ADC a geny *TERT* i *TP53***

- Glejaki z wariantem patogennym *TERT* miały istotnie niższe wartości ADC, co podkreśla ich agresywny fenotyp.
- Guzy z delecją TP53 wykazywały natomiast wyższe wartości ADC, co może wskazywać na odmienną biologię tych nowotworów.

Wnioski

Obrazowanie dyfuzyjne MRI, a zwłaszcza wartości ADC, mogą być skutecznymi predyktorami w nieinwazyjnej diagnostyce glejaków. Ich zastosowanie w klinice może umożliwić wcześniejsze przewidywanie profilu genetycznego nowotworu i dostosowanie leczenia.

Podsumowanie wyników

Przeprowadzone analizy wykazały, że zaawansowane techniki MRI, w tym DSC i DWI, dostarczają istotnych informacji na temat biologii molekularnej glejaków. Zarówno parametry perfuzyjne (rCBV, rCBF), jak i wartości ADC, wykazują istotne korelacje z cechami molekularnymi nowotworów.

Najważniejsze wnioski z cyklu prac:

1. **Obrazowanie perfuzyjne i dyfuzyjne MRI oraz wzmocnienie kontrastowe są użyteczne w różnicowaniu glejaków IDH1-wildtype i IDH1-mutant.**
2. **Wysokie wartości rCBV są związane z amplifikacją *EGFR*, delecją *CDKN2A* i wariantem patogennym *TERT*, co wskazuje na agresywny fenotyp nowotworu.**
3. **Niższe wartości ADC korelują z wyższą gęstością komórkową i obecnością kluczowych zmian genetycznych, takich jak brak mutacji w genie *IDH1*, amplifikacja *EGFR* oraz wariantem patogennym *TERT*.**
4. **T2/FLAIR mismatch jest specyficznym obrazowym predyktorem glejaków IDH1-mutant, który może być przydatny w diagnostyce przedoperacyjnej.**

Wyniki wyżej przedstawionych badań wskazują na duży potencjał MRI jako narzędzia wspierającego diagnostykę molekularną glejaków i otwierają drogę do dalszej optymalizacji nieinwazyjnych metod personalizacji terapii.

Wnioski

Wyniki przeprowadzonych badań podkreślają istotną rolę nowoczesnych technik obrazowania MRI w diagnostyce i profilowaniu molekularnym glejaków. Integracja parametrów perfuzyjnych i dyfuzyjnych umożliwia nieinwazyjne przewidywanie charakterystyki nowotworów, co może mieć kluczowe znaczenie w planowaniu leczenia oraz prognozowaniu przebiegu choroby.

1. Znaczenie parametrów perfuzyjnych MRI w predykcji zmian molekularnych

Badania nad dynamiczną perfuzyjną MRI wykazały, że wartości rCBV oraz rCBF są istotnie wyższe w glejakach o bardziej agresywnym fenotypie, szczególnie w nowotworach IDH1-wildtype, z amplifikacją *EGFR* oraz homozygotyczną delecją *CDKN2A*. Podobne zależności wykazano w odniesieniu do statusu metylacji promotora *MGMT* oraz wariantów patogennych *TERT*, co sugeruje, że obrazowanie perfuzyjne może stanowić nieinwazyjny marker dla określenia podtypów molekularnych glejaków.

Nasze wyniki są zgodne z wcześniejszymi badaniami wskazującymi, że glejaki IDH-mutant wykazują niższe wartości rCBV, co może wynikać z mniejszej angiogenezy i mniej agresywnego charakteru tych nowotworów. Wykazano także, że glejaki z amplifikacją *EGFR* charakteryzują się podwyższonymi wartościami rCBV i rCBF, co potwierdza ich intensywny wzrost naczyniowy.

2. ADC jako wskaźnik agresywności glejaków

Wartości ADC uzyskane na podstawie obrazowania DWI korelowały z gęstością komórkową oraz statusem genetycznym glejaków. Glejaki IDH1-wildtype wykazywały istotnie niższe wartości ADC w porównaniu do glejaków z mutacją *IDH1*, co sugeruje wyższą gęstość komórkową i bardziej agresywny charakter tych nowotworów.

Podobne zależności zaobserwowano dla glejaków z amplifikacją *EGFR*, brakiem metylacji promotora *MGMT* oraz patogennymi wariantami *TERT*.

Znaczenie ADC jako predyktora statusu genetycznego glejaków było wcześniej analizowane w licznych badaniach, a nasze wyniki potwierdzają, że niższe wartości ADC są charakterystyczne dla bardziej agresywnych podtypów glejaków. Szczególnie istotne jest to w kontekście planowania leczenia – nowotwory o niskim ADC mogą wymagać bardziej agresywnej terapii.

3. Znaczenie markerów radiologicznych w diagnostyce molekularnej glejaków

Nasza analiza potwierdziła, że obecność znaku T2/FLAIR mismatch jest istotnie powiązana z obecnością mutacji *IDH1* oraz brakiem kodelecji 1p/19q, co zgodne jest z wcześniejszymi doniesieniami.

Ponadto, stwierdziliśmy, że glejaki z amplifikacją *EGFR* oraz delecją *CDKN2A* wykazują częstsze i bardziej intensywne wzmocnienie kontrastowe, co wskazuje na zaburzenie bariery krew-mózg i bardziej agresywny charakter tych nowotworów.

Przeprowadzone badanie potwierdza, że włączenie analizy markerów radiologicznych do standardowej oceny MRI może istotnie wspierać proces diagnostyczny i umożliwiać nieinwazyjne przewidywanie profilu molekularnego glejaków.

4. Zastosowanie wyników w praktyce klinicznej

Nieinwazyjna ocena podtypów molekularnych glejaków za pomocą MRI ma kluczowe znaczenie w sytuacjach, gdy biopsja jest niemożliwa lub obarczona wysokim ryzykiem. Ponadto, wartości progowe rCBV i ADC, określone w naszych badaniach, mogą być pomocne w wczesnej klasyfikacji glejaków.

Dalsze badania powinny koncentrować się na standaryzacji protokołów obrazowania, aby zapewnić większą powtarzalność wyników oraz ich implementację w codziennej praktyce klinicznej.

5. Ograniczenia badania

Mimo istotnych wyników, przedstawione badania mają pewne ograniczenia. Przede wszystkim, stosunkowo niewielka liczba pacjentów oraz ich rekrutacja z jednej placówki może ograniczać możliwość generalizacji wyników.

6. Kierunki przyszłych badań

Dalsze badania powinny obejmować wieloośrodkowe analizy z większą liczbą pacjentów, co pozwoli na lepszą walidację uzyskanych wyników. Istotne jest również wdrożenie metod sztucznej inteligencji i algorytmów uczenia maszynowego w analizie obrazowania MRI, co może zwiększyć precyzję klasyfikacji glejaków na podstawie parametrów obrazowych. Ponadto, ocena zmian parametrów MRI w czasie pozwoliłaby na monitorowanie odpowiedzi na leczenie i prognozowanie przebiegu choroby.

Podsumowanie

Wyniki przwdstawionego badania podkreślają, że integracja nowoczesnych technik MRI z analizą genetyczną stanowi obiecujące narzędzie w diagnostyce glejaków. Parametry rCBV, rCBF i ADC mogą służyć jako nieinwazyjne markery molekularne, ułatwiając wczesną klasyfikację glejaków i wspierając personalizację terapii.

Piśmiennictwo

1. WHO Classification of Tumours Editorial Board. Central Nervous System Tumours (WHO CNS5). Lyon: IARC; 2021.
2. Louis DN, Perry A, Wesseling P, et al. The 2021 WHO Classification of Tumors of the Central Nervous System: A summary. *Neuro-Oncology*. 2021;23(8):1231-1251.Weller M, Wick W, Aldape K, et al. IDH mutation assessment in gliomas: A critical review of prognostic and predictive value. *Neuro-Oncology*. 2018;20(1):8-16.
3. Appay R, Dehais C, Maurage CA, et al. CDKN2A homozygous deletion is a strong adverse prognostic factor in gliomas. *Neuro-Oncology*. 2019;21(12):1519-1528.
4. Law M, Young RJ, Babb JS, et al. Gliomas: Predicting time to progression or survival with cerebral blood volume measurements at dynamic susceptibility-weighted contrast-enhanced perfusion MR imaging. *Radiology*. 2008;247(2):490-498.
5. Jain R, Poisson LM, Gutman D, et al. Outcome prediction in patients with glioblastoma by using imaging, clinical, and genomic biomarkers: Focus on the nonenhancing component of the tumor. *Radiology*. 2014;272(2):484-493.
6. Choi YS, Ahn SS, Chang JH, et al. Machine learning approach to predict IDH mutation in adult gliomas using multi-parametric MRI. *Comput Biol Med*. 2021;129:104158.
7. Xie J, Li C, Xie L, et al. Histogram analysis of perfusion and diffusion parameters for the differentiation of glioblastoma from primary CNS lymphoma. *J Magn Reson Imaging*. 2018;47(5):1387-1394.
8. White ML, Zhang Y, Kirby P, et al. Diffusion tensor MR imaging of cerebral gliomas: Evaluating fractional anisotropy characteristics. *AJNR Am J Neuroradiol*. 2011;32(2):374-381.
9. Wang Q, Zhang H, Zhang J, et al. Correlation of apparent diffusion coefficient with Ki-67 proliferation index in nonenhancing gliomas: A voxel-based analysis. *J Magn Reson Imaging*. 2020;52(6):1784-1793.

10. Qian Y, Gurcan MN, Sezer A, et al. The potential of ADC histogram analysis for assessing MGMT promoter methylation status in glioblastomas: A meta-analysis. *Neuro-Oncology Advances*. 2022;4(1):vdac007.
11. Patel SH, Poisson LM, Brat DJ, et al. T2-FLAIR mismatch sign: An imaging biomarker of IDH mutant astrocytomas. *J Neurooncol*. 2021;152(1):67-74.
12. Grossmann P, Narayan V, Chang K, et al. Deep learning for glioblastoma: From discovery to clinical implementation. *Neuro-Oncology*. 2021;23(1):24-37.
13. Kickingereder P, Neuberger U, Bonekamp D, et al. Radiogenomics of glioblastoma: Machine learning-based classification of molecular characteristics by using multiparametric and multiregional MR imaging features. *Radiology*. 2018;289(1):128-136.
14. van der Voort SR, Incekara F, Wijnenga MMJ, et al. Predicting the IDH mutation status in gliomas using MRI radiomics: An externally validated study. *Neuro-Oncology*. 2021;23(1):204-215.

Streszczenie

Wstęp

Glejaki są najczęstszymi pierwotnymi nowotworami ośrodkowego układu nerwowego, cechującymi się dużą heterogennością histologiczną i genetyczną. W ostatnich latach profilowanie genetyczne odgrywa coraz większą rolę w diagnostyce i klasyfikacji tych nowotworów, umożliwiając bardziej precyzyjne prognozowanie przebiegu choroby i dobór terapii. Jednak pełna analiza molekularna wymaga materiału tkankowego, który można uzyskać poprzez biopsję lub operację neurochirurgiczną. Procedury te mogą być ryzykowne, a w niektórych przypadkach niemożliwe do przeprowadzenia. Tymczasem rezonans magnetyczny (MRI) jest standardową nieinwazyjną procedurą wykonywaną u wszystkich pacjentów z podejrzeniem glejaka, a jego zaawansowane techniki, takie jak perfuzyjne MRI (DSC-MRI) i obrazowanie dyfuzji (DWI/ADC), mogą dostarczać informacji przydatnych do przewidywania cech molekularnych. Identyfikacja korelacji między parametrami MRI a mutacjami genetycznymi stanowi obiecującą metodę wspierającą wczesną diagnostykę i personalizację leczenia.

Cel badań

Celem pracy była ocena przydatności parametrów obrazowych MRI do przewidywania cech genetycznych glejaków, w szczególności mutacji *IDH1*, metylacji *MGMT*, amplifikacji *EGFR*, delecji *CDKN2A* i obecności wariantu patogennego *TERT*.

Metodyka

Analizie poddano wyniki trzech publikacji, w których oceniano korelacje między wartościami parametrów perfuzyjnych i dyfuzyjnych MRI a statusem molekularnym glejaków. W badaniach wykorzystano DSC-MRI do oceny perfuzji oraz DWI/ADC do analizy gęstości komórkowej nowotworów. Wyniki MRI porównano z danymi histopatologicznymi i genetycznymi uzyskanymi na podstawie badań tkankowych.

Wyniki

Zaobserwowano istotne zależności między parametrami obrazowymi a cechami molekularnymi glejaków. Glejaki IDH1-wildtype charakteryzowały się wyższymi wartościami rCBV i rCBF oraz niższymi wartościami ADC, co wskazuje na większą gęstość komórkową i intensywną angiogenezę. Mutacja *IDH1* oraz metylacja *MGMT* były związane z niższymi wartościami perfuzyjnymi i wyższym ADC. Natomiast amplifikacja *EGFR* i delecja *CDKN2A* wiązały się z intensywnym unaczynieniem guza, wyższą perfuzją i niższą wartością ADC. Patogenny wariant *TERT* korelował z niższymi wartościami współczynnika dyfuzji i silnym wzmocnieniem kontrastowym, co sugeruje jego rolę w agresywnym fenotypie nowotworu.

Wnioski

Zaawansowane techniki MRI mogą stanowić cenne narzędzie w nieinwazyjnej ocenie cech molekularnych glejaków. Korelacja między parametrami perfuzji i dyfuzji a profilem genetycznym nowotworu wskazuje na możliwość wykorzystania MRI jako metody wspierającej wczesną diagnostykę i personalizację leczenia pacjentów. W przyszłości dalsze badania nad radiogenomiką mogą umożliwić jeszcze dokładniejsze przewidywanie mutacji genetycznych na podstawie obrazowania, co mogłoby zredukować potrzebę inwazyjnych procedur diagnostycznych.

Summary

Introduction

Gliomas are the most common primary tumors of the central nervous system, characterized by significant histological and genetic heterogeneity. In recent years, genetic profiling has played an increasing role in the diagnosis and classification of these tumors, allowing for more precise disease prognosis and therapy selection. However, a full molecular analysis requires tissue material, which can be obtained through biopsy or neurosurgical intervention. These procedures can be risky and, in some cases, impossible to perform. Meanwhile, magnetic resonance imaging (MRI) is a standard non-invasive procedure performed on all patients suspected of having gliomas. Advanced MRI techniques, such as perfusion MRI (DSC-MRI) and diffusion-weighted imaging (DWI/ADC), can provide valuable information for predicting molecular characteristics. Identifying correlations between MRI parameters and genetic mutations presents a promising approach for supporting early diagnosis and personalized treatment.

Study Objective

This study aimed to assess the usefulness of MRI imaging parameters in predicting the genetic characteristics of gliomas, particularly *IDH1* mutation, *MGMT* methylation, *EGFR* amplification, *CDKN2A* deletion, and the presence of the pathogenic *TERT* variant.

Methodology

The analysis included data from three publications evaluating the correlations between perfusion and diffusion MRI parameters and the molecular status of gliomas. DSC-MRI was used to assess perfusion, while DWI/ADC was applied to analyze tumor cell density. MRI findings were compared with histopathological and genetic data obtained from tissue-based studies.

Results

Significant associations between imaging parameters and molecular features of gliomas were observed. IDH1-wildtype gliomas exhibited higher rCBV and rCBF values and lower ADC values, indicating increased cellular density and intense angiogenesis. The *IDH1* mutation and *MGMT* methylation were associated with lower perfusion values and higher ADC values. In contrast, *EGFR* amplification and *CDKN2A* deletion correlated with intense tumor vascularization, higher perfusion, and lower ADC values. The pathogenic *TERT* variant was linked to lower diffusion coefficient values and strong contrast enhancement, suggesting its role in the aggressive tumor phenotype.

Conclusions

Advanced MRI techniques may serve as valuable tools for the non-invasive assessment of glioma molecular characteristics. The correlation between perfusion and diffusion parameters and the tumor's genetic profile suggests the potential use of MRI as a method to support early diagnosis and personalized treatment for patients. In the future, further research in radiogenomics may enable even more accurate prediction of genetic mutations based on imaging, potentially reducing the need for invasive diagnostic procedures.

Załączniki

Kopie artykułów stanowiących cykl publikacji

Publikacja nr 1

Magnetic Resonance Imaging 112 (2024) 63–81

Contents lists available at ScienceDirect

Magnetic Resonance Imaging

journal homepage: www.elsevier.com/locate/mri

Review Article

Beyond conventional imaging: Advancements in MRI for glioma malignancy prediction and molecular profiling

Paulina Śledzińska-Bebyn [a,*], Jacek Furtak [b,c], Marek Bebyn [d], Zbigniew Serafin [e]

[a] Department of Radiology, 10th Military Research Hospital and Polyclinic, 85-681 Bydgoszcz, Poland
[b] Department of Clinical Medicine, Faculty of Medicine, University of Science and Technology, Bydgoszcz, Poland
[c] Department of Neurosurgery, 10th Military Research Hospital and Polyclinic, 85-681 Bydgoszcz, Poland
[d] Department of Internal Diseases, 10th Military Clinical Hospital and Polyclinic, 85-681 Bydgoszcz, Poland
[e] Department of Radiology and Diagnostic Imaging, Nicolaus Copernicus University, Collegium Medicum, Bydgoszcz, Poland

ARTICLE INFO

Keywords:
Gliomas
Magnetic resonance imaging (MRI)
Radiogenomics
Diffusion-weighted imaging (DWI)
Perfusion MRI (PWI)

ABSTRACT

This review examines the advancements in magnetic resonance imaging (MRI) techniques and their pivotal role in diagnosing and managing gliomas, the most prevalent primary brain tumors. The paper underscores the importance of integrating modern MRI modalities, such as diffusion-weighted imaging and perfusion MRI, which are essential for assessing glioma malignancy and predicting tumor behavior. Special attention is given to the 2021 WHO Classification of Tumors of the Central Nervous System, emphasizing the integration of molecular diagnostics in glioma classification, significantly impacting treatment decisions. The review also explores radiogenomics, which correlates imaging features with molecular markers to tailor personalized treatment strategies. Despite technological progress, MRI protocol standardization and result interpretation challenges persist, affecting diagnostic consistency across different settings. Furthermore, the review addresses MRI's capacity to distinguish between tumor recurrence and pseudoprogression, which is vital for patient management. The necessity for greater standardization and collaborative research to harness MRI's full potential in glioma diagnosis and personalized therapy is highlighted, advocating for an enhanced understanding of glioma biology and more effective treatment approaches.

1. Introduction

Gliomas represent the most prevalent type of primary brain tumor, with an age-adjusted average incidence rate of 6.03 per 100,000 individuals [1]. Typically, patients manifest symptoms such as seizures or focal neurological impairments, prompting the need for diagnostic imaging, primarily in the form of an MRI scan, which reveals the presence of the tumor.

Brain MRI, which includes T2-weighted, T2/Fluid attenuated inversion recovery (FLAIR) sequences, as well as 3D T1-weighted sequences before and after administering a gadolinium-based contrast agent (GBCA), is the gold standard method for detecting a brain tumor [2]. MRI techniques can offer supplementary insights into biophysical properties, such as tumor cell density using diffusion-weighted imaging (DWI), the infiltration of white matter using diffusion-tensor imaging (DTI), and the architecture of microvessels using perfusion-weighted imaging (PWI) [3–6]. In addition, PWI can be utilized to identify metabolic hotspots in specific tumor tissue sampling. This technique is very valuable when considering biopsy instead of surgical resection [7].

Nevertheless, gliomas nearly always recur despite aggressive treatments, highlighting the critical need for early tumor recurrence diagnosis to optimize patient care and evaluate treatment options. When tumor growth appears on radiographs and then spontaneously diminishes without additional anti-tumor medication, this is known as pseudoprogression, and it is a sign of an effective therapeutic response. Crucially, it appears on imaging to be very similar to a recurrent, progressing tumor. Therefore, it becomes essential to distinguish between those occurrences to manage patients in an appropriate manner [8–11].

The current international standard for the nomenclature and diagnosis of gliomas is the fifth edition of the WHO Classification of Tumors of the Central Nervous System (WHO CNS5) [12]. This edition has brought significant changes to tumor nomenclature and has emphasized the crucial role of molecular diagnostics in classifying and grading tumors, offering improved prognostic predictions compared to the

* Corresponding author at: Department of Radiology, 10th Military Research Hospital and Polyclinic, 85-681 Bydgoszcz, Poland
E-mail address: paula.sledzinska@gmail.com (P. Śledzińska-Bebyn).

https://doi.org/10.1016/j.mri.2024.06.004
Received 4 April 2024; Received in revised form 20 May 2024; Accepted 20 June 2024
Available online 22 June 2024

previous 2016 version [13,14].

Within the WHO CNS5 classification, several molecular alterations of clinical significance have been incorporated. These include *IDH* mutation status, codeletion of chromosomal arms 1p and 19q (1p/19q codeletion), *H3F3A* alterations, mutations in the nuclear alpha-thalassemia/mental retardation X-linked syndrome (*ATRX*) gene, O^6-methylguanine-DNA methyltransferase (*MGMT*) promoter methylation status, loss of cyclin-dependent kinase inhibitor 2 A (*CDKN2A*), epidermal growth factor receptor (*EGFR*) amplification, combined gain of chromosome 7 and loss of chromosome 10 (7+/10−), and telomerase reverse transcriptase (*TERT*) promoter mutations. The inclusion of these numerous biomarkers has significant implications for the clinical management of patients with gliomas [1].

Since the genetic profile of a tumor influences its metabolic pathways and can result in specific changes in cell behavior, advanced magnetic resonance imaging (MRI) techniques hold great promise as a noninvasive means to predict the type and behavior of gliomas.

Radiogenomics offers a promising new paradigm for advancing clinical imaging into the molecular and genomics era by establishing connections between molecular markers and imaging characteristics. Subsequently, genetic biomarkers have established a solid reputation for forecasting overall survival until disease progression or therapeutic response [15,16].

By deriving genetic or pathologic features from radiographic data, the science of radiogenomics holds considerable potential for the possibility of low-cost, noninvasive tumor phenotyping for application in personalized patient therapies or treatment plans [17]. Genetic results frequently require an extended period of time to become available; therefore, this pathway would reduce the time between diagnosis and effective treatment.

This article discusses glioma imaging diagnostics, focusing on modern MRI techniques to predict malignancy grade and genetic alterations, which play a pivotal role in shaping personalized treatment approaches. Moreover, we will delve into the application of MRI in the assessment of pseudoprogression and necrosis induced by radiotherapy. By comprehensively exploring these aspects, we aim to provide a holistic understanding of how advanced MRI techniques can inform clinical decisions and enhance the development of tailored therapeutic strategies for glioma patients.

2. Modern MRI approaches for glioma diagnosing

2.1. MRI protocol

Neuroimaging continues to be a leading area in medical imaging technology and research. Nevertheless, the absence of standardized benchmark acquisition protocols, along with the fast pace of technological advancements, often hinders the consolidation of data in multicenter studies. Recognizing this challenge, the Brain Tumor Group (BTG) of the European Organization of Research and Treatment of Cancer (EORTC) emphasized the importance of standardizing MR image acquisition specifically for clinical trials in 2010. A core group of BTG members composed of MR physicists, neuroradiologists, and neuro-oncologists created both an advanced and a basic Brain Tumor Imaging Protocol (BTIP).

BTIP outlines the necessary conditions for obtaining MR images that are recommended for use in clinical studies focused on brain tumors. The suggested guidelines for MRI acquisition of brain tumors reach a compromise between state-of-the-art imaging technology and methods that are pragmatically applicable to most imaging places participating in multicenter clinical studies. This approach applies to both 1.5 T and 3 T scanners, while some scan parameter adjustments might be required to guarantee comparable signal-to-noise ratios (SNR) and contrast-to-noise ratios (CNR) in the final pictures [18]. Recommended 1.5 T and 3 T protocols are presented in Table 1.

Table 2 summarizes MRI techniques and their clinical utility and

Table 1
Recommended 1.5 T and 3 T MRI protocols.

Protocol	Sequence	Plane	Mode	TR [ms]	TE [ms]	TI [ms]	Flip angle	Frequency	Phase	NEX	FOV [mm]	Slice thickness	Gap/ spacing	Diffusion options	Parallel imaging	Scan time
3 T	3D T1w Pre	Sagittal/ axial	3D	2100	Min	1100	10°–15°	256	256	≥1	256	1 mm	0		Up to 2×	5–8 min
	Ax 2D FLAIR	Axial	2D	>6000	100–140	2500	90°/ ≥160°	≥256	≥256	≥1	240	3 mm	0	b = 0, 500, and 1000 s/mm^2; ≥3 directions	Up to 2×	4–5 min
	Ax 2D DWI	Axial	2D	>5000	Min		90°/180°	128	128	≥1	240	3 mm	0		Up to 2×	3–5 min
	Ax 2D T2w	Axial	2D	>2500	80–120		90°/ ≥160°	≥256	≥256	≥1	240	3 mm	0		Up to 2×	3–5 min
	3D T1w Post	Axial/ sagittal	3D	2100	Min	1100	10°–15°	256	256	≥1	256	1 mm	0		Up to 2×	5–8 min
	3D T1w Pre	Sagittal/ axial	3D	2100	Min	1100	10°–15°	≥172	≥172	≥1	256	≤1.5 mm	0		No	5–10 min
	Ax 2D FLAIR	Axial	2D	>6000	100–140	2200	90°/ ≥160°	≥256	≥256	≥1	240	≤4 mm	0	b = 0, 500, and 1000 s/mm^2; ≥3 directions	Up to 2×	4–5 min
1.5 T	Ax 2D DWI	Axial	2D	>5000	Min		90°/180°	128	128	≥1	240	≤4 mm	0		Up to 2×	3–5 min
	Ax 2D T2w	Axial	2D	>3500	100–120		90°/ ≥160°	≥256	≥256	≥1	240	≤4 mm	0		Up to 2×	3–5 min
	3D T1w Post	Sagittal/ axial	3D	2100	Min	1100	10°–15°	≥172	≥172	≥1	256	≤1.5 mm	0		No	5–10 min

Note: Table based on Ellingson, Benjamin M et al. "Consensus recommendations for a standardized Brain Tumor Imaging Protocol in clinical trials." Neuro-oncology vol. 17,9 (2015): 1188–98. doi:https://doi.org/10.1093/neuonc/nov095.

Table 2
MRI techniques and their implications in clinical practice.

MRI Technique	Clinical Utility and Findings
T1	Anatomic MRI assesses the structure of tissues.
Pre-contrast	Hyperintensity caused by mineralization, blood products, or lipids
Post-contrast	Illustrates a non-specific breakdown of the BBB
T2/FLAIR	Anatomic MRI assesses the structure of tissues. "Hite matter injury," hyperintensity in peritumoral edema, non-enhancing tumor, and gliosis
DWI	Brownian motion of water molecules; an ADC map may be generated. High signal intensity (decreased diffusion) in regions of increased cellularity caused by tumors, cytotoxic edema, or postoperative injury
SWI	Sensitive to tissue susceptibility to magnetic fields Blood products produce a hypointense appearance, while calcification causes a hyperintense appearance.
DSC	Critical parameter: cerebral blood volume Elevated blood volume is indicative of either a more advanced tumor grade or a recurrence of the tumor.
DCE	The primary metric is K^{trans}, which quantifies capillary permeability. High permeability indicates a higher tumor grade.
ALS	Critical parameter is cerebral blood flow. Elevated blood flow is indicative of a tumor of a more advanced grade. Not necessitating contrast.
MRS	Assess the biochemical and metabolic profile of the tumor HGG has Cho, NAA, and Cho/Cr ratios that are greater than LGG.

Note: MRI – magnetic resonance imaging; BBB – blood-brain barrier; FLAIR – Fluid attenuated inversion recovery; DWI – diffusion-weighted imaging; ADC – apparent diffusion coefficient; SWI – Susceptibility-Weighted Imaging; DSC – dynamic susceptibility contrast; DCE – dynamic contrast-enhanced; ASL – arterial spin labeling; MRS – magnetic resonance spectroscopy; HGG – High grade gliomas; Cho – Choline; NAA – N-acetylaspartate; Cr – Creatine; LGG – low-grade gliomas.

findings.

2.2. T1 pre- and post-gadolinium and T2/T2 FLAIR sequences

The main functions of structural MRI in the initial assessment of brain tumors are to identify the precise lesion's location for treatment or biopsy planning, assess the mass effect of the tumor on the brain, ventricular system, and blood vessels [19].

T1 weighted image is a primary pulse sequence used in MRI. Utilizing short echo time (TE) and repetition time (TR) durations enables the production of T1-weighted images. The tissue's T1 properties mostly determine the contrast and brightness of the image [20].

T2 relaxation, also called spin-spin relaxation or transverse relaxation, is the progressive dephasing of spinning dipoles, leading to a decrease in magnetization in the transverse plane. T2-weighted images are generated by utilizing longer TE and TR. The contrast and brightness in these images are mostly influenced by the T2 characteristics of the tissue. The degree of T2 decay that a tissue experiences is contingent upon many circumstances. Every tissue possesses an inherent T2 value, however, extrinsic variables such as magnetic field inhomogeneity can diminish the T2 relaxation time. The additional effect is detected using T2* imaging [21].

The FLAIR sequence closely resembles a T2-weighted, with the exception that uses an inversion pulse to null out signal from the cerebrospinal fluid (CSF) in the final images. By employing this method, abnormalities remain bright, while the regular cerebrospinal fluid is reduced and become dark. This sequence holds high sensitivity to pathological conditions, facilitating the distinction between CSF and many abnormalities [19,22–24].

2.3. DWI MRI

DWI is extensively utilized in the field of neuro-oncology. MRI scan, which includes DWI sequences, should be performed within 48–72 h following surgery. This is important not only for evaluating the amount of the surgical removal, but also for identifying any local complications, such as postoperative ischemia [25].

DWI is a method that utilizes magnetic field gradients (b-values) to detect and measure the movement of molecules. The fundamental idea behind DWI based on signal decay resulting from water moving along field gradients. The signal strength is reduced depending on motion direction and magnitude. Therefore, DWI quantifies the movement of unbound water molecules caused by Brownian motion (Fig. 1). Water molecules diffuse relatively freely in the extracellular space; their movement is significantly restricted in the intracellular space. Greater water diffusivity results in a reduced initial T2* signal [26].

Quantifying diffusion can serve as an indicator of pathology as the water movement is influenced by factors that impact the microstructure, including cellularity, viscosity, and tortuosity of the extracellular environment [27]. For instance, diffusion, rapidly become restricted in ischemic brain tissue. During ischemia, the sodium - potassium pump shuts down and sodium accumulates intracellularly. Water then shifts from the extracellular to the intracellular space due to the osmotic gradient. As water movement becomes restricted intracellularly, this results in a bright signal on DWI. Thus, DWI is an extremely sensitive method for detecting acute stroke [28].

DWI may be obtained at varying levels of diffusion sensitization by modifying the crucial parameters, namely the amplitude and duration of the applied diffusion sensitization gradient. These parameters can encode various tissue attributes into DWI data while regulating the level of diffusion weighting in the resulting image. The sensitivity of the obtained DWI is represented by the b-value, which is quantified in units of seconds per square millimeter (s/mm^2). The b-value is directly related to both the time and the square of the amplitude of the applied diffusion sensitization gradient [29].

The evaluation of water molecule diffusion inside tissues is qualitatively determined using trace DWI, while quantitatively analyzed by using the apparent diffusion coefficient (ADC) parameter [29]. Furthermore, ADC is seen as an indicator of cellular density [30,31].

Recent advancements in time-dependent diffusion MRI, particularly the use of oscillating gradient spin echo (OGSE) diffusion MRI, have shown great promise in differentiating tumor types and evaluating pre-treatment and post-treatment gliomas. Time-dependent diffusivity at short diffusion times, as measured by OGSE, can characterize tissue microstructures in glioma patients. For instance, biopsy-confirmed solid enhancing tumors in high-grade glioblastoma show distinct diffusion characteristics compared to low-grade astrocytoma at the same OGSE frequency. Additionally, in post-treatment patients, enhancing lesions diagnosed with tumor progression exhibit different diffusion profiles compared to those with treatment effects, which helps in identifying infiltrative tumors and evaluating intra-tumoral volume fraction (cellular density) [32].

2.3.1. DTI

DTI is a key component of modern MRI approaches in glioma diagnosis. DTI assesses the magnitude and direction of water diffusion in tissues and allows for detailed visualization of the brain's white matter structure. This enables the mapping of neural pathways and the identification of brain areas that may be involved or threatened by the developing glioma [33].

Various metrics of DTI are employed for quantitative analysis. Mean diffusivity (MD) and fractional anisotropy (FA) are the most often utilized measures in DTI. MD is used to measure the rate of diffusion of water molecules, which is important for classifying tumors based on their cellularity. The cellularity of gliomas has an inverse relationship with the MD value [34,35]. The FA offers insights into the integrity of white matter. Reduced fractional anisotropy (FA) values may suggest increased penetration of malignant cells into the white matter, a characteristic commonly seen in more advanced gliomas. The additional

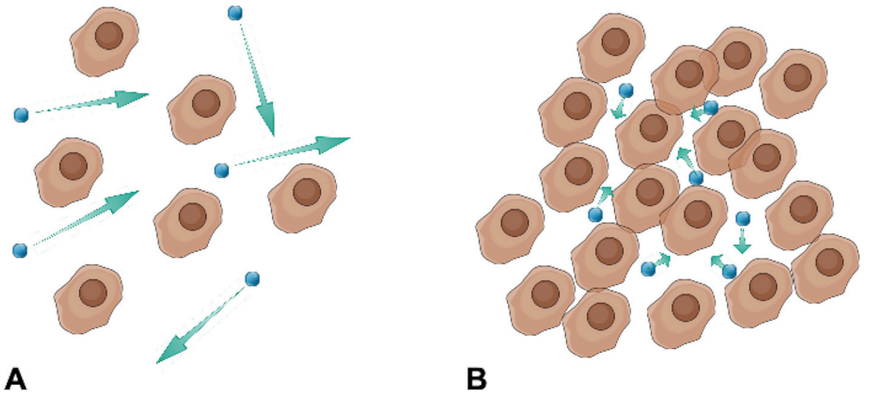

Fig. 1. Brownian movement of unbound water molecules. **A.** Free diffusion. The motion of water molecules (represented by blue dots) is comparatively unimpeded in a hypocellular environment, where the vast majority of the molecules freely diffuse in the extracellular space. It would appear that the voxel has a high apparent diffusion coefficient (ADC). **B.** Restricted diffusion. Frequent collisions between water molecules and cell membranes occur in hypercellular environments, such as viable tumors. The restriction of water molecule mobility is quantified as a low ADC within the voxel. (For interpretation of the references to color in this figure legend, the reader is referred to the web version of this article.)

fundamental metrics that quantify the shape of the DT are: axial diffusivity (DA), which characterizes diffusion primarily along the direction associated with the largest eigenvalue; radial diffusivity (RD), which indicates diffusion constrained to the plane formed by the two eigenvectors with the two largest eigenvalues [36–39]. DTI can also assist in surgical planning by allowing a better understanding of the relationship between the tumor and critical functional areas of the brain [40]. Fig. 2 provides a visual comparison between lower-grade (G2) and higher-grade (G4) gliomas, emphasizing the distinct MRI characteristics and diffusion metrics that reflect underlying pathological differences, particularly in axonal and myelin integrity.

In light of these capabilities, DTI is gaining importance as a tool for enhancing diagnostic precision in neurological oncology, opening new pathways in the understanding and treatment of gliomas.

In addition to conventional mono b-value DWI and diffusion tensor imaging (DTI), advanced diffusion imaging techniques such as diffusion kurtosis imaging (DKI), ultra-high b-value DWI, and intravoxel incoherent motion (IVIM) DWI provide valuable information for the preoperative evaluation of gliomas. DKI extends the analysis by quantifying non-Gaussian water diffusion, providing insight into tissue complexity and heterogeneity. Ultra-high b-value DWI enhances the sensitivity to tissue microstructural changes, allowing for better differentiation between tumor grades. IVIM DWI separates diffusion and perfusion components, offering a more comprehensive assessment of tumor vascularity and cellularity. These advanced techniques enhance the accuracy and specificity of glioma characterization, aiding in better treatment planning and prognosis [41,42].

2.4. Susceptibility-weighted imaging (SWI)

SWI is an MR sequence that visualizes variations in the magnetic field susceptibility and T2* differences across surrounding tissues [43]. Magnetic susceptibility is the measure of a material's ability to become magnetized when exposed to an external magnetic field. The sequence enables the assessment of substances such as deoxyhemoglobin in venous blood, iron accumulation in the brain, or calcium, hence providing crucial diagnostic information [44]. SWI images are produced by analyzing data obtained by an approach that involves using high-resolution (3.0 T) imaging, a long TE, full-flow correction, and a 3D gradient-echo. The obtained MR data is analyzed to identify variations in susceptibility among components present in tissues, including ferromagnetic materials (such as iron), paramagnetic substances (such deoxyhemoglobin and blood clots), and diamagnetic compounds (such as calcium) [45]. When magnetic fields are applied to calcium, which is diamagnetic, it appears bright on imaging. On the other hand, paramagnetic blood products look dark on imaging. SWI is the suitable method for imaging microhemorrhages due to its specific characteristics. This becomes especially important when differentiating between regions of necrosis or bleeding following radiation therapy [44,46,47]. The capacity of SWI to detect calcium on imaging can also assist in predicting tumor histology and/or grade before pathological confirmation, especially in cases when a CT scan has not been acquired. Intratumoral calcification, characterized by regions of reduced signal intensity, is predominantly observed in oligodendrogliomas, but can also occur in gangliogliomas, pilocytic astrocytomas, and ependymomas [47–49]. Moreover, there are studies that indicate that SWI can aid in distinguishing between brain abscess and necrotic glioblastoma in situations when it is challenging to identify them using T1 post-contrast imaging [50].

One parameter that is easily noticeable on SWI, as opposed to conventional MRI, is intra-tumoral susceptibility signal (ITSS) [51]. ITSS refers to regions within tumors that exhibit poor signal gathering or scattering, appearing either as linear or dot-like formations. Three categories of ITSS were classified based on their morphological characteristics: a cluster of dot-like formations, a cluster of fine linear formations, and the mixed formation. Thus, the ITSS grading method relied on the quantification of linear or dot-link structures seen in the largest cross-section of tumors on SWI. The grading scheme was as follows: Grade 0 indicates the absence of ITSS. Grade 1 represents the presence of 1–5 dot-like or fine linear ITSS. Grade 2 indicates the presence of 6–10 dot-like or fine linear ITSS. Grade 3 indicates the presence of 11 dot-like or fine linear ITSSs.

Prior research indicates that ITSS can serve as a tool to evaluate both the malignancy grade and the genetic characteristics of the tumor. Additional successful applications of SWI to distinguish glioma from other lesions have been identified in a study by Lai et al.. They successfully differentiated abscesses from necrotic gliomas using SWI and ADC, either separately or in combination.

2.5. PWI

PWI is an imaging technique used in MRI that allows the assessment of perfusion, or blood flow, in brain tissues. PWI is particularly useful in diagnosing and monitoring diseases and conditions that affect blood flow in the brain, such as stroke, brain tumors and neurodegenerative diseases. PWI is now seeing significant growth in its range of applications as it investigates the correlation between imaging parameters and the molecular features of gliomas in a noninvasive manner [52].

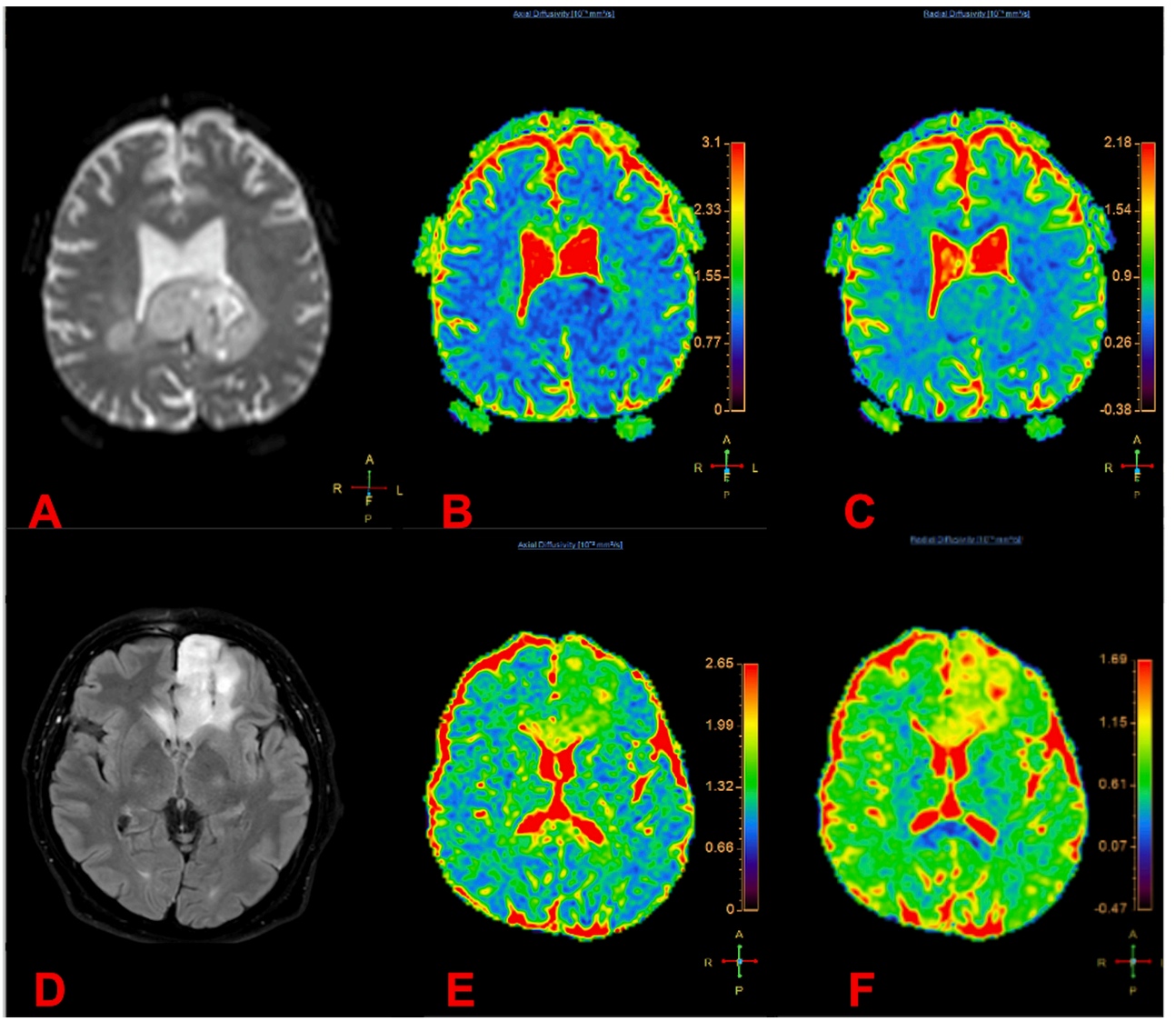

Fig. 2. Comparative MRI Analyses of Oligodendroglioma (G2) vs. Glioblastoma (G4). A-C. MRI scans of a patient diagnosed with Oligodendroglioma, Grade 2. A. T1-weighted post-gadolinium contrast image highlighting tumor contrast enhancement. B. Axial Diffusivity (AD) map indicating diffusion magnitude parallel to axonal fibers. Lower AD values may suggest axonal damage, reduced diameter, or a decrease in the parallel orientation of axons. C. Radial Diffusivity (RD) map illustrating diffusivity perpendicular to axonal fibers, typically associated with myelin alterations, indicating potential demyelination or dysmyelination processes. D–F. MRI scans of a patient diagnosed with Glioblastoma. D. Fluid-Attenuated Inversion Recovery (FLAIR) image showcasing the extensive infiltration and edema associated with high-grade gliomas. E. AD map for the glioblastoma case, serving a similar function as in panel B but applied to a more aggressive tumor type. F. RD map for the glioblastoma case.

According to the NCCN guidelines PWI can be valuable in distinguishing the tumor grade or differentiating between a tumor and radiation necrosis. The region with the greatest perfusion would be the optimal site for biopsy.

PWI approaches, such as dynamic contrast-enhanced (DCE) MRI, dynamic susceptibility contrast (DSC) MRI, and arterial spin labeling (ASL) MRI, have shown great promise as effective imaging biomarkers for managing gliomas, since they can offer insights into vascular hemodynamics [5,53]. PWI may be conducted using commonly accessible MRI scanners equipped with strong gradients and echo-planar (EPI) capabilities. This should be consider as a standard element of the imaging evaluation of brain tumors.

PWI relies on analyzing the time-intensity curve generated by the changes in susceptibility caused by the first passage of a GBCA bolus through the bloodstream, utilizing an EPI sequence (Fig. 3). The introduction of the contrast agent leads to a temporary signal loss, which is directly related to the amount of gadolinium in each voxel. This allows for the extraction of hemodynamic information from the perfusion scans. The signal intensity curve is utilized to estimate the Cerebral Blood Flow (CBF), the Cerebral Blood Volume (CBV), the Time-to-Peak (TTP), the Time of Arrival (ToA), and the Mean Transit Time (MTT) of the contrast-agent on a voxel-by-voxel basis. Following the administration of gadolinium, a thorough analysis of the time-intensity curve is conducted on a pixel-by-pixel basis. These data are then utilized to construct the relative perfusion maps [54].

2.5.1. DCE

DCE is a prominent approach in MRI perfusion. It determines perfusion parameters by analyzing the reduction in T1 relaxation time caused by the passage of a gadolinium-based contrast bolus through

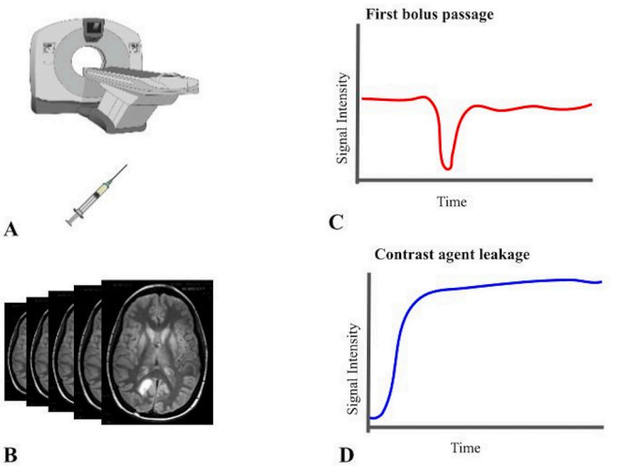

Fig. 3. Perfusion MRI. A. For PWI, a contrast agent is administered by intravenous injection. B. Following administration, repetitive image acquisition is performed, and the signal intensity for each pixel in the brain is plotted. C. Using a series of rapid scans, DSC provides the signal intensity curve—which can be utilized to approximate the CBV for individual pixels—during the initial passage of the contrast agent injection through the brain vasculature. D. DCE also involves the injection of a contrast agent into the bloodstream. However, it quantifies the signal strength in the brain tissue for an extended duration in order to map the leakage of contrast agent across the blood-brain barrier (K^{trans}).

tissue [55].

The principal application of DCE is to evaluate contrast agent leakage across the blood-brain barrier (BBB). The BBB is compromised in brain tumors due to neovascularization, which occurs when immature vessels form without the normal tight junctions that support the barrier; also, the endothelial barrier is directly impacted by dysregulation of growth factor release, pericytes, and immune responses [56].

DCE is frequently employed to characterize tumor microvasculature by capturing a fraction of extracellular extravascular space (EES), blood perfusion, and vessel permeability. By measuring the contrast arrival time, time to peak, maximum intensity, AUC, wash-in slope, and also wash-out rate, it is possible to semi-quantitatively evaluate the signal. Conversely, a quantitative analysis can be attained through the implementation of tracer kinetic models [57]. The extended Tofts model, which posits that the contrast tracer is distributed between two compartments—the intravascular space and the extravascular space—and undergoes a bidirectional exchange across the blood vessel wall—is the most commonly utilized model in tumor assessment [58]. The volume transfer constant (K^{trans}), the reflux exchange rate (Kep) from the EES to the blood plasma, the volume fraction of EES (Ve), and the volume fraction of plasma (Vp), can all be numerically estimated using the model. K^{trans}, the volume transfer constant that represents vascular permeability, is the DCE parameter most frequently employed in the context of glioma [59].

2.5.2. DSC

DSC is a commonly utilized method for assessing blood volume. It involves detecting the reduction in signal intensity on T2*-weighted sequences caused by the passage of a bolus of GBCA through a network of small blood vessels [55,60].

An intravenous injection of GBCA is administered, followed by rapid sequential imaging of the tissue, often the brain, during the first circulation of the contrast agent (Fig. 3). This leads to a series of images with the signal in each voxel representing intrinsic tissue T2/T2* signal attenuated by susceptibility-induced signal loss proportional to the amount of contrast primarily in the microvasculature [55,60]. Once an image has been acquired, the signal of a specific region is analyzed throughout the perfusion sequence in order to generate a signal intensity-time curve (Fig. 3).

This curve serves as a basis for calculating parameters such as CBV, CBF, and MTT. After obtaining these values, color maps of regional perfusion can be generated.

DSC can be helpful in distinguishing between cerebral metastases and glioblastoma [55,61]. The utility stems from underlying differences in the vascularity of metastases and primary brain tumors. Firstly, there can be substantial changes in the blood vessel distribution of the tumor component. Metastases lack a discernible BBB due to the similarity of their vessel structure to that of the host tissue. On the other hand, glioma vessels, even if they often present as abnormal, sometimes tend to remain intact BBB [61]. Second, the histological examination of the brain tissue surrounding metastases reveals normal vascularity. The absence of an enhancing high T2 signal can be attributed to vasogenic edema. As an alternative, the non-enhancing region of elevated T2 signal surrounding a glioma frequently corresponds to a non-enhancing tumor, which consequently possesses aberrant blood vessels [61].

CBV refers to the amount of blood present in a specific quantity of brain tissue, typically measured in milliliters of blood per 100 g of brain tissue [60]. Measuring CBF in absolute terms is usually challenging, therefore instead, relative CBF (rCBF) is computed by comparing it to normal white matter. The calculation of CBV involves evaluating the integral of the concentration-time curve, which can be derived from signal intensity-time curves obtained by techniques such as DSC or other methods. The calculation of absolute CBV using the approach described above is contingent upon two specific pharmacokinetic conditions: (a) the absence of contrast recirculation, and (b) the absence of capillary permeability. The first issue can be rectified by evaluating only the initial iteration of contrast. The second issue is more challenging due to the significant variability in permeability. In most cases, the calculation is focused on determining the CBV in relation to an internal control due to the challenges involved. Therefore, it is commonly known as relative CBV (rCBV) and is dimensionless, as it represents a mere ratio. However, the determination of rCBV can be hampered by the extravasation of GBCA due to a disturbed BBB, which is a frequently occurring situation in brain tumors. Although the "leakage effect" goes against the notion of GBCA vascular compartmentalization, DSC can still be effectively utilized to estimate brain tumor rCBV provided this leakage effect is taken into account [62–64]. Two recommended approaches for data gathering on brain tumors utilizing DSC have been established by a recent consensus [65]. The first entails providing a pre-dose of GBCA to mitigate the potential effects of T1 leakage. This is then followed by a second dose with a flip angle of either 30° or 60°, depending on the strength of the magnetic field. The second approach does not require a pre-dose, but instead utilizes a low flip angle and echo times that vary depending on the field strength. Both necessitate a suggested interval of repeat of 1000–1500 msec and incorporate a post-processing method for rectifying the leakage of contrast agent [63,66–68].

2.5.3. ASL

ASL is an alternative approach to MR perfusion that does not involve the administration of contrast agent intravenously. Hence, it is a non-invasive and non-ionizing MRI technique. ASL is a highly appropriate technique for implementation in pediatrics, where the utilization of radioactive tracers might be restricted. It is also safe to use in patients with allergies, impaired renal function or those who require serial follow-up [69].

The ASL technique utilizes an inversion pulse placed near the imaging area to magnetically determine the arterial blood water. Following a short delay, referred to as the post-labeling delay, an image is acquired in the brain that is influenced by the circulation of inverted spins in the blood. Obtained images are subtracted from control images that contain equivalent static tissue signals. The resulting CBF maps are constructed by averaging many control-label pairings. The disparity between an image acquired with and without this labeling eliminates

the tissue signal and retains only the signal from the incoming blood, enabling the measurement of the volume of labeled blood delivered to each voxel [70]. Several repeats of the measurement are required to obtain an adequate signal. The remaining signals are linear measures of the perfusion, which is proportionate to the CBF [71].

The ASL SNR is significantly low due to the fact that the signals originating from the tagged blood represent only 0.5–1.5% of the overall tissue signals. ASL capture utilizes EPI imaging due to its superior SNR. EPI can cause distortions in areas with strong magnetic fields. ASL capture has lately incorporated 3D sequences in order to enhance the SNR and minimize image distortion. In clinical practise it is necessary to get ASL data prior to administering GBCA, as gadolinium can induce T1 shortening, resulting in a reduction of detectable signals in both the labeled and controlled images [69,71].

ASL has demonstrated remarkable consistency, both within and between sessions that are separated by days to months. Various studies have demonstrated the significance of ASL in the process of diagnosing, assessing the tumor grade, and planning for surgery [72]. The ability of ASL to differentiate glioma from metastases, primary CNS lymphoma, and nonneoplastic brain lesions is highly diagnostic, as is typically based on detection increased blood flow in glioma [73,74].

2.6. MR spectroscopy (MRS)

Magnetic resonance spectroscopy (MRS) is used to gather data on the composition of metabolites. Sophisticated spectroscopic techniques have been employed to measure various indicators of tumor metabolism, such as glucose levels. Additionally, markers of membrane turnover and proliferation, such as choline (Cho), as well as indicators of energy homeostasis, such as creatine (Cr), are quantified. MRS also allows for the assessment of intact glioneuronal structures (*N*-acetylaspartate [NAA]) and the presence of necrosis (lactate [Lac] or lipids) [75].

The brain is a heterogeneous organ composed of various regions that possess distinct functions and structures. Consequently, the level of metabolites in healthy individuals differs across age groups and regions of the typical human brain [76]. According to the NCCN guidelines, MRS can be valuable in distinguishing between a tumor and radiation necrosis, as well as in grading tumors or evaluating their response. In addition, the most abnormal area in MRS would be the optimal location to focus on for a biopsy.

An MRS examination yields a spectrum that can be graphically represented as a relationship between signal intensity and frequency. The MR spectrum can be acquired through two distinct spectroscopic methods, which vary in accordance with the characteristics of the volume of interest (VOI) or sampled volume. Single-voxel spectroscopy (SVS) samples an MRS signal from a single, well-defined volume component - voxel. Conversely, multiple voxel spectroscopy acquires concurrently multiple MR spectra from adjacent spatial regions [77].

Chemical Exchange Saturation Transfer (CEST) imaging is a unique molecular MR method that permits the visualization of specific compounds at concentrations that are negligible in terms of affecting the contrast of conventional MR imaging and insufficient to be directly discernible in MRS at the resolution typically associated with water imaging [78]. The most explored form of CEST imaging is amide proton transfer (APT) [79]. APT has demonstrated effective application in imaging protein concentration and pH, with the latter being feasible owing to the amide proton exchange rate's significant dependence on pH. APT is demonstrating clinical promise, particularly in the characterization of brain tumors and the differentiation of treatment effects from recurrent tumors [80].

3. Predicting the malignancy of gliomas using MRI

3.1. Contrast enhancement

Gliomas can exhibit contrast enhancement due to either BBB disruptions or increased permeability of blood vessels. The BBB in glioma patients frequently sustains damage or exhibits aberrant morphology, facilitating the infiltration of GBCA from the bloodstream into the adjacent tumor tissue. Additionally, gliomas induce angiogenesis to facilitate nutrient supply through the formation of new blood vessels. Vessels that are newly developed in frequently exhibit irregularities and heightened permeability, hence facilitating the infiltration of contrast agents. Furthermore, gliomas have significant heterogeneity, indicating that various regions of the tumor may display varying levels of contrast enhancement. Moreover, tumors have the ability to provoke localized edema and inflammatory reactions within the brain. These disease circumstances can additionally compromise the integrity of the BBB, leading to an increased permeability of tissues to contrast agents. Extravasation of the contrast agent causes a decrease in T1 relaxation time and an increase in signal intensity (known as "contrast-enhancement") on T1-weighted imaging [81,82]. Thus, contrast enhancement of the solid area of a tumor in T1W images is frequently associated with the severity of the lesions [83].

High-grade gliomas (HGG) lead to abnormal growth of blood vessels and tissue death, which in effect causes the BBB to disrupt and allows GBCA to flow from the blood vessels into the brain [19,23,82]. However, regarding glioblastoma, it is widely recognized that malignant cells infiltrate also beyond contrast enhancing regions on T1 imaging [84].

Due to their slower growth and intact BBB, low-grade gliomas (LGG) show less enhancement on T1 post-contrast images. Therefore, the T2/FLAIR sequence is crucial for evaluating these tumors as well as regions of swelling and tumor development that extend beyond the CE areas on T1 images, which are indicative of HGG [85–87]. While LGG contrast enhanced it frequently exhibit a patchy or wispy appearance, which may suggest the presence of malignant transformation [88,89]. On the other hand, it is important to acknowledge that a significant number of LGG exhibit this enhancement. On the other hand, lack of contrast enhancement on MRI studies does not equate with low-grade tumors, and one-third of gliomas that do not demonstrate enhancement are malignant [19,85,90,91]. Furthermore, the likelihood of anaplasia occurring in non-enhancing lesions on MRI is notably higher as the patient's age increases. Consequently, when it comes to tumors that do not show improvement, it is often challenging to assess the grade of the tumor before surgery using traditional MRI. Consequently, contrast enhancement alone is not a reliable method for evaluating the malignancy of gliomas.

The ability of FLAIR to display areas of increased water content with prolonged transverse relaxation is valuable for visualizing peritumoral edema. This refers to the region surrounding the contrast-enhancing tumor core in HGG, which contains infiltrating tumor cells and higher levels of extracellular water due to plasma fluid leakage from abnormal tumor blood vessels [5,92–94]. T2/FLAIR imaging is important for guiding the surgical removal of HGG because it helps identify non-enhancing regions of infiltrative illness [82,95,96].

3.2. Diffusion techniques in predicting the malignancy of gliomas

An important parameter obtained during DWI used to assess the malignancy of the tumor is ADC. The ADC value corresponds to the motion of water molecules within the tissues. A higher ADC score may indicate a lower grade of glioma due to the increased intercellular space in lower grade tumors, which facilitates greater mobility of movement for water molecules (Fig. 5). Hence, when it comes to the preoperative quantitative evaluation of glioma using DWI, the ADC values have the potential to indicate both the density of tumor cells and the extent of the tumor.

ADC values were effectively utilized to distinguish between LGG and HGG. The analysis, which included 15 trials, yielded a summarized sensitivity of 0.85, and specificity of 0.80. Additionally, the summary receiver operating characteristic (ROC) curve-based AUC was calculated to be 0.9 [97]. The increased density of cells in anaplastic neoplasms leads to decreased ADC values. However, they also exhibit elevated levels of tissue death and fluid accumulation in the brain, along with increased ADC [30,98]. Hence, it is crucial to assess the tumor rather than the necrosis.

Advanced approaches, such as Diffusion Kurtosis Imaging (DKI) and Intravoxel Incoherent Motion (IVIM) imaging, have been utilized in preoperative imaging for neuro-oncology. More precisely, the mean kurtosis (MK) values obtained by DKI were utilized for the purpose of grading. It has been demonstrated that higher glioma malignancy is associated with an increase in MK values [99,100]. Moreover, studies have shown that both axial kurtosis and radial kurtosis values were higher in cases of HGG compared to LGG. This highlights the potential use of MK for classifying gliomas according to the WHO grades 2–4 and predicting Ki-67 as a measure of cellularity [101].

3.2.1. DTI

DTI has shown promise in glioma grade assessment. A study conducted by et al. on glioma patients who underwent DTI found significant differences in MD of the solid tumoral part between LGG and HGG. The best cutoff value for MD of the tumoral part was 1.42×10^3 mm^2/s, with an accuracy of 91.4% [102].

The peri-tumoral region is also a key site for distinguishing tumor types in DTI features due to structural changes and edema grade differences between LGG and HGG. MD and anisotropic metrics show significant differences between LGG and HGG, with LGG showing no or mild vasogenic edema and HGG showing evident edema. Moreover, peritumoral regions exhibited a notable decrease in FA values of HGG when compared to LGG. This reduction may be related to alterations in tubular anisotropy [103].

The study found that over half of the LGG samples had a white matter tract displacement pattern, followed by infiltration, with a combination of infiltration and disruption accounting for 10% of the total pattern. In contrast, 25% of HGG samples had an infiltration pattern, 23% had an "infiltration and disruption" combination, and 6% had more than two patterns [104].

3.3. SWI MRI techniques in the assessment of malignancy of gliomas

The glioma microenvironment reflects the biological features of tumor lesions. SWI sequences provide high sensitivity in detecting blood and vascular structures, enabling the visualization of microhemorrhages and neoangiogenesis that are not detectable on standard MRI sequences.

Statistical analyses reveal notable disparities in hemorrhage occurrence in small blood vessels and microvessels among gliomas of varying grades. Higher tumor grades correspond to a higher prevalence of small blood vessels and hemorrhage within the tumor. Consequently, the greater the grade of a glioma, the higher its ITSS grade [105]. Kong et al. found significant ITSS grade differences between HGG and LGG. LGG had significantly lower ITSS grades than HGG [106].

3.4. Perfusion techniques in the malignancy assessment of gliomas

3.4.1. DCE

Malignant gliomas exhibit a significant increase in angiogenesis, resulting in atypical vascular anatomy, irregular blood flow, and heightened permeability in the vessels. The potential of DCE-driven parameters as markers of angiogenic activity in gliomas has been studied, and they are now being utilized for tumor monitoring [107]. A comprehensive systematic analysis synthesized findings from research on the discriminating between LGG and HGG using DCE parameters. The study found that all of these investigations exhibited significant specificity and sensitivity in regards to the examined factors, indicating a high level of diagnostic precision in distinguishing between LGG and HGG (AUC 0.96) [108].

Research is ongoing to investigate the compatibility of rCBV measurements in single-dose and double-dose contrast injection perfusion examinations for gliomas. An up-to-date study conducted by Jain et al. found that using a single dose of contrast medium in DCE is equally successful as using a double-dose procedure for grading gliomas using 3 T MRI [109].

3.4.2. DSC

One of the most crucial roles of preoperative rCBV obtained during DSC is to assist in establishing an accurate diagnosis, as the gliomas' heterogeneity can result in misinterpretation and underestimated assessment [110]. Moreover, it has been demonstrated that brain tumor rCBV is useful in identifying the optimal locations for surgical biopsy [111].

Research has demonstrated that rCBV can serve as a reliable indicator of the glioma grade [62,112–114]. Both the preoperative measurement of blood volume within the tumor (intra-tumoral rCBV) and the measurement of blood volume surrounding the tumor (peri-tumoral rCBV) were found to be reliable in distinguishing between HGG and LGG. This differentiation was made with remarkable sensitivity and accuracy [115]. HGG (WHO grades 3 and 4) have been found to have a greater rCBV compared to LGG (WHO grades 1 and 2) [51,90,116]. Previous research has proposed a suitable cut-off value of 1.75 for rCBVmax [90,117]. Moreover, rCBV can assist in distinguishing between gliomas of WHO grade 2 and 3. The study conducted by Delgado et al. found that the average difference in relative maximal CBV between glioma grades 2 and 3, with a sample size of 727, was 1.76 (95% CI, 1.27–2.24; $p = 0.001$) [118].

The rCBV maps have demonstrated superior sensitivity compared to other imaging techniques in early tumor growth prediction. They are particularly sensitive to minor regional changes, exceeding conventional MR imaging, PET, and single photon emission computed tomography (SPECT) [111,119,120].

Moreover, there is a more powerful correlation between the maximal rCBV and the malignant grade defined by the WHO compared to the contrast enhancement observed in morphologic MR imaging [90,121,122]. It is crucial to acknowledge that the use of the area of interest- (ROI-) based method to acquire rCBV is not effective in grading oligodendrogliomas. This is because oligodendrogliomas show increased rCBV levels regardless of their grade [30]. The use of histogram analysis to calculate rCBV provides a more objective and dependable approach to assess the severity of glioma compared to methods that rely on ROI. It has the potential to measure the degree of tumor heterogeneity and differentiate between oligodendroglioma and other LGG [121,123]. Law et al. conducted a study to assess the effectiveness of histogram evaluation in grading gliomas by comparing the perfusion parameters acquired from ROI and histogram rCBV analysis. In the end, they postulated that utilizing histogram analysis would offer a reliable and unbiased method for measuring perfusion data in cerebral gliomas [121]. In a separate investigation, Law et al. determined that histogram analysis of rCBV is equally beneficial as maximum rCBV analysis in correlating with the grade of glioma. Nevertheless, histogram analyses are more suitable for inexperienced operators as they can achieve perfusion measures that are comparable to those achieved by experienced operators using ROI analysis [121].

3.4.3. ASL

Two meta-analyses have shown that ASL can be effective in differentiating between HGG and LGG. The highest level of blood flow in the tumor compared to healthy tissue on the opposite side has been found to provide the most accurate differentiation [74,124,125]. HGG commonly displays elevated perfusion and vascularity, which aligns with the increased metabolic activity of the tumor tissue. Additionally, it

demonstrates an elevated signal on ASL imaging. On the other hand, LGG often exhibits decreased blood flow, except for cases of pilocytic astrocytoma and ganglioglioma [72,73].

A study conducted by Flies et al. aimed to explore the effectiveness of ASL in detecting malignant progression in patients with LGG before it becomes visible on T1w-MRI. A significant association was found between ASL positivity and malignant progression within 12 months in LGG, even after stratifying for radiotherapy and assessing IDH-mutational status. Patients with LGG and positive ASL should be considered at high risk for malignant progression [126].

3.5. MRS

Spectroscopy combined with other advanced imaging techniques can improve diagnostic accuracy and be helpful in distinguishing between LGG and HGG by analyzing the Cho/Cr, NAA/Cr, and particularly Cho/NAA ratios [127]. Furthermore, 1H-MRS has been proposed as a method to distinguish between high- and low-grade oligodendrogliomas [128]. HGG exhibit metabolic alterations, including decreased levels of NAA, reduced Cr, and lower MI. Additionally, there is an increase in lactate levels that is proportional to the volume of the necrotic lesion, as well as restricted water diffusion [129,130]. APT CEST can also be used to differentiate between LGG and HGG. The presence of higher protein levels in glioma relative to the surrounding tissues, as well as the rapid exchange of protons inside cells, results in an elevated APT level [131]. Regrettably, this methodology is not universally accessible at all institutions and its use on a broad scale poses significant challenges.

Table 3
The clinical applications of the molecular subtypes in gliomas as they are discussed in this review.

Imaging Modality	Feature	Molecular marker	
T1	Contrast enhancement	*EGFR* amplification	↑
		IDH1 mutant 1p/19	
T2/FLAIR	T2/FLAIR mimatch	noncodeleted glioma	
DSC	rCBV	*EGFR* amplification	↑
DSC	rCBV	*TERTp* mutation	↑
DSC	rCBV	*MGMT* methylation	↓
DSC	rCBV	*IDH1* mutation	↓
DCE	K^{trans} and Ve	*IDH1* mutation	↓
DCE	K^{trans}	*MGMT* methylation	↑
DCE	Vp	*TERTp* mutation	↑
DCE	K^{trans} and Vp	*EGFR* amplification	↑
ASL	CBF	*IDH1* mutation	↓
ASL	CBF	*p53*	↓
ASL	CBF	*MGMT* methylation	↓
DWI	ADC	*IDH1* mutation	↑
DWI	ADC	*MGMT* methylation	↑
DWI	ADC	*EGFR* amplification	↓
DWI	ADC	*H3F3A K27*	↓
DWI	FA	*IDH1* mutation	↓
SWI	ITSS	*IDH1* mutation	↓
SWI	ITSS	*MGMT* methylation	↓
MRS	2HG	*IDH1* mutation	↑
MRS	NADPH, GSH, Glu, Gln, NAA	*IDH1* mutation	↓

Note: EGFR – epidermal growth factor receptor; MGMT – The O6-methylguanine-DNA methyl-transferase; FLAIR – Fluid attenuated inversion recovery; IDH – Isocitrate dehydrogenase; DSC – Dynamic susceptibility contrast; rCBV – Relative Cerebral Blood Volume; K^{trans} – volume transfer constant; Ve – volume fraction of extracellular extravascular space; Vp – volume fraction of plasma; CBF – Cerebral blood flow; DCE – Dynamic contrast enhanced; ASL – Arterial spin labeling; DWI – Diffusion-weighted imaging; ADC – Apparent diffusion coefficient; ITSS – Intratumoral Susceptibility Signal; SWI – Susceptibility weighted imaging; MRS – Magnetic resonance spectroscopy; 2HG – 2-Hydroxyglutarate; NADPH – Nicotinamide adenine dinucleotide phosphate; GSH – Glutathione; Glu – glutamate; Gln – glutamine; NAA – N-acetylaspartate; Cho – choline.

4. Assessment of genetic alterations using MRI

Table 3 provides a summary of the clinical applications parameters derived from MRI discussed in this review that pertain to predicting molecular subtypes in gliomas.

4.1. Contrast enhancement

Contrast enhancement on conventional MRI can be valuable not only for evaluating the level of tumor malignancy, but also for evaluating molecular features (Fig. 6). Prior research has demonstrated a correlation between elevated contrast enhancement volume and enhancement/necrosis ratio on conventional MRI scans and the presence of *EGFR* overexpression [132,133]. The likelihood of detecting EGFRvIII mutation was higher when there was an increased ratio of T2 intensity to enhancing volume [134]. The findings suggest that the presence of aberrant blood vessel formation and the ability of tumors to receive blood supply and allow substances to pass through may be indicative of the status of the *EGFR* gene.

Contrast enhancement can also be employed to forecast the presence of *MGMT* methylation. Hypermethylated *MGMT* tumors exhibit a mixed-nodular enhancement, and lesions outside the temporal lobe [135]. In contrast, tumors with unmethylated *MGMT* exhibit a high prevalence of temporal lobe lesions and ring enhancement [136].

4.2. T2/FLAIR mismatch

The T2/FLAIR mismatch sign refers to the MRI presentation of a T2-hyperintense lesion that appears hypointense on FLAIR imaging. The radiogenomic signature is regarded as a very specific indicator for astrocytomas IDH-mutant gliomas with intact 1p19q, distinguishing them from other LGG [137,138]. A 2021 meta-analysis demonstrated that the identification of tumors with IDH-mutant, 1p19q non-codeleted status had a pooled specificity of 100%. However, the pooled sensitivity was just 42% [139].

A study conducted by Lee et al. demonstrated that including the T2/FLAIR mismatch sign with the ADC or CBV histogram parameters enhances the detection of IDH-mutant, 1p19q-noncodel diffuse LGG. The study population was categorized into three groups based on molecular subtype: IDH-mutant 1p19q-codel, IDH-wildtype, and IDH-mutant 1p19q-noncodel. The presence of a positive visual T2/FLAIR mismatch sign and increased CBV skewness were found to be significant factors in distinguishing the IDH-mutant 1p19q-noncodel group from the other two groups. The AUC for this distinction was 0.88, with a 95% CI of 0.81–0.96. A lower ADC value was a crucial factor in differentiating the IDH-mutant 1p19q-noncodel group from the IDH-wildtype group, with an AUC of 0.75 and a 95% CI ranging from 0.62 to 0.89. The inclusion of ADC or CBV histogram characteristics to the T2/FLAIR mismatch sign enhanced the accuracy in differentiating IDH-mutant 1p19q-noncodel from the other two groups (AUC 0.882 vs. AUC 0.810) or from IDH-wildtype (AUC 0.923 vs. AUC 0.868) [140].

4.3. Diffusion MRI techniques in the molecular evaluation of gliomas

The ADC results showed a notable increase in IDH-mutant gliomas compared to IDH-wildtype gliomas (Fig. 4) [141]. The evaluation of ADC values in various brain parenchyma and tumor regions has been examined. In patients with IDH-mutant tumors, the ADC values were notably higher in the tumor tissue compared to the surrounding areas of the tumor. However, in patients with IDH-wildtype tumors, there were no significant variations in ADC values between the tumor tissue and the surrounding areas of the tumor [142]. Additionally, a greater level of spatial variability has been noticed in unmethylated *MGMT* tumors that show contrast enhancement [83,143,144].

ADC values were effectively utilized in a multi-center investigation to predict the *EGFR* amplification status of IDH-wildtype WHO grade

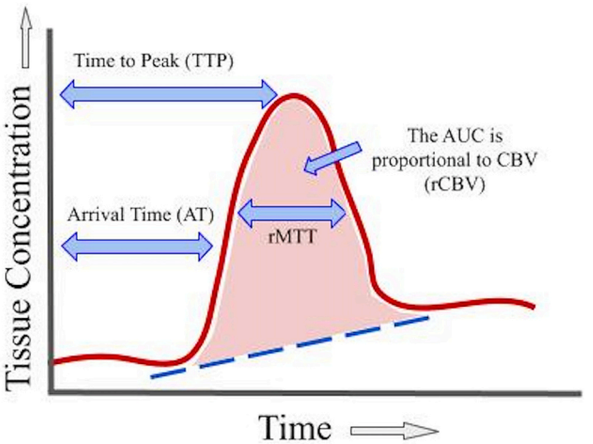

Fig. 4. Schematic of DSC perfusion time-intensity curve. Gadolinum-chelate tissue concentration is on the Y-axis and time on the X. Essentially, the area under the curve is proportional to the relative cerebral blood volume (CBV) in the voxel. The most typically utilized parameters are arrival (AT) and peak (TTP). Full width and half maximum concentration is relative mean transit time (rMTT).

2–3 gliomas. Which is crucial according to the new classification, because *EGFR* amplification in the case of an IDH-wildtype grade 2–3 tumor classifies it as a tumor with the highest degree of malignancy. More precisely, a decrease in the ADC and the lower 5th percentile of ADC values showed potential as imaging biomarkers for identifying *EGFR* amplification in glioma without *IDH* mutation [145]. A recent study conducted by Park et al. found that tumors with *EGFR* amplification had lower mean ADC levels compared to tumors without *EGFR* amplification ($p = 0.019$). The average ADC value was found to be a reliable indicator of *EGFR* amplification, with an AUC of 0.75 [146].

The ADC of the tumor in the H3 K27-altered group was lower (7.83×10^{-4} mm^2/s) than the corresponding values in the no H3 K27-altered group (13.5×10^{-4} mm^2/s) [147]. A separate study examined the diffuse midline glioma *H3 K27*-altered and found that decreased ADC values in non-enhancing regions may be associated with the normal expression of *ATRX* [148].

4.3.1. DTI

Diffusion tensor imaging has demonstrated potential value in the molecular evaluation of glioma. Previous studies proved DTI distinguishes the *IDH* genotype of gliomas. In all the adult-type diffuse gliomas, the average and minimum MD values of the IDH-wildtype group were significantly lower than those of the IDH-mutant group ($p < 0.001$) [149].

In addition, studies have examined the potential to assess *IDH* mutation status utilizing the maximal FA and the ratio of maximal FA (rmFA). The results showed that there were significant differences in these measures between IDH-mutant oligodendroglial tumors and those without *IDH* mutation. The patients with *IDH1/2* mutations had lower maximal FA and rmFA values compared to the patients without *IDH1/2* mutations. The AUC values for maximal FA and the ratio of maximal FA were 0.79 and 0.82, respectively [150].

4.4. SWI MRI in the molecular assessment of gliomas

A study conducted by Kong et al. found that the ITSS grade had a substantial impact on predicting both the pathological grade and the

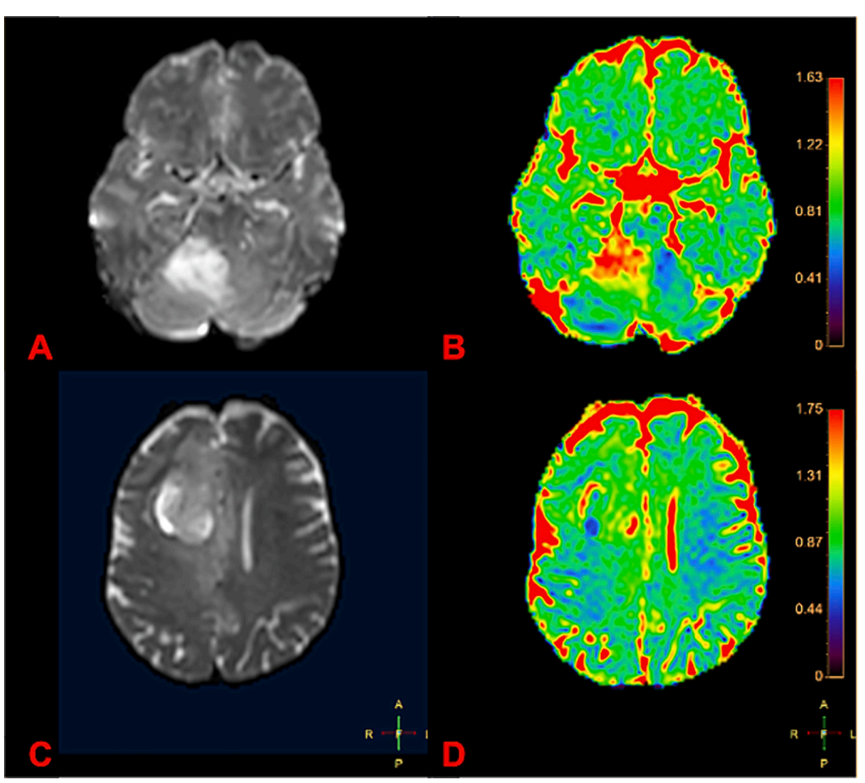

Fig. 5. ADC value can assist in glioma grade forecasting. A higher ADC score may indicate a lower grade of glioma. A-B. A patient diagnosed with Glioblastoma (G4); molecular characteristics: *IHD1*-wt, *MGMT* methylated, *EGFR* amplification, *CDKN2A* homozygous deletion, 1p19q non-codeleted, *TERT* pathogenic variant. A. DWI. B. ADC map. C—D. A patient diagnosed with Astrocytoma (G2); molecular characteristics: *IHD1*-mt, *MGMT* methylated, *EGFR* non-amplification, *CDKN2A* non-deleted, 1p19q non-deleted, no *TERT* pathogenic variant. A. DWI. B. ADC map.

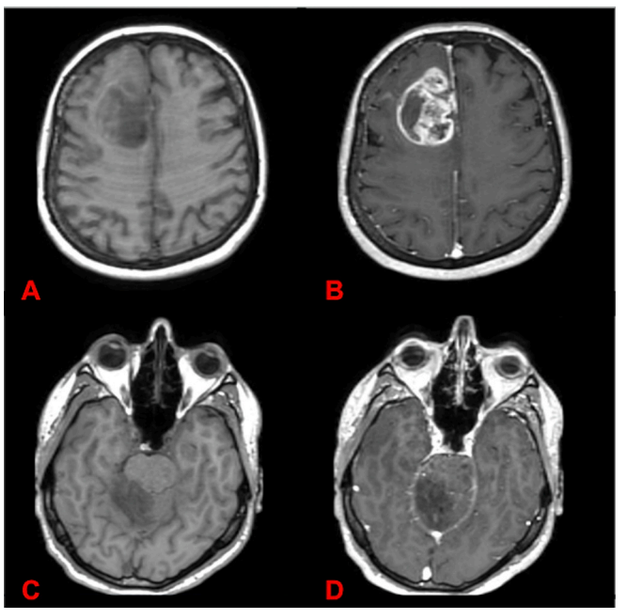

Fig. 6. Contrast enhancement can also be employed to forecast glioma grade and some of vital genetic alteration. A-B. A patient diagnosed with Glioblastoma (G4); molecular characteristics: *IHD1*-wt, *MGMT* methylated, *EGFR* amplification, *CDKN2A* homozygous deletion, 1p19q non-codeleted, *TERT* pathogenic variant. A. T1-pre Gadolinum contrast. B. T1-post Gadolinum contrast - contrast enhanced lesion. C—D. A patient diagnosed with Astrocytoma (G2); molecular characteristics: *IHD1*-mt, *MGMT* methylated, *EGFR* non-amplification, *CDKN2A* non-deleted, 1p19q non-deleted, no *TERT* pathogenic variant. A. T1-pre Gadolinum contrast. B. T1-post Gadolinum contrast - non-enhancing lesion after contrast administration.

expression status of *IDH1* and *MGMT*. The optimal cut-off value to predict *IDH1* status was shown to be 2.5, with a sensitivity of 75%, specificity of 83.6%, and an AUC of 0.80. Similarly, the best cut-off value to predict *MGMT* methylation status was found to be 2.5, with a sensitivity of 80%, specificity of 76.5%, and an AUC of 0.79. Nevertheless, the ITSS grade did not demonstrate a substantial impact in accurately predicting the expression status of 1p19q (AUC = 0.58) [106]. Therefore, the ITSS grades of gliomas with *IDH1* mutations and *MGMT* methylation were markedly lower than those of IDH-mutant *MGMT* unmethylated gliomas.

Ozturk et al. conducted a study to analyse SWI and DWI to differentiate atypical glioblastoma and primary CNS lymphoma. They found that glioblastomas IDH-wildtype had lower rSWI values than astrocytoma IDH-mutant grade 4 and PCNSL. Moreover, combining ADC and SWI effectively differentiated astrocytoma grade 4 with *IDH1* mutations, achieving a sensitivity of 94.3% and a specificity of 100% [151].

The multicenter study conducted by Saini et al. discovered that utilizing a combination of rCBV and SWI-derived ITSS enhanced the precision of diagnosing grade 2/3 gliomas as distinct from grade 4 gliomas [152].

4.5. MRI perfusion techniques in the molecular evaluation of gliomas

4.5.1. DSC

DSC perfusion imaging is highly useful for the molecular assessment of gliomas. Prior studies have established multiple associations between imaging characteristics acquired during DSC and various significant genetic alterations vital for the categorization of tumors (Fig. 7).

Some prior studies observed a significant decrease in CBV values in IDH-mutant glioblastomas compared to IDH-wildtype glioblastomas [153,154]. The presence of *IDH* mutation has been related to resistance against the angiogenesis. This association may provide an explanation for the observed CBV values in glioblastomas with *IDH* mutation [155].

Tykocinski et al. found that the rCBV was significantly elevated in glioblastoma cases that were positive for the *EGFRvIII* mutation, as compared to those who were negative for the mutation. The acquired rCBV threshold value of 4.34 on a 1.5 T system demonstrated both 100% sensitivity and specificity [156]. Moreover, Gupta et al. examined the association between *EGFR* amplification and preoperative DSC measures, specifically rCBV, permeability-surface area product (PSR), and relative peak height (rPH). It was observed that glioblastoma with *EGFR* amplification exhibited a larger median rCBV and a lower PSR. Additionally, there was a correlation between a higher median rPH and the presence of *EGFRvIII* mutation [157]. Additional studies have also

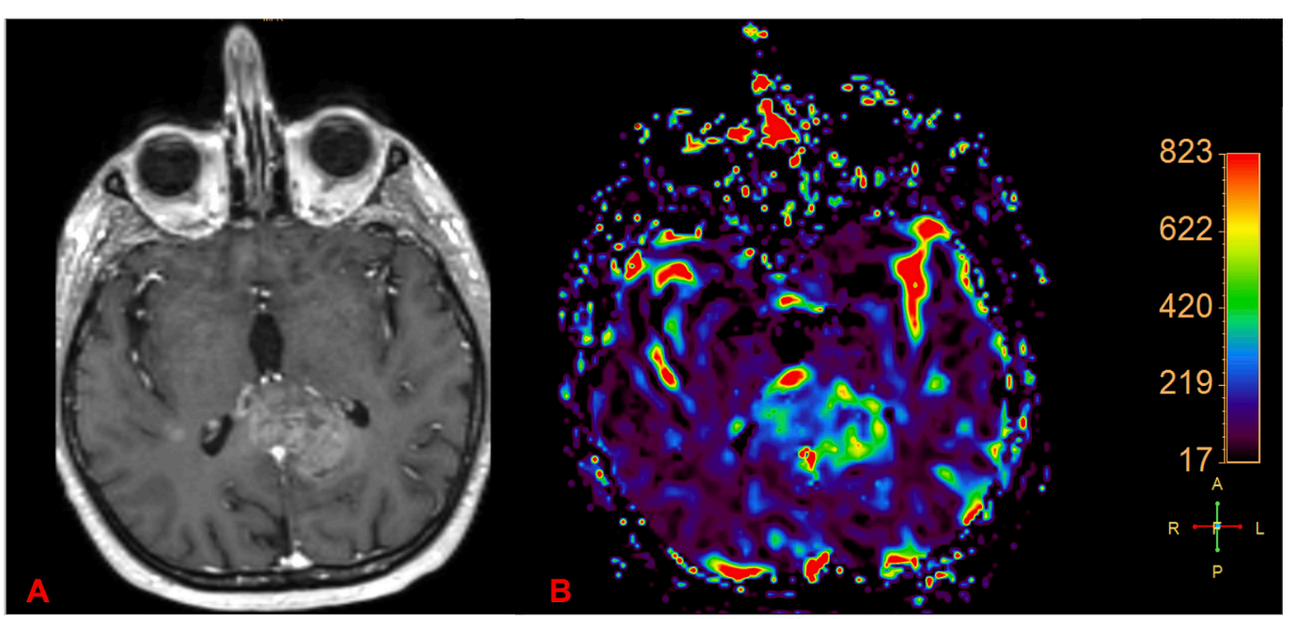

Fig. 7. MRI examination of a patient diagnosed with Glioblastoma (G4). Molecular characteristics: *IHD1*-wt, *MGMT* unmethylated, *EGFR* amplification, *CDKN2A* homozygous deletion, 1p19q non-codeleted, *TERT* pathogenic variant. Imaging analysis: rCBV = 10.7; rCBF = 6.3. A. T1 post-contrast. B. DSC MRI - CBV map.

confirmed that *EGFR* abnormality is associated with angiogenesis, leading to an increase in CBV, CBF, plasma volume, and contrast transfer coefficient in MR perfusion [129,158,159].

Another crucial factor to take into account concerning genetic modifications in the CNS5 is the *TERTp* mutation, which may be evaluated by PWI. Tumors with *TERTp* mutations exhibited significantly increased average CBV ($p = 0.020$) and average CBF ($p = 0.017$) compared to *TERTp* wildtype tumors [146]. Jung et al. examined the relationship between CBV and the status of the *MGMT* promoter. The glioblastoma with *MGMT* methylation exhibit decreased CBV, demonstrating a sensitivity of 73.3% and specificity of 85.7% for differentiation [160]. Furthermore, the presence of raised relative CBV in gliomas with 1p/19q codeletions indicates an increased formation of new blood vessels (neovascularity) in tumors that contain oligodendroglial components [161].

4.5.2. DCE

Recent studies have shown that DCE-driven parameters can assist in the initial assessment of some molecular characteristics that are currently used to classify glioma tumors, such as *IDH* mutation, *TERT* promoter mutation, *EGFR* amplification, or *MGMT* methylation.

Hu et al. observed significant statistical disparities in the histogram characteristics of K^{trans} and Ve between gliomas with *IDH* mutations and those without *IDH* mutations [162]. In addition, Zhang et al. observed that glioblastoma with *MGMT* methylation exhibited a notably elevated $K^{trans,}$ suggesting that *MGMT* methylation might have a role in the angiogenesis associated with glioma, which is characterized by vasculatures with high endothelial permeability [59]. A study conducted by Park et al. found that *TERTp* mutant tumors had a higher mean Vp (0.12 versus 0.06, $p = 0.002$) compared to *TERTp* wildtype tumors. In the context of multivariate logistic regression analysis, the average Vp value emerged as the sole predictor of *TERTp* mutation status, exhibiting an AUC value of 0.85 [146]. Furthermore, Arevalo-Perez et al. assessed the capacity of DCE to indicate the presence of EGFRvIII expression in patients with glioblastoma. EGFRvIII-positive glioblastoma exhibited a notable rise in both K^{trans} and Vp mean/histogram values. Furthermore, Vp demonstrated superior predictive capability compared to K^{trans} [159].

4.5.3. ASL

ASL has been found to be predictive of *IDH1*, *MGMT* promoter methylation, and *p53* status. Decreased blood flow is reported in relation to *IDH1* and *MGMT*. Moreover, *p53* mutant tumors exhibit reduced blood flow. Moreover, ASL seems to be associated with tumor microvascular density and VEGF production [163–166].

For instance, a recent study by Yoo et al. assessed the effectiveness of ASL in predicting molecular biomarkers and survival in patients with glioblastoma. The CBF was markedly elevated in the IDH-wildtype group compared to the IDH-mutant group ($p = 0.013$), and in the *MGMT* unmethylated group compared to the methylated group ($p = 0.047$). The AUC were 0.678 for *IDH* mutation ($p = 0.022$) and 0.601 for *MGMT* promoter methylation ($p = 0.043$) [164].

However, further research is required to investigate the precise categorization of gliomas using ASL.

4.6. MRS in the molecular assessment of gliomas

Recent studies using 1H-MRS/I have focused on glioma with mutations in the IDH enzyme that may cause accumulation of the oncometabolite 2HG. A review conducted by Suh et al. estimated that the pooled sensitivity and specificity of 2HG diagnostic scores for predicting IDH-mutated glioma were 95% and 91%, respectively [167]. Moreover, in instances when the IDH-mutant status is ambiguous, the presence of 2HG has enhanced the accuracy of the diagnostic process [168]. Alongside increased 2HG, IDH-mutant gliomas presented decreased levels of NADPH, GSH, Glu, and Gln, as well as higher mI, and NAA. >88% of IDH-mutant gliomas have been identified using these metabolic markers in combination [169]. HGG demonstrates metabolic alterations, such as decreased NAA, Cr, and MI concentrations. Additionally, an increase in lactate concentrations proportional to the volume of the necrotic lesion and a restriction in water diffusion are observed and associated with *EGFR* amplification, overexpression, or mutation [101,170–172]. An additional unfavorable prognostic indicator in CNS5 WHO 2021 is the mutation in *TERTp*. Recent research suggests that gliomas that are exclusively *TERTp* can be distinguished with an exceptional 92.6% accuracy rate by analyzing the levels of total Cho, Glu, and Gln complex (Glx) [169].

5. Progression vs pseudoprogression

The exact cause of pseudoprogression is not well understood, although it is believed that the inflammation of epithelial cells and tissue, together with edema and abnormal vascular permeability, may be triggered by the combination of chemotherapy and radiation [173,174]. The clinical definition of pseudoprogression lacks clarity, since some studies suggest that the lesion must exhibit no symptoms of advancement for a minimum of 6 months, while others recommend a 2-month delay following the initial scan to confirm the diagnosis of pseudoprogression [174]. This disparity could potentially account for the significant divergence in the documented occurrence of this phenomena. A recent meta-analysis revealed that the combined occurrence rate of pseudoprogression in individuals with newly diagnosed glioblastoma was 36% (95% CI 33–40), although tumor progression was observed in 60% of cases.

According to the Response Assessment in Neuro-Oncology (RANO) criteria, tumor growth occurring within 12 weeks after radiotherapy can only be detected through imaging if there is new tumor enhancement outside of the radiation region [175]. Indicators of real progression discussed in other articles consist of the expansion of T2/FLAIR signal beyond the area that received radiation, as well as the expansion of the corpus callosum, a signal that crosses the midline, and the involvement of the subependymal region [176–178]. Serial imaging conducted over a period of time can be used to differentiate between pseudoprogression and actual tumor recurrence. Pseudoprogression on consecutive imaging is defined by the gradual decrease in signal or volume of post-contrast enhancement [24]. Nevertheless, this approach may have limitations since the after-effects of treatment gradually increase, typically throughout the initial 3–6 months following postoperative radiation therapy, necessitating multiple sequential scans until eventually regresing. Inaccurate identification of pseudoprogression can result in unnecessary surgery, premature discontinuation of a beneficial treatment, or the use of unnecessary chemotherapy drugs [179].

It is crucial to acquire MRI scans shortly after surgery (specifically, within 48 h) to accurately distinguish between pseudoprogression and actual progression. This is necessary to prevent any misleading factors that may affect the signal strength or augmentation on future MRI scans, such as tissue ischemia. Nevertheless, the majority of studies indicate that the ability of anatomic MR sequences to accurately predict progression of HGG is limited, with sensitivity and specificity rates of just 68% and 77%, respectively. Hence, further imaging techniques such as PWI, DWI, and MRS can be utilized to assist in the diagnosis [180].

PWI is commonly employed to facilitate the differentiation between recurrence and treatment efficacy. Recurrent HGG shows elevated rCBV values compared to the effects of radiation therapy after treatment [181,182]. Progressive disease showed elevated rCBV and reduced PSR, whereas pseudoprogression displayed decreased rCBV and rPH [183–187]. Due to the notable variability of tumors and the extensive alterations in vascular structures caused by chemoradiation, the use of the ROI-based method to measure rCBV is subjective and inadequate for accurately describing the complete tumor characteristics. The percentage changes in skewness and kurtosis of CBV histograms were highly effective in predicting the early tumor progression. Additionally, the

histographic pattern of CBV showed the highest level of independent predictive accuracy [188].

In the context of possible pseudoprogression, DWI/ADC imaging is beneficial. Tumor progression is associated with lower ADC values compared to pseudoprogression. This is likely because genuine tumors have a more cellular nature, while pseudoprogression is characterized by edema caused by the inflammatory response [189,190].

Moreover, DTI can be utilized in differentiation between progression and pseudoprogression. In a study conducted by Wang et al. FA, linear anisotropy coefficient, and planar anisotropy coefficient and decreased spheric anisotropy coefficient were observed in true progression compared with pseudoprogression ($p < 0.05$) [191]. Furthermore, according to a number of studies, pseudoprogression displays greater MD values from the enhanced region than tumor preogression, in part because of the degree of vascular alterations and cellular death in pseudoprogression [189,192].

A comprehensive meta-analysis conducted by Charalampos Tsakiris et al. examined the distinction between actual tumor development of glioblastoma and pseudoprogression utilizing DWI and PWI. The analysis included 24 studies and a total of 900 participants. DWI had slightly higher sensitivity and specificity compared to PWI. The sensitivity of DWI was 0.88 (95% CI 0.83–0.92) and the specificity was 0.85 (95% CI 0.78–0.91). In contrast, the sensitivity of PWI was 0.85 (95% CI 0.81–0.89) and the specificity was 0.79 (95% CI 0.74–0.84). The study specifically examined cases of individuals who experienced pseudoprogression within 6 months after completing concurrent chemoradiotherapy [193].

Emphasizing the distinctions between pseudoprogression and radiation necrosis is crucial, as these are separate clinical phenomena. The primary distinction lies in the timing of occurrence, with pseudoprogression often manifesting 3–6 months following the conclusion of chemoradiotherapy, while radiation necrosis arises 6 months to several years after treatment. The duration between treatment and identification of radiation necrosis varies depending on the radiotherapy method, with carbon ion therapy exhibiting a longer lag compared to proton or photon therapy [194]. Distinguishing between glioma recurrence and radiation necrosis remains a significant difficulty. The two entities have distinct prognoses, although frequently exhibit similar symptoms and characteristics in conventional morphologic imaging such as CT and MRI [195].

Utilizing thresholds that are specific to each study, PWI parameters distinguish viable tumors from radiation necrosis with a reasonable degree of sensitivity and specificity. In aggregate, the most frequently assessed parameters, rCBVmean and rCBVmax, as well as in the pseudoprogression subgroup where sensitivity and specificity values are primarily within the range of 80–90%, exhibit comparable accuracy between the highest performing DSC and DCE parameters from each study. The pooled sensitivities and specificities of the highest performing parameter in each method, DSC and DCE, were 95% and 88% (95% CI: 0.85–0.94; 0.83–0.92) and 89% and 85% (95% CI 0.78–0.96; 0.77–0.91), respectively. The two parameters most frequently assessed in the literature - mean rCBV (threshold range: 0.9–2.15) and maximum rCBV (threshold range: 1.49–3.1) - were pooled to determine sensitivity and specificity. The respective ratios were 93% and 76% (95% CI: 0.86–0.98; 0.66–0.85) and 88% and 88% (95% CI: 0.81–0.94; 0.78–0.95) [182]. Okuchi et al. evaluated the application of DCE in distinguishing between recurrence and necrosis after radiotherapy, based on data from 9 trials involving 298 patients. The combined sensitivity, specificity, and AUC for distinguishing tumor relapse from treatment-related changes were 0.88, 0.86, and 0.89, respectively [108].

DWI is also useful for distinguishing between recurrent glioblastoma and radiation treatment effects due to the contrasting cell density observed in these two conditions. Recurrent glioma tumors often exhibit high cell density, while areas affected by treatment alterations show low cell density. The result of this is that the genuine glioma recurrence groups exhibit lower ADC values compared to the pseudoprogression and post-radiation alterations groups [196].

CBV, as evaluated by DCE employing the deconvolution approach, has the potential to provide comparable or superior assessment when compared to fluorodeoxyglucose-positron emission tomography (FDG-PET) for differentiating purposes [197]. The utilization of a CBV threshold of 2.0 ml/100 g allowed for the accurate identification of regressing lesions, achieving a sensitivity and specificity rate of 100%. Furthermore, when DTI and DSC were used together, the evaluation of features such as ADC and rCBV led to enhanced discrimination, especially in the lesions exhibiting higher rCBV and lower ADC values [198].

MRS can also be employed to distinguish glioma from the effects of therapy. Specifically for HGG, MRS reveals an increased Cho/Cr ratio in regions where tumor recurrence occurs, as opposed to regions affected by radiation-induced necrosis or therapeutic effects. Furthermore, there have been documented variations in Cho/NAA ratios between recurring tumor and regions affected by radiation-induced necrosis [199]. A meta-analysis conducted by Zhang et al. demonstrates that MRS by itself has modest diagnostic accuracy in distinguishing between glioma recurrence and radiation necrosis. This is achieved by analyzing metabolite ratios such as Cho/Cr and Cho/NAA. The quantitative synthesis of investigations revealed that the combined sensitivity and specificity for the Cho/Cr ratio were 0.83 (95% CI: 0.77, 0.89) and 0.83 (95% CI: 0.74, 0.90) respectively. The combined sensitivity and specificity for the Cho/NAA ratio were 0.88 (95% CI: 0.81, 0.93) and 0.86 (95% CI: 0.76, 0.93), respectively. The AUC curve was 0.9185. It is highly advisable for MRS to integrate additional modern imaging technologies in order to enhance diagnostic precision [200].

Although advanced imaging techniques are superior than anatomic MRI in differentiating between pseudoprogression, therapeutic effect, and genuine progression, their accuracy and effectiveness are constrained. Consequently, surgical biopsy with histological examination is frequently required to validate the diagnosis [201].

6. Limitations and challenges

Although there have been technical advancements, there are still difficulties related to visualizing gliomas [202]. A significant obstacle is the absence of thorough validation for sophisticated MRI-derived biomarkers. Although there are suggestions for accelerate the progress of imaging biomarkers in brain tumors, there is a lack of regulatory certifications or well-defined protocols that have been implemented into practice. Furthermore, variations existed in the administration of GBCA, including preload, dynamic bolus, injection dose and rate, and timing. Advanced sequences beyond traditional structural MRI may include specialized hardware and/or software, as well as the need for devoted expertise in acquisition, post-processing, and evaluation [203–205]. This makes advanced imaging of gliomas time-consuming and frequently necessitates manual data management and specialized, custom-built pipelines.

Furthermore, they also exhibited variations in the methodologies employed to address contrast leakage and recirculation correction for DSC imaging. Hu et al. conducted a study where they evaluated rCBV using various acquisition and postprocessing methods. They discovered that the accuracy of the diagnostic results differed depending on whether contrast preloading and baseline subtraction procedures were employed. This highlights the need of optimizing these variables for the purpose of DSC imaging [206]. However, multiple factors affect optimization, including type of contrast agent, incubation time, pulse-sequence parameters, and correction algorithm, which limits comparison of quantitative metrics across studies.

It is important to acknowledge that perfusion parameters are unavoidably affected by different hemodynamic conditions, types of GBCAs, and the overall duration of the acquisition. For instance, K^{trans} is defined by the rate of blood flow and the PSR. When there is a large level of leakage or when low-molecular-weight contrast agents are used, K^{trans} is mostly determined by blood flow. Insufficient temporal precision

during the acquisition process might lead to inaccuracies in K^{trans} estimation, causing an underestimation.

Furthermore, the comparability among research is also constrained by factors such as the size, number, location, and technique of identification of ROIs. Normalization to contralateral white matter exhibited variability across DCE and DSC experiments [206,207]. Moreover, a notable factor contributing to the diversity observed among research was the extensive range of criteria that were assessed. The DSC metric that is most frequently assessed, normalized rCBV, varied depending on whether mean, maximum, or histogram-derived percentile values were used. DCE parameters exhibited comparable levels of variability, encompassing certain semi-quantitative metrics (such as the maximum rate of enhancement during the initial vascular phase and the ratio of the initial AUC). These metrics are unlikely to be suitable for routine utilization unless integrated into automated commercial software [208,209].

Lastly, several studies have used PWI to differentiate between pseudoprogression and progression in glioblastoma. However, the cut-off values for specific parameters that indicate the presence of each condition vary across different institutions. This is due to the small sample sizes used in these studies, as well as the lack of standardized imaging protocols and consistent inclusion criteria for participants.

7. Future directions

The future directions in glioma diagnostics and treatment are poised to be significantly influenced by the integration of advanced MRI techniques and the expanding field of radiogenomics. As we move forward, a key focus will be on enhancing the precision and accessibility of DWI and PWI. These techniques, when combined with rapidly evolving molecular diagnostics, have the potential to revolutionize personalized medicine in neuro-oncology. Future research should aim at standardizing MRI protocols and developing automated, AI-driven analysis tools to ensure consistency and accuracy across different clinical settings. Additionally, there's an emerging need to explore non-invasive methods for real-time monitoring of tumor progression and treatment response, potentially through the development of novel biomarkers detectable by advanced imaging modalities.

Looking ahead, one of the most promising aspects of these advancements in MRI technology is the potential to initiate chemotherapy or radiotherapy based on advanced MRI results. This approach could significantly shorten the time required to obtain a reliable diagnosis, allowing for quicker intervention and potentially improving patient outcomes. Currently, the time gap between initial imaging and the start of treatment can be critical, especially in fast-progressing gliomas. By enabling the initiation of therapy based on sophisticated MRI findings, we could see a paradigm shift in how quickly patients receive essential treatment.

However, it is crucial to note that more research is needed to further confirm the correspondence between MRI findings and genetic changes in gliomas. This research will play a pivotal role in validating the use of advanced MRI techniques as a reliable stand-alone diagnostic tool in the clinical setting. Once there is stronger evidence of this correlation, it could lead to international societies such as the National Comprehensive Cancer Network (NCCN) or the European Association of Neuro-Oncology (EANO) issuing new recommendations. These guidelines would allow oncologists to base their treatment decisions on advanced MRI results, paving the way for more timely and targeted interventions in glioma management.

8. Conclusions

In conclusion, MR scans have revolutionized the management of glioma patients. The integration of advanced MRI techniques, such as DWI and PWI, alongside the advancements in radiogenomics, marks a significant leap forward in the diagnostics and management of gliomas. These technologies offer a deeper understanding of tumor biology and enable more precise and personalized treatment strategies. However, challenges such as the standardization of MRI protocols and the interpretation of complex imaging data remain. Overcoming these hurdles necessitates collaborative efforts among researchers, clinicians, and technologists. As we move forward, continued innovation and research in this field are essential to fully realize the potential of advanced imaging techniques in enhancing glioma patient care, potentially transforming prognosis and treatment efficacy in neuro-oncology.

Funding

This research received no external funding.

Ethics approval

This is a review article. No ethical approval is required.

Informed consent

This is a review article. No Informed consent is required.

CRediT authorship contribution statement

Paulina Śledzińska-Bebyn: Writing – review & editing, Writing – original draft, Visualization, Resources, Project administration, Conceptualization. **Jacek Furtak:** Writing – review & editing, Funding acquisition. **Marek Bebyn:** Writing – original draft, Visualization. **Zbigniew Serafin:** Writing – review & editing, Supervision, Resources, Conceptualization.

Declaration of competing interest

The authors declare no conflict of interest.

References

[1] Louis DN, Perry A, Wesseling P, Brat DJ, Cree IA, Figarella-Branger D, et al. The 2021 WHO classification of tumors of the central nervous system: a summary. Neuro-Oncol 2021;noab106. https://doi.org/10.1093/neuonc/noab106.
[2] Ellingson BM, Wen PY, Cloughesy TF. Modified criteria for radiographic response assessment in glioblastoma clinical trials. Neurother J Am Soc Exp Neurother 2017;14:307–20. https://doi.org/10.1007/s13311-016-0507-6.
[3] Stadlbauer A, Ganslandt O, Buslei R, Hammen T, Gruber S, Moser E, et al. Gliomas: histopathologic evaluation of changes in directionality and magnitude of water diffusion at diffusion-tensor MR imaging. Radiology 2006;240:803–10. https://doi.org/10.1148/radiol.2403050937.
[4] Price SJ, Jena R, Burnet NG, Hutchinson PJ, Dean AF, Peña A, et al. Improved delineation of glioma margins and regions of infiltration with the use of diffusion tensor imaging: an image-guided biopsy study. AJNR Am J Neuroradiol 2006;27:1969–74.
[5] Barajas RF, Phillips JJ, Parvataneni R, Molinaro A, Essock-Burns E, Bourne G, et al. Regional variation in histopathologic features of tumor specimens from treatment-naive glioblastoma correlates with anatomic and physiologic MR imaging. Neuro-Oncol 2012;14:942–54. https://doi.org/10.1093/neuonc/nos128.
[6] Hu LS, Eschbacher JM, Dueck AC, Heiserman JE, Liu S, Karis JP, et al. Correlations between perfusion MR imaging cerebral blood volume, microvessel quantification, and clinical outcome using stereotactic analysis in recurrent high-grade glioma. AJNR Am J Neuroradiol 2012;33:69–76. https://doi.org/10.3174/ajnr.A2743.
[7] Albert NL, Weller M, Suchorska B, Galldiks N, Soffietti R, Kim MM, et al. Response assessment in neuro-oncology working group and European Association for Neuro-Oncology recommendations for the clinical use of PET imaging in gliomas. Neuro-Oncol 2016;18:1199–208. https://doi.org/10.1093/neuonc/now058.
[8] Stupp R, Mason WP, van den Bent MJ, Weller M, Fisher B, Taphoorn MJB, et al. Radiotherapy plus concomitant and adjuvant temozolomide for glioblastoma. N Engl J Med 2005;352:987–96. https://doi.org/10.1056/NEJMoa043330.
[9] Stupp R, Hegi ME, Mason WP, van den Bent MJ, Taphoorn MJB, Janzer RC, et al. Effects of radiotherapy with concomitant and adjuvant temozolomide versus radiotherapy alone on survival in glioblastoma in a randomised phase III study: 5-year analysis of the EORTC-NCIC trial. Lancet Oncol 2009;10:459–66. https://doi.org/10.1016/S1470-2045(09)70025-7.

[10] Stupp R, Brada M, van den Bent MJ, Tonn J-C, Pentheroudakis G, ESMO Guidelines Working Group. High-grade glioma: ESMO clinical practice guidelines for diagnosis, treatment and follow-up. Ann Oncol Off J Eur Soc Med Oncol 2014; 25(Suppl. 3). https://doi.org/10.1093/annonc/mdu050. iii93–101.

[11] Chaskis C, Neyns B, Michotte A, De Ridder M, Everaert H. Pseudoprogression after radiotherapy with concurrent temozolomide for high-grade glioma: clinical observations and working recommendations. Surg Neurol 2009;72:423–8. https://doi.org/10.1016/j.surneu.2008.09.023.

[12] Śledzińska P, Bebyn MG, Furtak J, Kowalewski J, Lewandowska MA. Prognostic and predictive biomarkers in gliomas. Int J Mol Sci 2021;22:10373. https://doi.org/10.3390/ijms221910373.

[13] Horbinski C, Berger T, Packer RJ, Wen PY. Clinical implications of the 2021 edition of the WHO classification of central nervous system tumours. Nat Rev Neurol 2022;18:515–29. https://doi.org/10.1038/s41582-022-00679-w.

[14] Louis DN, Perry A, Reifenberger G, von Deimling A, Figarella-Branger D, Cavenee WK, et al. The 2016 World Health Organization classification of tumors of the central nervous system: a summary. Acta Neuropathol (Berl) 2016;131: 803–20. https://doi.org/10.1007/s00401-016-1545-1.

[15] Rutman AM, Kuo MD. Radiogenomics: creating a link between molecular diagnostics and diagnostic imaging. Eur J Radiol 2009;70:232–41. https://doi.org/10.1016/j.ejrad.2009.01.050.

[16] Narang S, Lehrer M, Yang D, Lee J, Rao A. Radiomics in glioblastoma: current status, challenges and potential opportunities. Transl Cancer Res 2016:5. https://doi.org/10.21037/tcr.2016.06.31.

[17] Singh G, Manjila S, Sakla N, True A, Wardeh AH, Beig N, et al. Radiomics and radiogenomics in gliomas: a contemporary update. Br J Cancer 2021;125:641–57. https://doi.org/10.1038/s41416-021-01387-w.

[18] Ellingson BM, Bendszus M, Boxerman J, Barboriak D, Erickson BJ, Smits M, et al. Consensus recommendations for a standardized brain tumor imaging protocol in clinical trials. Neuro-Oncol 2015;17:1188–98. https://doi.org/10.1093/neuonc/nov095.

[19] Upadhyay N, Waldman AD. Conventional MRI evaluation of gliomas. Br J Radiol 2011;84(2):S107–11. https://doi.org/10.1259/bjr/65711810.

[20] Curry TS, Dowdey JE, Murry RC. Christensen's physics of diagnostic radiology. Lippincott Williams & Wilkins; 1990.

[21] Allisy-Roberts PJ, Williams J. Farr's physics for medical imaging. Elsevier Health Sciences; 2007.

[22] Okuda T, Korogi Y, Shigematsu Y, Sugahara T, Hirai T, Ikushima I, et al. Brain lesions: when should fluid-attenuated inversion-recovery sequences be used in MR evaluation? Radiology 1999;212:793–8. https://doi.org/10.1148/radiology.212.3.r99se07793.

[23] Ellingson BM, Chung C, Pope WB, Boxerman JL, Kaufmann TJ. Pseudoprogression, radionecrosis, inflammation or true tumor progression? Challenges associated with glioblastoma response assessment in an evolving therapeutic landscape. J Neuro-Oncol 2017;134:495–504. https://doi.org/10.1007/s11060-017-2375-2.

[24] Li J, Liu S, Qin Y, Zhang Y, Wang N, Liu H. High-order radiomics features based on T2 FLAIR MRI predict multiple glioma immunohistochemical features: a more precise and personalized gliomas management. PLoS One 2020;15:e0227703. https://doi.org/10.1371/journal.pone.0227703.

[25] Weller M, Le Rhun E, Van den Bent M, Chang SM, Cloughesy TF, Goldbrunner R, et al. Diagnosis and management of complications from the treatment of primary central nervous system tumors in adults. Neuro-Oncol 2023;25:1200–24. https://doi.org/10.1093/neuonc/noad038.

[26] Hagmann P, Jonasson L, Maeder P, Thiran J-P, Wedeen VJ, Meuli R. Understanding diffusion MR imaging techniques: from scalar diffusion-weighted imaging to diffusion tensor imaging and beyond. Radiogr Rev Publ Radiol Soc N Am Inc 2006;26(Suppl. 1):S205–23. https://doi.org/10.1148/rg.26si065510.

[27] Hirschler L, Sollmann N, Schmitz-Abecassis B, Pinto J, Arzanforoosh F, Barkhof F, et al. Advanced MR techniques for preoperative glioma characterization: part 1. J Magn Reson Imaging 2023;57:1655–75. https://doi.org/10.1002/jmri.28662.

[28] Srinivasan A, Goyal M, Al Azri F, Lum C. State-of-the-art imaging of acute stroke. Radiogr Rev Publ Radiol Soc N Am Inc 2006;26(Suppl. 1):S75–95. https://doi.org/10.1148/rg.26si065501.

[29] Vijithananda SM, Jayatilake ML, Gonçalves TC, Rato LM, Weerakoon BS, Kalupahana TD, et al. Texture feature analysis of MRI-ADC images to differentiate glioma grades using machine learning techniques. Sci Rep 2023;13:15772. https://doi.org/10.1038/s41598-023-41353-5.

[30] Cha S. Update on brain tumor imaging: from anatomy to physiology. AJNR Am J Neuroradiol 2006;27:475–87.

[31] Sugahara T, Korogi Y, Kochi M, Ikushima I, Shigematu Y, Hirai T, et al. Usefulness of diffusion-weighted MRI with echo-planar technique in the evaluation of cellularity in gliomas. J Magn Reson Imaging 1999;9:53–60. https://doi.org/10.1002/(sici)1522-2586(199901)9:1<53::aid-jmri7>3.0.co;2-2.

[32] Zhu A, Shih R, Huang RY, DeMarco JK, Bhushan C, Morris HD, et al. Revealing tumor microstructure with oscillating diffusion encoding MRI in pre-surgical and post-treatment glioma patients. Magn Reson Med 2023;90:1789–801. https://doi.org/10.1002/mrm.29758.

[33] Le Bihan D. Diffusion, perfusion and functional magnetic resonance imaging. J Mal Vasc 1995;20:203–14.

[34] Yamasaki F, Kurisu K, Satoh K, Arita K, Sugiyama K, Ohtaki M, et al. Apparent diffusion coefficient of human brain tumors at MR imaging. Radiology 2005;235: 985–91. https://doi.org/10.1148/radiol.2353031338.

[35] Abdel Razek AAK. Diffusion magnetic resonance imaging of chest tumors. Cancer Imaging 2012;12:452–63. https://doi.org/10.1102/1470-7330.2012.0041.

[36] Alexander AL, Hasan K, Kindlmann G, Parker DL, Tsuruda JS. A geometric analysis of diffusion tensor measurements of the human brain. Magn Reson Med 2000;44:283–91. https://doi.org/10.1002/1522-2594(200008)44:2<283::aid-mrm16>3.0.co;2-v.

[37] Westin C-F, Maier SE, Mamata H, Nabavi A, Jolesz FA, Kikinis R. Processing and visualization for diffusion tensor MRI. Med Image Anal 2002;6:93–108. https://doi.org/10.1016/s1361-8415(02)00053-1.

[38] Toh C-H, Castillo M, Wong AM-C, Wei K-C, Wong H-F, Ng S-H, et al. Primary cerebral lymphoma and glioblastoma multiforme: differences in diffusion characteristics evaluated with diffusion tensor imaging. AJNR Am J Neuroradiol 2008;29:471–5. https://doi.org/10.3174/ajnr.A0872.

[39] Beppu T, Inoue T, Shibata Y, Kurose A, Arai H, Ogasawara K, et al. Measurement of fractional anisotropy using diffusion tensor MRI in supratentorial astrocytic tumors. J Neuro-Oncol 2003;63:109–16. https://doi.org/10.1023/A:1023977520909.

[40] Pierpaoli C, Jezzard P, Basser PJ, Barnett A, Di Chiro G. Diffusion tensor MR imaging of the human brain. Radiology 1996;201:637–48. https://doi.org/10.1148/radiology.201.3.8939209.

[41] Togao O, Hiwatashi A, Yamashita K, Kikuchi K, Mizoguchi M, Yoshimoto K, et al. Differentiation of high-grade and low-grade diffuse gliomas by intravoxel incoherent motion MR imaging. Neuro-Oncol 2016;18:132–41. https://doi.org/10.1093/neuonc/nov147.

[42] Kang Y, Choi SH, Kim Y-J, Kim KG, Sohn C-H, Kim J-H, et al. Gliomas: histogram analysis of apparent diffusion coefficient maps with standard- or high-b-value diffusion-weighted MR imaging—correlation with tumor grade. Radiology 2011; 261:882–90. https://doi.org/10.1148/radiol.11110686.

[43] Reichenbach JR, Venkatesan R, Schillinger DJ, Kido DK, Haacke EM. Small vessels in the human brain: MR venography with deoxyhemoglobin as an intrinsic contrast agent. Radiology 1997;204:272–7. https://doi.org/10.1148/radiology.204.1.9205259.

[44] Löbel U, Sedlacik J, Sabin N, Kocak M, Broniscer A, Hillenbrand C, et al. Three-dimensional susceptibility-weighted imaging and two-dimensional T2*-weighted gradient-Echo imaging of Intratumoral hemorrhages in pediatric diffuse intrinsic pontine glioma. Neuroradiology 2010;52:1167–77. https://doi.org/10.1007/s00234-010-0771-9.

[45] Haacke EM, Xu Y, Cheng Y-CN, Reichenbach JR. Susceptibility weighted imaging (SWI). Magn Reson Med 2004;52:612–8. https://doi.org/10.1002/mrm.20198.

[46] Li C, Ai B, Li Y, Qi H, Wu L. Susceptibility-weighted imaging in grading brain astrocytomas. Eur J Radiol 2010;75:e81–5. https://doi.org/10.1016/j.ejrad.2009.08.003.

[47] Mohammed W, Xunning H, Haibin S, Jingzhi M. Clinical applications of susceptibility-weighted imaging in detecting and grading intracranial gliomas: a review. Cancer Imaging 2013;13:186–95. https://doi.org/10.1102/1470-7330.2013.0020.

[48] Emblem KE, Scheie D, Due-Tonnessen P, Nedregaard B, Nome T, Hald JK, et al. Histogram analysis of MR imaging–derived cerebral blood volume maps: combined glioma grading and identification of low-grade oligodendroglial subtypes. AJNR Am J Neuroradiol 2008;29:1664–70. https://doi.org/10.3174/ajnr.A1182.

[49] Hsu CC-T, Watkins TW, Kwan GNC, Haacke EM. Susceptibility-weighted imaging of glioma: update on current imaging status and future directions. J Neuroimaging Off J Am Soc Neuroimaging 2016;26:383–90. https://doi.org/10.1111/jon.12360.

[50] Toh CH, Wei K-C, Chang C-N, Hsu P-W, Wong H-F, Ng S-H, et al. Differentiation of pyogenic brain abscesses from necrotic glioblastomas with use of susceptibility-weighted imaging. AJNR Am J Neuroradiol 2012;33:1534–8. https://doi.org/10.3174/ajnr.A2986.

[51] Park MJ, Kim HS, Jahng G-H, Ryu C-W, Park SM, Kim SY. Semiquantitative assessment of Intratumoral susceptibility signals using non-contrast-enhanced high-field high-resolution susceptibility-weighted imaging in patients with gliomas: comparison with MR perfusion imaging. AJNR Am J Neuroradiol 2009; 30:1402–8. https://doi.org/10.3174/ajnr.A1593.

[52] Chung C, Metser U, Ménard C. Advances in magnetic resonance imaging and positron emission tomography imaging for grading and molecular characterization of glioma. Semin Radiat Oncol 2015;25:164–71. https://doi.org/10.1016/j.semradonc.2015.02.002.

[53] Jain R. Measurements of tumor vascular leakiness using DCE in brain tumors: clinical applications. NMR Biomed 2013;26:1042–9. https://doi.org/10.1002/nbm.2994.

[54] Chaskis C, Stadnik T, Michotte A, Van Rompaey K, D'Haens J. Prognostic value of perfusion-weighted imaging in brain glioma: a prospective study. Acta Neurochir 2006;148:277–85. https://doi.org/10.1007/s00701-005-0718-9.

[55] Essig M, Shiroishi MS, Nguyen TB, Saake M, Provenzale JM, Enterline D, et al. Perfusion MRI: the five most frequently asked technical questions. AJR Am J Roentgenol 2013;200:24–34. https://doi.org/10.2214/AJR.12.9543.

[56] Hoque MM, Abdelazim H, Jenkins-Houk C, Wright D, Patel BM, Chappell JC. The cerebral microvasculature: basic and clinical perspectives on stroke and glioma. Microcirc N Y 1994;2021(28):e12671. https://doi.org/10.1111/micc.12671.

[57] Khalifa F, Soliman A, El-Baz A, Abou El-Ghar M, El-Diasty T, Gimel'farb G, et al. Models and methods for analyzing DCE-MRI: a review. Med Phys 2014;41: 124301. https://doi.org/10.1118/1.4898202.

[58] Tofts PS, Brix G, Buckley DL, Evelhoch JL, Henderson E, Knopp MV, et al. Estimating kinetic parameters from dynamic contrast-enhanced t1-weighted MRI of a diffusable tracer: standardized quantities and symbols. J Magn Reson Imaging 1999;10:223–32. https://doi.org/10.1002/(SICI)1522-2586(199909)10:3<223::AID-JMRI2>3.0.CO;2-S.

[59] Zhang J, Liu H, Tong H, Wang S, Yang Y, Liu G, et al. Clinical applications of contrast-enhanced perfusion MRI techniques in gliomas: recent advances and current challenges. Contrast Media Mol Imaging 2017;2017:7064120. https://doi.org/10.1155/2017/7064120.
[60] Petrella JR, Provenzale JM. MR perfusion imaging of the brain: techniques and applications. AJR Am J Roentgenol 2000;175:207–19. https://doi.org/10.2214/ajr.175.1.1750207.
[61] Cha S, Lupo JM, Chen M-H, Lamborn KR, McDermott MW, Berger MS, et al. Differentiation of glioblastoma multiforme and single brain metastasis by peak height and percentage of signal intensity recovery derived from dynamic susceptibility-weighted contrast-enhanced perfusion MR imaging. AJNR Am J Neuroradiol 2007;28:1078–84. https://doi.org/10.3174/ajnr.A0484.
[62] Donahue KM, Krouwer HG, Rand SD, Pathak AP, Marszalkowski CS, Censky SC, et al. Utility of simultaneously acquired gradient-echo and spin-echo cerebral blood volume and morphology maps in brain tumor patients. Magn Reson Med 2000;43:845–53. https://doi.org/10.1002/1522-2594(200006)43:6<845::aid-mrm10>3.0.co;2-j.
[63] Boxerman JL, Schmainda KM, Weisskoff RM. Relative cerebral blood volume maps corrected for contrast agent extravasation significantly correlate with glioma tumor grade, whereas uncorrected maps do not. AJNR Am J Neuroradiol 2006;27:859–67.
[64] Paulson ES, Schmainda KM. Comparison of dynamic susceptibility-weighted contrast-enhanced MR methods: recommendations for measuring relative cerebral blood volume in brain tumors. Radiology 2008;249:601–13. https://doi.org/10.1148/radiol.2492071659.
[65] Boxerman JL, Quarles CC, Hu LS, Erickson BJ, Gerstner ER, Smits M, et al. Consensus recommendations for a dynamic susceptibility contrast MRI protocol for use in high-grade gliomas. Neuro-Oncol 2020;22:1262–75. https://doi.org/10.1093/neuonc/noaa141.
[66] Quarles CC, Ward BD, Schmainda KM. Improving the reliability of obtaining tumor hemodynamic parameters in the presence of contrast agent extravasation. Magn Reson Med 2005;53:1307–16. https://doi.org/10.1002/mrm.20497.
[67] Bjornerud A, Sorensen AG, Mouridsen K, Emblem KE. T1- and T2*-dominant extravasation correction in DSC-MRI: part I - theoretical considerations and implications for assessment of tumor hemodynamic properties. J Cereb Blood Flow Metab Off J Int Soc Cereb Blood Flow Metab 2011;31:2041–53. https://doi.org/10.1038/jcbfm.2011.52.
[68] Leu K, Boxerman JL, Cloughesy TF, Lai A, Nghiemphu PL, Liau LM, et al. Improved leakage correction for single-echo dynamic susceptibility contrast perfusion MRI estimates of relative cerebral blood volume in high-grade gliomas by accounting for bidirectional contrast agent exchange. AJNR Am J Neuroradiol 2016;37:1440–6. https://doi.org/10.3174/ajnr.A4759.
[69] Petcharunpaisan S, Ramalho J, Castillo M. Arterial spin labeling in neuroimaging. World J Radiol 2010;2:384–98. https://doi.org/10.4329/wjr.v2.i10.384.
[70] Alsop DC, Detre JA, Golay X, Günther M, Hendrikse J, Hernandez-Garcia L, et al. Recommended implementation of arterial spin-labeled perfusion MRI for clinical applications: a consensus of the ISMRM perfusion study group and the European consortium for ASL in dementia. Magn Reson Med 2015;73:102–16. https://doi.org/10.1002/mrm.25197.
[71] Haller S, Zaharchuk G, Thomas DL, Lovblad K-O, Barkhof F, Golay X. Arterial spin labeling perfusion of the brain: emerging clinical applications. Radiology 2016;281:337–56. https://doi.org/10.1148/radiol.2016150789.
[72] Falk Delgado A, De Luca F, van Westen D, Falk Delgado A. Arterial spin labeling MR imaging for differentiation between high- and low-grade glioma-a meta-analysis. Neuro-Oncol 2018;20:1450–61. https://doi.org/10.1093/neuonc/noy095.
[73] Abdel Razek AAK, Talaat M, El-Serougy L, Gaballa G, Abdelsalam M. Clinical applications of arterial spin labeling in brain tumors. J Comput Assist Tomogr 2019;43:525–32. https://doi.org/10.1097/RCT.0000000000000873.
[74] Soldozy S, Galindo J, Snyder H, Ali Y, Norat P, Yağmurlu K, et al. Clinical utility of arterial spin labeling imaging in disorders of the nervous system. Neurosurg Focus 2019;47:E5. https://doi.org/10.3171/2019.9.FOCUS19567.
[75] Dhermain FG, Hau P, Lanfermann H, Jacobs AH, van den Bent MJ. Advanced MRI and PET imaging for assessment of treatment response in patients with gliomas. Lancet Neurol 2010;9:906–20. https://doi.org/10.1016/S1474-4422(10)70181-2.
[76] Komoroski RA, Heimberg C, Cardwell D, Karson CN. Effects of gender and region on proton MRS of normal human brain. Magn Reson Imaging 1999;17:427–33. https://doi.org/10.1016/s0730-725x(98)00186-6.
[77] Bulik M, Jancalek R, Vanicek J, Skoch A, Mechl M. Potential of MR spectroscopy for assessment of glioma grading. Clin Neurol Neurosurg 2013;115:146–53. https://doi.org/10.1016/j.clineuro.2012.11.002.
[78] Wu B, Warnock G, Zaiss M, Lin C, Chen M, Zhou Z, et al. An overview of CEST MRI for non-MR physicists. EJNMMI Phys 2016;3:19. https://doi.org/10.1186/s40658-016-0155-2.
[79] Aquino D, Gioppo A, Finocchiaro G, Bruzzone MG, Cuccarini V. MRI in glioma immunotherapy: evidence, pitfalls, and perspectives. J Immunol Res 2017;2017:5813951. https://doi.org/10.1155/2017/5813951.
[80] Zhou J, Heo H-Y, Knutsson L, van Zijl PCM, Jiang S. APT-weighted MRI: techniques, current neuro applications, and challenging issues. J Magn Reson Imaging 2019;50:347–64. https://doi.org/10.1002/jmri.26645.
[81] Hervey-Jumper SL, Berger MS. Maximizing safe resection of low- and high-grade glioma. J Neuro-Oncol 2016;130:269–82. https://doi.org/10.1007/s11060-016-2110-4.
[82] Hu LS, Hawkins-Daarud A, Wang L, Li J, Swanson KR. Imaging of intratumoral heterogeneity in high-grade glioma. Cancer Lett 2020;477:97–106. https://doi.org/10.1016/j.canlet.2020.02.025.
[83] Guzmán-De-Villoria JA, Mateos-Pérez JM, Fernández-García P, Castro E, Desco M. Added value of advanced over conventional magnetic resonance imaging in grading gliomas and other primary brain tumors. Cancer Imaging Off Publ Int Cancer Imaging Soc 2014;14:35. https://doi.org/10.1186/s40644-014-0035-8.
[84] Berman JI, Berger MS, Chung SW, Nagarajan SS, Henry RG. Accuracy of diffusion tensor magnetic resonance imaging tractography assessed using intraoperative subcortical stimulation mapping and magnetic source imaging. J Neurosurg 2007;107:488–94. https://doi.org/10.3171/JNS-07/09/0488.
[85] Scott JN, Brasher PMA, Sevick RJ, Rewcastle NB, Forsyth PA. How often are nonenhancing supratentorial gliomas malignant? A population study. Neurology 2002;59:947–9. https://doi.org/10.1212/wnl.59.6.947.
[86] Harpold HLP, Alvord EC, Swanson KR. The evolution of mathematical modeling of glioma proliferation and invasion. J Neuropathol Exp Neurol 2007;66:1–9. https://doi.org/10.1097/nen.0b013e31802d9000.
[87] Gupta A, Dwivedi T. A simplified overview of World Health Organization classification update of central nervous system tumors 2016. J Neurosci Rural Pract 2017;8:629–41. https://doi.org/10.4103/jnrp.jnrp_168_17.
[88] Whitfield GA, Kennedy SR, Djoukhadar IK, Jackson A. Imaging and target volume delineation in glioma. Clin Oncol 2014;26:364–76. https://doi.org/10.1016/j.clon.2014.04.026.
[89] Zhang Z, Tan Z, Lv Q, Wang L, Yu K, Yang H, et al. High expression of C1ORF112 predicts a poor outcome: a potential target for the treatment of low-grade gliomas. Front Genet 2021;12:710944. https://doi.org/10.3389/fgene.2021.710944.
[90] Law M, Yang S, Wang H, Babb JS, Johnson G, Cha S, et al. Glioma grading: sensitivity, specificity, and predictive values of perfusion MR imaging and proton MR spectroscopic imaging compared with conventional MR imaging. AJNR Am J Neuroradiol 2003;24:1989–98.
[91] Furtak J, Śledzińska P, Bebyn MG, Szylberg T, Krajewski S, Birski M, et al. Infratentorial stereotactic biopsy of brainstem and cerebellar lesions. Brain Sci 2021;11:1432. https://doi.org/10.3390/brainsci11111432.
[92] Saadoun S, Papadopoulos MC, Davies DC, Bell BA, Krishna S. Increased aquaporin 1 water channel expression inhuman brain tumours. Br J Cancer 2002;87:621–3. https://doi.org/10.1038/sj.bjc.6600512.
[93] Warth A, Simon P, Capper D, Goeppert B, Tabatabai G, Herzog H, et al. Expression pattern of the water channel aquaporin-4 in human gliomas is associated with blood-brain barrier disturbance but not with patient survival. J Neurosci Res 2007;85:1336–46. https://doi.org/10.1002/jnr.21224.
[94] Barajas RF, Hess CP, Phillips JJ, Von Morze CJ, Yu JP, Chang SM, et al. Super-resolution track density imaging of glioblastoma: histopathologic correlation. AJNR Am J Neuroradiol 2013;34:1319–25. https://doi.org/10.3174/ajnr.A3400.
[95] Henker C, Hiepel MC, Kriesen T, Scherer M, Glass Å, Herold-Mende C, et al. Volumetric assessment of glioblastoma and its predictive value for survival. Acta Neurochir 2019;161:1723–32. https://doi.org/10.1007/s00701-019-03966-6.
[96] Verburg N, de Witt Hamer PC. State-of-the-art imaging for glioma surgery. Neurosurg Rev 2021;44:1331–43. https://doi.org/10.1007/s10143-020-01337-9.
[97] Zhang L, Min Z, Tang M, Chen S, Lei X, Zhang X. The utility of diffusion MRI with quantitative ADC measurements for differentiating high-grade from low-grade cerebral gliomas: evidence from a meta-analysis. J Neurol Sci 2017;373:9–15. https://doi.org/10.1016/j.jns.2016.12.008.
[98] Sanvito F, Castellano A, Falini A. Advancements in neuroimaging to unravel biological and molecular features of brain tumors. Cancers 2021;13:424. https://doi.org/10.3390/cancers13030424.
[99] Raab P, Hattingen E, Franz K, Zanella FE, Lanfermann H. Cerebral gliomas: diffusional kurtosis imaging analysis of microstructural differences. Radiology 2010;254:876–81. https://doi.org/10.1148/radiol.09090819.
[100] Tietze A, Hansen MB, Østergaard L, Jespersen SN, Sangill R, Lund TE, et al. Mean diffusional kurtosis in patients with glioma: initial results with a fast imaging method in a clinical setting. Am J Neuroradiol 2015;36:1472–8. https://doi.org/10.3174/ajnr.A4311.
[101] Van Cauter S, De Keyzer F, Sima DM, Sava AC, D'Arco F, Veraart J, et al. Integrating diffusion kurtosis imaging, dynamic susceptibility-weighted contrast-enhanced MRI, and short echo time chemical shift imaging for grading gliomas. Neuro-Oncol 2014;16:1010–21. https://doi.org/10.1093/neuonc/not304.
[102] El-Serougy L, Abdel Razek AAK, Ezzat A, Eldawoody H, El-Morsy A. Assessment of diffusion tensor imaging metrics in differentiating low-grade from high-grade gliomas. Neuroradiol J 2016;29:400–7. https://doi.org/10.1177/1971400916665382.
[103] Ma L, Song ZJ. Differentiation between low-grade and high-grade glioma using combined diffusion tensor imaging metrics. Clin Neurol Neurosurg 2013;115:2489–95. https://doi.org/10.1016/j.clineuro.2013.10.003.
[104] Kovanlikaya I, Firat Z, Kovanlikaya A, Uluğ AM, Cihangiroglu MM, John M, et al. Assessment of the corticospinal tract alterations before and after resection of brainstem lesions using diffusion tensor imaging (DTI) and tractography at 3T. Eur J Radiol 2011;77:383–91. https://doi.org/10.1016/j.ejrad.2009.08.012.
[105] Li X, Zhu Y, Kang H, Zhang Y, Liang H, Wang S, et al. Glioma grading by microvascular permeability parameters derived from dynamic contrast-enhanced MRI and intratumoral susceptibility signal on susceptibility weighted imaging. Cancer Imaging 2015;15:4. https://doi.org/10.1186/s40644-015-0039-z.
[106] Kong L-W, Chen J, Zhao H, Yao K, Fang S-Y, Wang Z, et al. Intratumoral susceptibility signals reflect biomarker status in gliomas. Sci Rep 2019;9:17080. https://doi.org/10.1038/s41598-019-53629-w.

[107] Harrer JU, Parker GJM, Haroon HA, Buckley DL, Embelton K, Roberts C, et al. Comparative study of methods for determining vascular permeability and blood volume in human gliomas. J Magn Reson Imaging 2004;20:748–57. https://doi.org/10.1002/jmri.20182.
[108] Okuchi S, Rojas-Garcia A, Ulyte A, Lopez I, Ušinskienė J, Lewis M, et al. Diagnostic accuracy of dynamic contrast-enhanced perfusion MRI in stratifying gliomas: a systematic review and meta-analysis. Cancer Med 2019;8:5564–73. https://doi.org/10.1002/cam4.2369.
[109] Jain KK, Sahoo P, Tyagi R, Mehta A, Patir R, Vaishya S, et al. Prospective glioma grading using single-dose dynamic contrast-enhanced perfusion MRI. Clin Radiol 2015;70:1128–35. https://doi.org/10.1016/j.crad.2015.06.076.
[110] McCullough BJ, Ader V, Aguedan B, Feng X, Susanto D, Benkers TL, et al. Preoperative relative cerebral blood volume analysis in gliomas predicts survival and mitigates risk of biopsy sampling error. J Neuro-Oncol 2018;136:181–8. https://doi.org/10.1007/s11060-017-2642-2.
[111] Maeda M, Itoh S, Kimura H, Iwasaki T, Hayashi N, Yamamoto K, et al. Tumor vascularity in the brain: evaluation with dynamic susceptibility-contrast MR imaging. Radiology 1993;189:233–8. https://doi.org/10.1148/radiology.189.1.8372199.
[112] Sugahara T, Korogi Y, Kochi M, Ikushima I, Hirai T, Okuda T, et al. Correlation of MR imaging-determined cerebral blood volume maps with histologic and angiographic determination of vascularity of gliomas. AJR Am J Roentgenol 1998;171:1479–86. https://doi.org/10.2214/ajr.171.6.9843274.
[113] Lev MH, Ozsunar Y, Henson JW, Rasheed AA, Barest GD, Harsh GR, et al. Glial tumor grading and outcome prediction using dynamic spin-echo MR susceptibility mapping compared with conventional contrast-enhanced MR: confounding effect of elevated rCBV of oligodendrogliomas [corrected]. AJNR Am J Neuroradiol 2004;25:214–21.
[114] Schmainda KM, Rand SD, Joseph AM, Lund R, Ward BD, Pathak AP, et al. Characterization of a first-pass gradient-Echo spin-Echo method to predict brain tumor grade and angiogenesis. AJNR Am J Neuroradiol 2004;25:1524–32.
[115] Soliman RK, Gamal SA, Essa A-HA, Othman MH. Preoperative grading of glioma using dynamic susceptibility contrast MRI: relative cerebral blood volume analysis of intra-tumoural and peri-tumoural tissue. Clin Neurol Neurosurg 2018;167:86–92. https://doi.org/10.1016/j.clineuro.2018.01.003.
[116] Law M, Young R, Babb J, Rad M, Sasaki T, Zagzag D, et al. Comparing perfusion metrics obtained from a single compartment versus pharmacokinetic modeling methods using dynamic susceptibility contrast-enhanced perfusion MR imaging with glioma grade. AJNR Am J Neuroradiol 2006;27:1975–82.
[117] Nasseri M, Gahramanov S, Netto JP, Fu R, Muldoon LL, Varallyay C, et al. Evaluation of pseudoprogression in patients with glioblastoma multiforme using dynamic magnetic resonance imaging with ferumoxytol calls RANO criteria into question. Neuro-Oncol 2014;16:1146–54. https://doi.org/10.1093/neuonc/not328.
[118] Delgado AF, Delgado AF. Discrimination between glioma grades II and III using dynamic susceptibility perfusion MRI: a meta-analysis. Am J Neuroradiol 2017;38:1348–55. https://doi.org/10.3174/ajnr.A5218.
[119] Martin WH, Delbeke D, Patton JA, Sandler MP. Detection of malignancies with SPECT versus PET, with 2-[fluorine-18]fluoro-2-deoxy-D-glucose. Radiology 1996;198:225–31. https://doi.org/10.1148/radiology.198.1.8539384.
[120] Watanabe M, Tanaka R, Takeda N. Magnetic resonance imaging and histopathology of cerebral gliomas. Neuroradiology 1992;34:463–9. https://doi.org/10.1007/BF00598951.
[121] Law M, Young R, Babb J, Pollack E, Johnson G. Histogram analysis versus region of interest analysis of dynamic susceptibility contrast perfusion MR imaging data in the grading of cerebral gliomas. AJNR Am J Neuroradiol 2007;28:761–6.
[122] Hilario A, Ramos A, Perez-Nuñez A, Salvador E, Millan JM, Lagares A, et al. The added value of apparent diffusion coefficient to cerebral blood volume in the preoperative grading of diffuse gliomas. AJNR Am J Neuroradiol 2012;33:701–7. https://doi.org/10.3174/ajnr.A2846.
[123] Emblem KE, Nedregaard B, Nome T, Due-Tonnessen P, Hald JK, Scheie D, et al. Glioma grading by using histogram analysis of blood volume heterogeneity from MR-derived cerebral blood volume maps. Radiology 2008;247:808–17. https://doi.org/10.1148/radiol.2473070571.
[124] Kong L, Chen H, Yang Y, Chen L. A meta-analysis of arterial spin labelling perfusion values for the prediction of glioma grade. Clin Radiol 2017;72:255–61. https://doi.org/10.1016/j.crad.2016.10.016.
[125] Alsaedi A, Doniselli F, Jäger HR, Panovska-Griffiths J, Rojas-Garcia A, Golay X, et al. The value of arterial spin labelling in adults glioma grading: systematic review and meta-analysis. Oncotarget 2019;10:1589–601. https://doi.org/10.18632/oncotarget.26674.
[126] Flies CM, Snijders TJ, Van Seeters T, Smits M, De Vos FYF, Hendrikse J, et al. Perfusion imaging with arterial spin labeling (ASL)–MRI predicts malignant progression in low-grade (WHO grade II) gliomas. Neuroradiology 2021;63:2023–33. https://doi.org/10.1007/s00234-021-02737-4.
[127] Wang Q, Zhang H, Zhang J, Wu C, Zhu W, Li F, et al. The diagnostic performance of magnetic resonance spectroscopy in differentiating high-from low-grade gliomas: a systematic review and meta-analysis. Eur Radiol 2016;26:2670–84. https://doi.org/10.1007/s00330-015-4046-z.
[128] Smits M. Imaging of oligodendroglioma. Br J Radiol 2016;89:20150857. https://doi.org/10.1259/bjr.20150857.
[129] Wang Y, Fan X, Zhang C, Zhang T, Peng X, Qian T, et al. Identifying radiographic specificity for phosphatase and tensin homolog and epidermal growth factor receptor changes: a quantitative analysis of glioblastomas. Neuroradiology 2014;56:1113–20. https://doi.org/10.1007/s00234-014-1427-y.
[130] Young RJ, Gupta A, Shah AD, Graber JJ, Schweitzer AD, Prager A, et al. Potential role of preoperative conventional MRI including diffusion measurements in assessing epidermal growth factor receptor gene amplification status in patients with glioblastoma. AJNR Am J Neuroradiol 2013;34:2271–7. https://doi.org/10.3174/ajnr.A3604.
[131] Choi YS, Ahn SS, Lee S-K, Chang JH, Kang S-G, Kim SH, et al. Amide proton transfer imaging to discriminate between low- and high-grade gliomas: added value to apparent diffusion coefficient and relative cerebral blood volume. Eur Radiol 2017;27:3181–9. https://doi.org/10.1007/s00330-017-4732-0.
[132] Diehn M, Nardini C, Wang DS, McGovern S, Jayaraman M, Liang Y, et al. Identification of noninvasive imaging surrogates for brain tumor gene-expression modules. Proc Natl Acad Sci 2008;105:5213–8. https://doi.org/10.1073/pnas.0801279105.
[133] Gutman DA, Cooper LAD, Hwang SN, Holder CA, Gao J, Aurora TD, et al. MR imaging predictors of molecular profile and survival: multi-institutional study of the TCGA glioblastoma data set. Radiology 2013;267:560–9. https://doi.org/10.1148/radiol.13120118.
[134] Aghi M, Gaviani P, Henson JW, Batchelor TT, Louis DN, Barker FG. Magnetic resonance imaging characteristics predict epidermal growth factor receptor amplification status in glioblastoma. Clin Cancer Res Off J Am Assoc Cancer Res 2005;11:8600–5. https://doi.org/10.1158/1078-0432.CCR-05-0713.
[135] Yoon RG, Kim HS, Paik W, Shim WH, Kim SJ, Kim JH. Different diagnostic values of imaging parameters to predict pseudoprogression in glioblastoma subgroups stratified by MGMT promoter methylation. Eur Radiol 2017;27:255–66. https://doi.org/10.1007/s00330-016-4346-y.
[136] Ellingson BM, Lai A, Harris RJ, Selfridge JM, Yong WH, Das K, et al. Probabilistic radiographic atlas of glioblastoma phenotypes. AJNR Am J Neuroradiol 2013;34:533–40. https://doi.org/10.3174/ajnr.A3253.
[137] Deguchi S, Oishi T, Mitsuya K, Kakuda Y, Endo M, Sugino T, et al. Clinicopathological analysis of T2-FLAIR mismatch sign in lower-grade gliomas. Sci Rep 2020;10:10113. https://doi.org/10.1038/s41598-020-67244-7.
[138] Juratli TA, Tummala SS, Riedl A, Daubner D, Hennig S, Penson T, et al. Radiographic assessment of contrast enhancement and T2/FLAIR mismatch sign in lower grade gliomas: correlation with molecular groups. J Neuro-Oncol 2019;141:327–35. https://doi.org/10.1007/s11060-018-03034-6.
[139] Park SI, Suh CH, Guenette JP, Huang RY, Kim HS. The T2-FLAIR mismatch sign as a predictor of IDH-mutant, 1p/19q-noncodeleted lower-grade gliomas: a systematic review and diagnostic meta-analysis. Eur Radiol 2021;31:5289–99. https://doi.org/10.1007/s00330-020-07467-4.
[140] Lee MK, Park JE, Jo Y, Park SY, Kim SJ, Kim HS. Advanced imaging parameters improve the prediction of diffuse lower-grade gliomas subtype, IDH mutant with no 1p19q codeletion: added value to the T2/FLAIR mismatch sign. Eur Radiol 2020;30:844–54. https://doi.org/10.1007/s00330-019-06395-2.
[141] Wang C, Xu Z, Wang S, Peng L, Zhang W, Li X, et al. Clinical importance of ADC in the prediction of 125I in the treatment for gliomas. J Cancer 2021;12:1945–51. https://doi.org/10.7150/jca.50789.
[142] Fujita Y, Nagashima H, Tanaka K, Hashiguchi M, Hirose T, Itoh T, et al. The histopathologic and radiologic features of T2-FLAIR mismatch sign in IDH-mutant 1p/19q non-codeleted astrocytomas. World Neurosurg 2021;149:e253–60. https://doi.org/10.1016/j.wneu.2021.02.042.
[143] Ellingson BM. Radiogenomics and imaging phenotypes in glioblastoma: novel observations and correlation with molecular characteristics. Curr Neurol Neurosci Rep 2015;15:506. https://doi.org/10.1007/s11910-014-0506-0.
[144] Moffat BA, Chenevert TL, Lawrence TS, Meyer CR, Johnson TD, Dong Q, et al. Functional diffusion map: a noninvasive MRI biomarker for early stratification of clinical brain tumor response. Proc Natl Acad Sci USA 2005;102:5524–9. https://doi.org/10.1073/pnas.0501532102.
[145] Park YW, Park JE, Ahn SS, Kim EH, Kang S-G, Chang JH, et al. Magnetic resonance imaging parameters for noninvasive prediction of epidermal growth factor receptor amplification in Isocitrate dehydrogenase-wild-type lower-grade gliomas: a multicenter study. Neurosurgery 2021;89:257–65. https://doi.org/10.1093/neuros/nyab136.
[146] Park YW, Ahn SS, Park CJ, Han K, Kim EH, Kang S-G, et al. Diffusion and perfusion MRI may predict EGFR amplification and the TERT promoter mutation status of IDH-wildtype lower-grade gliomas. Eur Radiol 2020;30:6475–84. https://doi.org/10.1007/s00330-020-07090-3.
[147] Zhao J, Liu X, Lin H, Cui C, Yue Y, Gao S, et al. MRI comparative study of diffuse midline glioma, H3 K27-altered and glioma in the midline without H3 K27-altered. BMC Neurol 2022;22:498. https://doi.org/10.1186/s12883-022-03026-0.
[148] Seong M, Kim ST, Noh JH, Kim YK, Kim H-J. Radiologic findings and the molecular expression profile of diffuse midline glioma H3 K27M mutant. Acta Radiol Stockh Swed 1987;2021(62):1404–11. https://doi.org/10.1177/0284185120968560.
[149] Wang P, He J, Ma X, Weng L, Wu Q, Zhao P, et al. Applying MAP-MRI to identify the WHO grade and Main genetic features of adult-type diffuse gliomas: a comparison of three diffusion-weighted MRI models. Acad Radiol 2023;30:1238–46. https://doi.org/10.1016/j.acra.2022.10.009.
[150] Xiong J, Tan W-L, Pan J-W, Wang Y, Yin B, Zhang J, et al. Detecting isocitrate dehydrogenase gene mutations in oligodendroglial tumors using diffusion tensor imaging metrics and their correlations with proliferation and microvascular density. J Magn Reson Imaging 2016;43:45–54. https://doi.org/10.1002/jmri.24958.
[151] Ozturk K, Soylu E, Cayci Z. Differentiation between primary CNS lymphoma and atypical glioblastoma according to major genomic alterations using diffusion and

susceptibility-weighted MR imaging. Eur J Radiol 2021;141:109784. https://doi.org/10.1016/j.ejrad.2021.109784.
[152] Saini J, Gupta PK, Sahoo P, Singh A, Patir R, Ahlawat S, et al. Differentiation of grade II/III and grade IV glioma by combining "T1 contrast-enhanced brain perfusion imaging" and susceptibility-weighted quantitative imaging. Neuroradiology 2018;60:43–50. https://doi.org/10.1007/s00234-017-1942-8.
[153] Wang X, Chen X-Z, Shi L, Dai J-P. Glioma grading and IDH1 mutational status: assessment by intravoxel incoherent motion MRI. Clin Radiol 2019;74:651.e7–651.e14. https://doi.org/10.1016/j.crad.2019.03.020.
[154] Lu J, Li X, Li H. Perfusion parameters derived from MRI for preoperative prediction of IDH mutation and MGMT promoter methylation status in glioblastomas. Magn Reson Imaging 2021;83:189–95. https://doi.org/10.1016/j.mri.2021.09.005.
[155] Rohwer N, Zasada C, Kempa S, Cramer T. The growing complexity of HIF-1α's role in tumorigenesis: DNA repair and beyond. Oncogene 2013;32:3569–76. https://doi.org/10.1038/onc.2012.510.
[156] Tykocinski ES, Grant RA, Kapoor GS, Krejza J, Bohman L-E, Gocke TA, et al. Use of magnetic perfusion-weighted imaging to determine epidermal growth factor receptor variant III expression in glioblastoma. Neuro-Oncol 2012;14:613–23. https://doi.org/10.1093/neuonc/nos073.
[157] Gupta A, Young RJ, Shah AD, Schweitzer AD, Graber JJ, Shi W, et al. Pretreatment dynamic susceptibility contrast MRI perfusion in glioblastoma: prediction of EGFR gene amplification. Clin Neuroradiol 2015;25:143–50. https://doi.org/10.1007/s00062-014-0289-3.
[158] Kickingereder P, Bonekamp D, Nowosielski M, Kratz A, Sill M, Burth S, et al. Radiogenomics of glioblastoma: machine learning-based classification of molecular characteristics by using multiparametric and multiregional MR imaging features. Radiology 2016;281:907–18. https://doi.org/10.1148/radiol.2016161382.
[159] Arevalo-Perez J, Thomas AA, Kaley T, Lyo J, Peck KK, Holodny AI, et al. T1-weighted dynamic contrast-enhanced MRI as a noninvasive biomarker of epidermal growth factor receptor vIII status. AJNR Am J Neuroradiol 2015;36:2256–61. https://doi.org/10.3174/ajnr.A4484.
[160] Jung SC, Choi SH, Yeom JA, Kim J-H, Ryoo I, Kim SC, et al. Cerebral blood volume analysis in glioblastomas using dynamic susceptibility contrast-enhanced perfusion MRI: a comparison of manual and semiautomatic segmentation methods. PLoS One 2013;8:e69323. https://doi.org/10.1371/journal.pone.0069323.
[161] Law M, Brodsky JE, Babb J, Rosenblum M, Miller DC, Zagzag D, et al. High cerebral blood volume in human gliomas predicts deletion of chromosome 1p: preliminary results of molecular studies in gliomas with elevated perfusion. J Magn Reson Imaging 2007;25:1113–9. https://doi.org/10.1002/jmri.20920.
[162] Hu Y, Chen Y, Wang J, Kang JJ, Shen DD, Jia ZZ. Non-invasive estimation of glioma IDH1 mutation and VEGF expression by histogram analysis of dynamic contrast-enhanced MRI. Front Oncol 2020;10:593102. https://doi.org/10.3389/fonc.2020.593102.
[163] Mao J, Deng D, Yang Z, Wang W, Cao M, Huang Y, et al. Pretreatment structural and arterial spin labeling MRI is predictive for p53 mutation in high-grade gliomas. Br J Radiol 2020;93:20200661. https://doi.org/10.1259/bjr.20200661.
[164] Yoo R-E, Yun TJ, Hwang I, Hong EK, Kang KM, Choi SH, et al. Arterial spin labeling perfusion-weighted imaging aids in prediction of molecular biomarkers and survival in glioblastomas. Eur Radiol 2020;30:1202–11. https://doi.org/10.1007/s00330-019-06379-2.
[165] Pang H, Dang X, Ren Y, Zhuang D, Qiu T, Chen H, et al. 3D-ASL perfusion correlates with VEGF expression and overall survival in glioma patients: comparison of quantitative perfusion and pathology on accurate spatial location-matched basis. J Magn Reson Imaging 2019;50:209–20. https://doi.org/10.1002/jmri.26562.
[166] Dangouloff-Ros V, Deroulers C, Foissac F, Badoual M, Shotar E, Grévent D, et al. Arterial spin labeling to predict brain tumor grading in children: correlations between histopathologic vascular density and perfusion MR imaging. Radiology 2016;281:553–66. https://doi.org/10.1148/radiol.2016152228.
[167] Suh CH, Kim HS, Jung SC, Choi CG, Kim SJ. 2-Hydroxyglutarate MR spectroscopy for prediction of isocitrate dehydrogenase mutant glioma: a systemic review and meta-analysis using individual patient data. Neuro-Oncol 2018;20:1573–83. https://doi.org/10.1093/neuonc/noy113.
[168] Di Ieva A, Magnussen JS, McIntosh J, Mulcahy MJ, Pardey M, Choi C. Magnetic resonance spectroscopic assessment of Isocitrate dehydrogenase status in gliomas: the new frontiers of spectrobiopsy in neurodiagnostics. World Neurosurg 2020;133:e421–7. https://doi.org/10.1016/j.wneu.2019.09.040.
[169] Ozturk-Isik E, Cengiz S, Ozcan A, Yakicier C, Ersen Danyeli A, Pamir MN, et al. Identification of IDH and TERTp mutation status using 1 H-MRS in 112 hemispheric diffuse gliomas. J Magn Reson Imaging 2020;51:1799–809. https://doi.org/10.1002/jmri.26964.
[170] Fudaba H, Shimomura T, Abe T, Matsuta H, Momii Y, Sugita K, et al. Comparison of multiple parameters obtained on 3T pulsed arterial spin-labeling, diffusion tensor imaging, and MRS and the Ki-67 labeling index in evaluating glioma grading. AJNR Am J Neuroradiol 2014;35:2091–8. https://doi.org/10.3174/ajnr.A4018.
[171] Carrillo JA, Lai A, Nghiemphu PL, Kim HJ, Phillips HS, Kharbanda S, et al. Relationship between tumor enhancement, edema, IDH1 mutational status, MGMT promoter methylation, and survival in glioblastoma. AJNR Am J Neuroradiol 2012;33:1349–55. https://doi.org/10.3174/ajnr.A2950.
[172] Mahajan A, Goh V, Basu S, Vaish R, Weeks AJ, Thakur MH, et al. Bench to bedside molecular functional imaging in translational cancer medicine: to image or to imagine? Clin Radiol 2015;70:1060–82. https://doi.org/10.1016/j.crad.2015.06.082.
[173] Brandsma D, Stalpers L, Taal W, Sminia P, van den Bent MJ. Clinical features, mechanisms, and management of pseudoprogression in malignant gliomas. Lancet Oncol 2008;9:453–61. https://doi.org/10.1016/S1470-2045(08)70125-6.
[174] Thust SC, van den Bent MJ, Smits M. Pseudoprogression of brain tumors. J Magn Reson Imaging 2018;48:571–89. https://doi.org/10.1002/jmri.26171.
[175] Wen J, Chen W, Zhu Y, Zhang P. Clinical features associated with the efficacy of chemotherapy in patients with glioblastoma (GBM): a surveillance, epidemiology, and end results (SEER) analysis. BMC Cancer 2021;21:81. https://doi.org/10.1186/s12885-021-07800-0.
[176] Mullins ME, Barest GD, Schaefer PW, Hochberg FH, Gonzalez RG, Lev MH. Radiation necrosis versus glioma recurrence: conventional MR imaging clues to diagnosis. AJNR Am J Neuroradiol 2005;26:1967–72.
[177] Abel R, Jones J, Mandelin P, Cen S, Pagnini P. Distinguishing pseudoprogression from true progression by FLAIR volumetric characteristics compared to 45 Gy Isodose volumes in treated glioblastoma patients. Int J Radiat Oncol Biol Phys 2012;84:S275. https://doi.org/10.1016/j.ijrobp.2012.07.716.
[178] Strauss SB, Meng A, Ebani EJ, Chiang GC. Imaging glioblastoma posttreatment: progression, pseudoprogression, pseudoresponse, radiation necrosis. Radiol Clin North Am 2019;57:1199–216. https://doi.org/10.1016/j.rcl.2019.07.003.
[179] Khan MN, Sharma AM, Pitz M, Loewen SK, Quon H, Poulin A, et al. High-grade glioma management and response assessment—recent advances and current challenges. Curr Oncol 2016;23:e383–91. https://doi.org/10.3747/co.23.3082.
[180] van Dijken BRJ, van Laar PJ, Holtman GA, van der Hoorn A. Diagnostic accuracy of magnetic resonance imaging techniques for treatment response evaluation in patients with high-grade glioma, a systematic review and meta-analysis. Eur Radiol 2017;27:4129–44. https://doi.org/10.1007/s00330-017-4789-9.
[181] Sadeghi N, D'Haene N, Decaestecker C, Levivier M, Metens T, Maris C, et al. Apparent diffusion coefficient and cerebral blood volume in brain gliomas: relation to tumor cell density and tumor microvessel density based on stereotactic biopsies. AJNR Am J Neuroradiol 2008;29:476–82. https://doi.org/10.3174/ajnr.A0851.
[182] Patel P, Baradaran H, Delgado D, Askin G, Christos P, John Tsiouris A, et al. MR perfusion-weighted imaging in the evaluation of high-grade gliomas after treatment: a systematic review and meta-analysis. Neuro-Oncol 2017;19:118–27. https://doi.org/10.1093/neuonc/now148.
[183] Shiroishi MS, Boxerman JL, Pope WB. Physiologic MRI for assessment of response to therapy and prognosis in glioblastoma. Neuro-Oncol 2016;18:467–78. https://doi.org/10.1093/neuonc/nov179.
[184] Mangla R, Singh G, Ziegelitz D, Milano MT, Korones DN, Zhong J, et al. Changes in relative cerebral blood volume 1 month after radiation-temozolomide therapy can help predict overall survival in patients with glioblastoma. Radiology 2010;256:575–84. https://doi.org/10.1148/radiol.10091440.
[185] Prager AJ, Martinez N, Beal K, Omuro A, Zhang Z, Young RJ. Diffusion and perfusion MRI to differentiate treatment-related changes including pseudoprogression from recurrent tumors in high-grade gliomas with histopathologic evidence. AJNR Am J Neuroradiol 2015;36:877–85. https://doi.org/10.3174/ajnr.A4218.
[186] Shin KE, Ahn KJ, Choi HS, Jung SL, Kim BS, Jeon SS, et al. DCE and DSC MR perfusion imaging in the differentiation of recurrent tumour from treatment-related changes in patients with glioma. Clin Radiol 2014;69:e264–72. https://doi.org/10.1016/j.crad.2014.01.016.
[187] Young RJ, Gupta A, Shah AD, Graber JJ, Chan TA, Zhang Z, et al. MRI perfusion in determining pseudoprogression in patients with glioblastoma. Clin Imaging 2013;37:41–9. https://doi.org/10.1016/j.clinimag.2012.02.016.
[188] Baek HJ, Kim HS, Kim N, Choi YJ, Kim YJ. Percent change of perfusion skewness and kurtosis: a potential imaging biomarker for early treatment response in patients with newly diagnosed glioblastomas. Radiology 2012;264:834–43. https://doi.org/10.1148/radiol.12112120.
[189] Lee WJ, Choi SH, Park C-K, Yi KS, Kim TM, Lee S-H, et al. Diffusion-weighted MR imaging for the differentiation of true progression from pseudoprogression following concomitant radiotherapy with temozolomide in patients with newly diagnosed high-grade gliomas. Acad Radiol 2012;19:1353–61. https://doi.org/10.1016/j.acra.2012.06.011.
[190] Matsusue E, Fink JR, Rockhill JK, Ogawa T, Maravilla KR. Distinction between glioma progression and post-radiation change by combined physiologic MR imaging. Neuroradiology 2010;52:297–306. https://doi.org/10.1007/s00234-009-0613-9.
[191] Wang S, Martinez-Lage M, Sakai Y, Chawla S, Kim SG, Alonso-Basanta M, et al. Differentiating tumor progression from pseudoprogression in patients with glioblastomas using diffusion tensor imaging and dynamic susceptibility contrast MRI. Am J Neuroradiol 2016;37:28–36. https://doi.org/10.3174/ajnr.A4474.
[192] Cha J, Kim ST, Kim H-J, Kim B-J, Kim YK, Lee JY, et al. Differentiation of tumor progression from pseudoprogression in patients with posttreatment glioblastoma using multiparametric histogram analysis. AJNR Am J Neuroradiol 2014;35:1309–17. https://doi.org/10.3174/ajnr.A3876.
[193] Tsakiris C, Siempis T, Alexiou GA, Zikou A, Sioka C, Voulgaris S, et al. Differentiation between true tumor progression of glioblastoma and pseudoprogression using diffusion-weighted imaging and perfusion-weighted imaging: systematic review and meta-analysis. World Neurosurg 2020;144:e100–9. https://doi.org/10.1016/j.wneu.2020.07.218.
[194] Viselner G, Farina L, Lucev F, Turpini E, Lungarotti L, Bacila A, et al. Brain MR findings in patients treated with particle therapy for skull base tumors. Insights Imaging 2019;10:94. https://doi.org/10.1186/s13244-019-0784-9.

[195] Chao ST, Ahluwalia MS, Barnett GH, Stevens GHJ, Murphy ES, Stockham AL, et al. Challenges with the diagnosis and treatment of cerebral radiation necrosis. Int J Radiat Oncol Biol Phys 2013;87:449–57. https://doi.org/10.1016/j.ijrobp.2013.05.015.

[196] Li C, Gan Y, Chen H, Chen Y, Deng Y, Zhan W, et al. Advanced multimodal imaging in differentiating glioma recurrence from post-radiotherapy changes. Int Rev Neurobiol 2020;151:281–97. https://doi.org/10.1016/bs.irn.2020.03.009.

[197] Larsen VA, Simonsen HJ, Law I, Larsson HBW, Hansen AE. Evaluation of dynamic contrast-enhanced T1-weighted perfusion MRI in the differentiation of tumor recurrence from radiation necrosis. Neuroradiology 2013;55:361–9. https://doi.org/10.1007/s00234-012-1127-4.

[198] Masch WR, Wang PI, Chenevert TL, Junck L, Tsien C, Heth JA, et al. Comparison of diffusion tensor imaging and magnetic resonance perfusion imaging in differentiating recurrent brain neoplasm from radiation necrosis. Acad Radiol 2016;23:569–76. https://doi.org/10.1016/j.acra.2015.11.015.

[199] Chuang M-T, Liu Y-S, Tsai Y-S, Chen Y-C, Wang C-K. Differentiating radiation-induced necrosis from recurrent brain tumor using MR perfusion and spectroscopy: a meta-analysis. PLoS One 2016;11:e0141438. https://doi.org/10.1371/journal.pone.0141438.

[200] Zhang H, Ma L, Wang Q, Zheng X, Wu C, Xu B. Role of magnetic resonance spectroscopy for the differentiation of recurrent glioma from radiation necrosis: a systematic review and meta-analysis. Eur J Radiol 2014;83:2181–9. https://doi.org/10.1016/j.ejrad.2014.09.018.

[201] Li C, Yi C, Chen Y, Xi S, Guo C, Yang Q, et al. Identify glioma recurrence and treatment effects with triple-tracer PET/CT. BMC Med Imaging 2021;21:92. https://doi.org/10.1186/s12880-021-00624-1.

[202] Clement P, Booth T, Borovečki F, Emblem KE, Figueiredo P, Hirschler L, et al. GliMR: cross-border collaborations to promote advanced MRI biomarkers for glioma. J Med Biol Eng 2021;41:115–25. https://doi.org/10.1007/s40846-020-00582-z.

[203] Manfrini E, Smits M, Thust S, Geiger S, Bendella Z, Petr J, et al. From research to clinical practice: a European neuroradiological survey on quantitative advanced MRI implementation. Eur Radiol 2021;31:6334–41. https://doi.org/10.1007/s00330-020-07582-2.

[204] Hu LS, Kelm Z, Korfiatis P, Dueck AC, Elrod C, Ellingson BM, et al. Impact of software modeling on the accuracy of perfusion MRI in glioma. AJNR Am J Neuroradiol 2015;36:2242–9. https://doi.org/10.3174/ajnr.A4451.

[205] Kelm ZS, Korfiatis PD, Lingineni RK, Daniels JR, Buckner JC, Lachance DH, et al. Variability and accuracy of different software packages for dynamic susceptibility contrast magnetic resonance imaging for distinguishing glioblastoma progression from pseudoprogression. J Med Imaging Bellingham Wash 2015;2:026001. https://doi.org/10.1117/1.JMI.2.2.026001.

[206] Hu LS, Baxter LC, Pinnaduwage DS, Paine TL, Karis JP, Feuerstein BG, et al. Optimized preload leakage-correction methods to improve the diagnostic accuracy of dynamic susceptibility-weighted contrast-enhanced perfusion MR imaging in posttreatment gliomas. AJNR Am J Neuroradiol 2010;31:40–8. https://doi.org/10.3174/ajnr.A1787.

[207] Hu LS, Baxter LC, Smith KA, Feuerstein BG, Karis JP, Eschbacher JM, et al. Relative cerebral blood volume values to differentiate high-grade glioma recurrence from posttreatment radiation effect: direct correlation between image-guided tissue histopathology and localized dynamic susceptibility-weighted contrast-enhanced perfusion MR imaging measurements. AJNR Am J Neuroradiol 2009;30:552–8. https://doi.org/10.3174/ajnr.A1377.

[208] Narang J, Jain R, Arbab AS, Mikkelsen T, Scarpace L, Rosenblum ML, et al. Differentiating treatment-induced necrosis from recurrent/progressive brain tumor using nonmodel-based semiquantitative indices derived from dynamic contrast-enhanced T1-weighted MR perfusion. Neuro-Oncol 2011;13:1037–46. https://doi.org/10.1093/neuonc/nor075.

[209] Suh CH, Kim HS, Choi YJ, Kim N, Kim SJ. Prediction of pseudoprogression in patients with glioblastomas using the initial and final area under the curves ratio derived from dynamic contrast-enhanced T1-weighted perfusion MR imaging. AJNR Am J Neuroradiol 2013;34:2278–86. https://doi.org/10.3174/ajnr.A3634.

Publikacja nr 2

Magnetic Resonance Imaging 117 (2025) 110318

Contents lists available at ScienceDirect

Magnetic Resonance Imaging

journal homepage: www.elsevier.com/locate/mri

Investigating glioma genetics through perfusion MRI: rCBV and rCBF as predictive biomarkers

Paulina Śledzińska-Bebyn [a,*], Jacek Furtak [b,c], Marek Bebyn [d], Alicja Bartoszewska-Kubiak [e], Zbigniew Serafin [f]

[a] Department of Radiology, 10th Military Research Hospital and Polyclinic, 85-681 Bydgoszcz, Poland
[b] Department of Clinical Medicine, Faculty of Medicine, University of Science and Technology, Bydgoszcz, Poland
[c] Department of Neurosurgery, 10th Military Research Hospital and Polyclinic, 85-681 Bydgoszcz, Poland
[d] Department of Internal Diseases, 10th Military Clinical Hospital and Polyclinic, 85-681 Bydgoszcz, Poland
[e] Laboratory of Clinical Genetics and Molecular Pathology, Department of Medical Analytics, 10th Military Research Hospital and Polyclinic, 85-681 Bydgoszcz, Poland
[f] Department of Radiology and Diagnostic Imaging, Nicolaus Copernicus University, Collegium Medicum, Bydgoszcz, Poland

ARTICLE INFO

Keywords:
Brain tumors
Genetic markers
MRI perfusion
Neurooncology radiogenomics
rCBV

ABSTRACT

Background: Brain tumors exhibit diverse genetic landscapes and hemodynamic properties, influencing diagnosis and treatment outcomes.
Purpose: To explore the relationship between MRI perfusion metrics (rCBV, rCBF), genetic markers, and contrast enhancement patterns in gliomas, aiming to enhance diagnostic accuracy and inform personalized therapeutic strategies. Additionally, other radiological features, such as the T2/FLAIR mismatch sign, are evaluated for their predictive utility in *IDH* mutations.
Study type: Retrospective cohort study.
Population: 67 patients with brain tumors (including glioblastoma, astrocytoma, oligodendroglioma) undergoing surgical resection.
Field strength: 1.5 Tesla MRI, including T1 pre- and post-contrast, FLAIR, DWI, and DSC sequences.
Assessment: Semiquantitative perfusion metrics (rCBV, rCBF) were evaluated against genetic markers (*IDH1*, *EGFR*, *CDKN2A*, *PDGFRA*, *MGMT*, *TERT*, 1p19q, *PTEN*, *TP53*, *H3F3A*) through advanced MRI techniques. Contrast enhancement was assessed, and genetic alterations were confirmed via histopathological and molecular analyses.
Statistical tests: Chi-square test, sensitivity, specificity, and ROC analysis for predictive modeling; significance level set at $p < 0.05$.
Results: Statistically significant differences in perfusion metrics were observed among tumors with distinct genetic profiles, with primary tumors and those harboring specific mutations (*IDH1* wildtype, *EGFR* amplification, *CDKN2A* homozygous deletion, *PDGFRA* amplification) showing higher perfusion values. A cut-off value of <4 for rCBV in predicting *IDH1* mutation yielded a sensitivity of 61.5 % and specificity of 82.1 %. For *CDKN2A* deletion, a cut-off of >5 resulted in a sensitivity of 75 % and specificity of 74.6 %, with an ROC value of 0.78.
Data conclusion: Integrating perfusion MRI with genetic analysis offers a promising approach to improving the diagnostic and therapeutic landscape for brain tumors, indicating a substantial step toward personalized neuro-oncology. Additionally, findings like the T2/FLAIR mismatch sign highlight the potential for preoperative molecular predictions when biopsy is not feasible. These findings support further validation in larger, multi-institutional studies to solidify their role in clinical practice.
Data conclusion: Integrating perfusion MRI with genetic analysis offers a promising approach to improving the diagnostic and therapeutic landscape for brain tumors, indicating a substantial step toward personalized neuro-oncology. These findings support further validation in larger, multi-institutional studies to solidify their role in clinical practice.

* Corresponding author at: Department of Radiology, 10th Military Research Hospital and Polyclinic, Powstańców Warszawy 5, 85-681 Bydgoszcz, Poland.
E-mail address: paula.sledzinska@gmail.com (P. Śledzińska-Bebyn).

https://doi.org/10.1016/j.mri.2024.110318
Received 22 May 2024; Received in revised form 19 December 2024; Accepted 26 December 2024
Available online 29 December 2024

1. Introduction

Gliomas, the most common primary brain tumors, represent a major diagnostic and therapeutic challenge in neuro-oncology due to their histological and molecular diversity and complexity [1]. These glial cell-derived tumors vary widely in prognosis based on their histopathological grade and genomic profile, with molecular features now playing a central role in classification and treatment strategies. Despite standard treatment with surgery, chemotherapy, and radiotherapy, the prognosis remains poor, especially for high-grade gliomas, highlighting the need for novel, patient-tailored therapies [2,3].

Magnetic Resonance Imaging (MRI) is the most reliable method for detecting brain tumors, offering precise spatial data and valuable insights into the features of the tumor [4]. Over the years, various MRI modalities have been utilized to study gliomas, including T1- and T2-weighted imaging, Fluid-attenuated Inversion Recovery (FLAIR), Diffusion-weighted Imaging (DWI), and Dynamic Susceptibility Contrast (DSC) imaging. Among these, DSC-MRI, which assesses cerebral blood volume (CBV), serves as a quantitative measure of vascular density and tumor-induced angiogenesis [5].

The fifth edition of the World Health Organization Classification of Tumors of the Central Nervous System (WHO CNS5) has revolutionized glioma diagnosis and grading by integrating molecular parameters alongside traditional histological features. Key genetic markers such as *IDH1* mutation, 1p/19q codeletion, and *MGMT* promoter methylation status, *TERT* promoter mutation, *EGFR* amplification, *CDKN2A* homozygous deletion, now play a central role in glioma classification [6].

Previous studies have explored the correlation between MRI features and glioma genotypes, demonstrating the potential of imaging modalities to reflect underlying genetic profiles. However, these studies have been limited by small sample sizes, heterogeneous imaging protocols, and the need for the integration of advanced imaging techniques. The growing field of radiogenomics addresses these challenges by systematically linking imaging features with molecular data to predict tumor behavior, offering non-invasive insights into tumor genetics.

In this context, radiogenomics is emerging as a promising field that bridges the gap between clinical imaging and genomic data. It focuses on identifying relationships between imaging features and molecular markers, offering the potential for targeted therapies based on the tumor's genetic profile derived from imaging features. This integration of radiomics and genomics provides a more comprehensive understanding of gliomas and holds the potential for personalized treatment strategies [7–9].

This study aims to advance the current state of knowledge by identifying correlations between perfusion MRI findings and genetic markers in gliomas, thereby improving the accuracy of diagnosis and prognosis. The use of advanced perfusion MRI metrics as non-invasive biomarkers could significantly enhance routine clinical assessments, especially in situations where biopsy is not feasible or carries significant risks. Additionally, this research contributes valuable data to the field of neuro-oncology, potentially influencing future diagnostic and therapeutic strategies.

By leveraging the interdisciplinary nature of neuro-oncology, this study seeks to improve patient care and advance scientific understanding of brain tumors, ultimately supporting the development of more effective, personalized treatment approaches.

2. Materials and methods

2.1. Patient cohort

The study population consisted of patients undergoing surgery for brain tumors at the hospital. The inclusion criteria were: patients over 18 years of age with a confirmed diagnosis of glioma by histopathological examination and who underwent preoperative MRI with perfusion imaging (DSC). Exclusion criteria were incomplete data sets—patients who did not have the complete set of data required for a thorough analysis (Fig. 1).

2.2. Ethical considerations and patient consent

The Ethics Committee approved the study protocol. Rigorous data protection measures were employed to maintain the privacy and security of sensitive patient information.

2.3. Clinical data collection

The study conducted a thorough compilation of clinical data for every patient, encompassing essential criteria for evaluating performance status and tumor features. The information collected consisted of demographic factors such as age and sex, tumor characteristics such as location, laterality, and multiplicity, clinical symptoms, recurrence history, functional assessment using the Karnofsky Performance Status (KPS), handedness, smoking status, specific tumor diagnosis, tumor grade, and Body Mass Index (BMI). The large dataset provided an opportunity to conduct a thorough examination of the relationships between clinical variables, imaging findings, and genetic profiles.

2.4. MRI imaging

The MRI studies were conducted using a 1.5 T machine. This standardized protocol, presented in Table S1, was meticulously followed to ensure consistency and reliability of the imaging data. The MRI sequences included pre-and post-gadolinium T1- and T2-weighted images, Fluid-attenuated inversion recovery (FLAIR), Diffusion-weighted imaging (DWI), and dynamic susceptibility contrast (DSC) perfusion imaging. Special emphasis was placed on the perfusion imaging techniques, which are crucial for assessing the tumor's hemodynamic properties [10].

DSC perfusion MRI involves the administration of a bolus injection of a gadolinium-based contrast agent (dose: 0.1 mmol/kg body weight) followed by a saline flush. As the contrast agent passes through the brain vasculature, dynamic changes in signal intensity are captured using T2-weighted echo-planar imaging (EPI). This method allows for the calculation of perfusion parameters such as rCBF, rCBV, mean transit time (MTT), and time to peak (TTP).* The “relative” nature of these metrics refers to their normalization to reference regions, making them semi-quantitative measures rather than absolute values. DSC perfusion MRI is

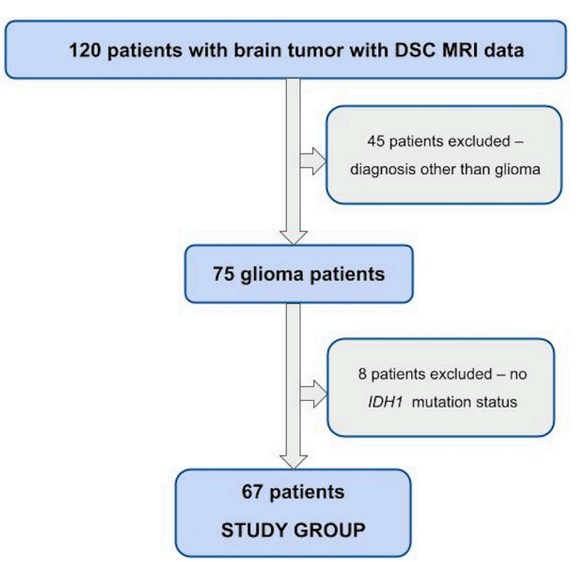

Fig. 1. Flowchart of the study.

a widely used technique in neuro-oncology because it provides key insights into tumor vascularity and angiogenesis.

2.5. Imaging data analysis

The imaging data were analyzed using advanced software tools specifically designed for neuro-oncology imaging. First, the raw imaging data underwent preprocessing to correct for motion artifacts and to align the images accurately, ensuring that images from different sequences and time points were properly registered for consistent analysis.

For the perfusion data from the DSC MRI, we employed a software package that implements deconvolution algorithms to extract key perfusion parameters. The arterial input function (AIF) was automatically identified, and parameters such as rCBF, rCBV, MTT, and TTP were calculated. These parameters were visualized as parametric maps, which facilitated the identification of regions with abnormal perfusion characteristics. Semiquantitative metrics were extracted from the parametric maps and regions of interest (ROIs), including mean values, standard deviations, and histogram analyses of the perfusion parameters within the ROIs.

The ROIs were identified and marked on areas of solid tumor tissue that exhibited the strongest enhancement on imaging and showed no evidence of necrosis, indicating regions of viable, actively proliferating tumor cells. Initially, the ROIs were drawn by a junior radiologist under the supervision of an experienced neuroradiologist with over 20 years of expertise in neuro-oncology imaging. The ROIs were delineated on all relevant slices displaying the target characteristics to ensure comprehensive coverage and accuracy.

To assess the T2/FLAIR mismatch, we used established radiological criteria. This concept, as clarified earlier in the manuscript, refers to a region where there is hyperintensity on T2-weighted images without corresponding hyperintensity on FLAIR images, which is suggestive of specific tumor characteristics. This evaluation was performed by the experienced neuroradiologist, ensuring the consistent application of criteria across all cases.

By following these rigorous analysis methods, we ensured the reliability and robustness of the derived perfusion parameters, providing valuable insights into the hemodynamic properties of the tumors.

2.6. Histopathological examination

The histopathological examination was an essential part of our study, providing detailed insights into the tumor's characteristics. Tissue samples were obtained during surgical resection of the brain tumors. These samples were immediately preserved and processed according to standard histopathological protocols. The preserved tissue was then sectioned and stained using routine hematoxylin and eosin staining for initial assessment.

These samples were analyzed by experienced neuropathologists, who classified the tumors according to the latest WHO classification of central nervous system tumors. The classification included an assessment of morphological features and the presence of specific histological patterns [6].

2.7. Genetic analysis

In addition to the histopathological examination, genetic analysis was performed on the tumor tissues. The genetic markers analyzed included *IDH1* mutation status, *MGMT* methylation, *EGFR* amplification, *CDKN2A* deletion, *TP53* deletion, *PDGFRA* amplification, *PTEN* deletion, 1p19q codeletion, *TERT* pathogenic variants, and H3F3A (K27M) pathogenic variants. These genetic markers were selected due to their established relevance in brain tumor pathology and prognosis. The analysis of these genetic markers was carried out using standard molecular techniques, such as polymerase chain reaction (PCR), fluorescence in situ hybridization (FISH), and next-generation sequencing (NGS), to provide a comprehensive genetic profile of each tumor.

2.8. Statistical analysis

The Shapiro–Wilk test was performed to test the normality of data. The Mann–Whitney and chi-square tests were used to determine statistically significant differences between two groups of independent variables, depending on whether the data were continuous or categorical, respectively. We performed cut-off point analysis using ROC curve sensitivity and specificity to identify optimal threshold values for differentiating between genetic profiles of brain tumors. To ensure the accuracy and reliability of our results, samples with NA (Not Available) genetic data were excluded from the statistical analysis. This exclusion was consistently applied across all groups to maintain uniformity in our comparisons and conclusions. The findings were measured using 95 % confidence intervals (95 % CI), and a p-value of 0.05 was considered statistically significant. All statistical analyses were conducted using the R Studio.

3. Results

3.1. Patient characteristics

Table 1 presents a detailed overview of the demographic and clinical characteristics of the study participants.

The cohort comprised 67 individuals, with a gender distribution of 29 females (43.3 %) and 38 males (56.7 %). The mean age of the participants was 51 years, with a standard deviation (SD) of 15.

The table also illustrates the prevalence of various neurological symptoms among the study participants. Paresis, characterized by muscle weakness or paralysis, was observed in 18 cases (26.9 %). The same number of patients had symptoms of epilepsy. Headaches were observed in 14 (20.9 %) cases. Balance disorders, affecting coordination, were present in 7 (10.4 %) cases, while speech disorders were identified in 11 cases (16.4 %). Memory disorders, disturbances of consciousness, and blurred vision were reported in 6 (9 %), 10 (14.9 %), and 8 (11.9 %) cases, respectively. Other symptoms such as retardation, and paresthesia (abnormal sensations) were less frequent, with 2 (3 %), and 4 cases (6 %) respectively.

Table 1
Patients' characteristics.

		N	%
Gender			
	Male	38	56.7
	Female	29	43.3
Age (Mean; SD)		51	15
KPS (Mean; SD)		83	11
Handedness			
	Right	57	95
	Left	2	3.3
	Both	1	1.7
Smoker			
	No	42	77.8
	Yes	12	22.2
BMI (Mean; SD)		26.1	5.8
Symptoms			
	Epilepsy	18	26.9
	Paresis	18	26.9
	Headache	14	20.9
	Speech disorders	11	16.4
	Disturbances of consciousness	10	14.9
	Blurred vision	8	11.9
	Balance disorders	7	10.4
	Memory disorders	6	9.0
	Paresthesia	4	6.0
	Retardation	2	3.0

Note: N = 67; SD – Standard Deviation, KPS – Karnofsky Performance Status; BMI – Body Mass Index.

3.2. Tumor characteristics

In this study, a comprehensive analysis of the diagnosed brain tumors was conducted, revealing diverse molecular and pathological characteristics (see Table 2). The distribution of primary brain tumor diagnoses among the studied population includes 39 cases of glioblastoma, 19 cases of astrocytoma, and 9 cases of oligodendroglioma. Tumor grades were stratified into Grade 2 (9 cases, 13.4 %), Grade 3 (19 cases, 28.4 %), and the most prevalent Grade 4 (39 cases, 58.2 %). This classification provides important insights into the spectrum of malignancy levels observed in the cohort.

Examining the molecular landscape, the study assessed the presence of key genetic alterations. Notably, *IDH1* mutation status revealed 58.2 % of cases as wildtype and 41.8 % as mutant. *MGMT* methylation, a critical marker for treatment response, demonstrated 63.1 % of cases as methylated and 36.9 % as unmethylated. Further exploration of molecular markers included *EGFR* amplification (47 %), *CDKN2A* deletion (50.7 % non-deleted, 35.8 % heterozygous deletion, 11.9 % homozygous deletion), *TP53* deletion (98.4 % non-deleted, 1.6 % deleted), *PDGFRA* amplification (34.4 % amplified, 86.9 % non-amplified), *PTEN* deletion (13.1 % deleted, 65.6 % non-deleted), 1p19q codeletion (12.1 % codeleted, 87.9 % non-codeleted), *TERT* pathogenic variant (53.6 % present, 46.4 % absent), and H3K27M pathogenic variant (100 % absent). Fig. 2 presents the landscape of genetic alteration in the examined cohort.

Table 2
Diagnosis and molecular characteristics.

		N	%
Diagnosis			
	Astrocytoma	20	
	Glioblastoma	38	
	Oligodendroglioma	9	
Grade			
	2	10	14.9
	3	19	28.4
	4	38	56.7
IDH1 mutation			
	Wildtype	39	58.2
	Mutant	28	41.8
MGMT methylation			
	Unmethylated	24	36.9
	Methylated	41	63.1
EGFR amplification			
	No	35	53
	Yes	31	47
CDKN2A deletion			
	Non-deleted	34	50.7
	Heterozygous deletion	24	35.8
	Homozygous deletion	8	11.9
	NA	1	1.5
TP53 deletion			
	Non-deleted	60	98.4
	Deleted	1	1.6
PDGFRA amplification			
	Non-amplified	53	86.9
	Amplified	21	34.4
PTEN deletion			
	Deleted	8	13.1
	Non-deleted	40	65.6
1p19q codeletion			
	Non-codeleted	58	87.9
	Codeleted	8	12.1
TERT pathogenic variant			
	No	26	46.4
	Yes	30	53.6
H3K27M pathogenic variant			
	No	47	100

Note: *IDH1* – isocitrate dehydrogenase 1; *MGMT* – O^6-methylguanine-DNA methyltransferase; *EGFR* – epidermal growth factor receptor; *CDKN2 A* – loss of cyclin-dependent kinase inhibitor 2 A; *PDGFRA* – platelet-derived growth factor receptor alpha gene; *PTEN* – phosphatase and tensin homolog; *TERT* – telomerase reverse transcriptase.

3.3. Imaging findings

In this investigation, a thorough analysis of imaging and perfusion parameters has been conducted to provide a detailed characterization of the observed brain lesions (Table 3).

The distribution of contrast enhancement revealed that 40.3 % of cases exhibited no contrast enhancement, while 59.7 % showed contrast enhancement. Contrast enhancement serves as a critical indicator of blood-brain barrier disruption, commonly observed in higher-grade gliomas such as glioblastomas, and reflects the tumor's vascular permeability and aggressiveness.

The presence of the T2/FLAIR mismatch sign was noted in 13.4 % of cases, whereas the majority (86.6 %) exhibited no such mismatch. The T2/FLAIR mismatch sign, a hallmark feature strongly associated with IDH1-mutant astrocytomas, underscores its value in identifying specific molecular subtypes of gliomas and differentiating them from other tumor types.

Numerical values representing the mean and standard deviation for various ROIs were also analyzed. These include:

- Region of Interests (ROIs): regions representing the most viable tumor tissue with the strongest contrast enhancement, excluding necrotic or cystic regions.
- Relative Cerebral Blood Flow (rCBF): rCBF values were measured in ROI1 (tumor core) and ROI2 (reference tissue). Higher rCBF values in ROI1 indicate increased vascular activity, characteristic of aggressive or high-grade tumors.
- Relative Cerebral Blood Volume (rCBV): rCBV values were similarly assessed in ROI1 and ROI2. Increased rCBV values reflect greater tumor vascularity and angiogenesis, serving as a reliable marker for glioma grading and molecular profiling.
- Mean Transit Time (MTT) and Time to Peak (TTP): These parameters provide insights into blood flow dynamics within the tumor. Prolonged MTT and altered TTP values in ROI1 compared to ROI2 may indicate abnormal perfusion patterns associated with tumor-induced angiogenesis.

These semiquantitative metrics reflect differences in tumor grade, vascularity, and molecular subtypes. Higher rCBV and rCBF values in glioblastomas compared to astrocytomas and oligodendrogliomas align with their aggressive angiogenic profiles. The T2/FLAIR mismatch sign in IDH1-mutant astrocytomas further highlights the role of advanced imaging in identifying genetic alterations. This study underscores the potential of perfusion parameters as non-invasive biomarkers for glioma diagnosis, grading, and molecular classification.

3.3.1. Correlations between radiological features and genetic alterations in primary brain tumors

In our comprehensive analysis of the study results, we investigated the intricate relationship between basic radiological features and genetic alterations in patients diagnosed with brain tumors.

Table 4 sheds light on the associations between contrast enhancement, T2/FLAIR mismatch, and key genetic markers, providing valuable insights into the interplay between molecular characteristics and radiological manifestations.

We observed a statistically significant association between contrast enhancement patterns and several genetic alterations. Notably, *IDH1* wildtype cases exhibited a distinct propensity for contrast enhancement, 32 out of 39 had contrast enhancement (82 %), while 8 out of 28 (29 %) *IDH1* mutant had contrast enhancement ($p = 0.000$). Similarly, cases with *EGFR* amplification were notably more likely to exhibit contrast enhancement ($p = 0.019$), emphasizing the potential influence of this genetic alteration on radiological characteristics. The relationship between *CDKN2 A* deletion and contrast enhancement was also statistically significant ($p = 0.038$). Non-deleted and heterozygous deletion cases exhibited a lower likelihood of contrast enhancement, suggesting a

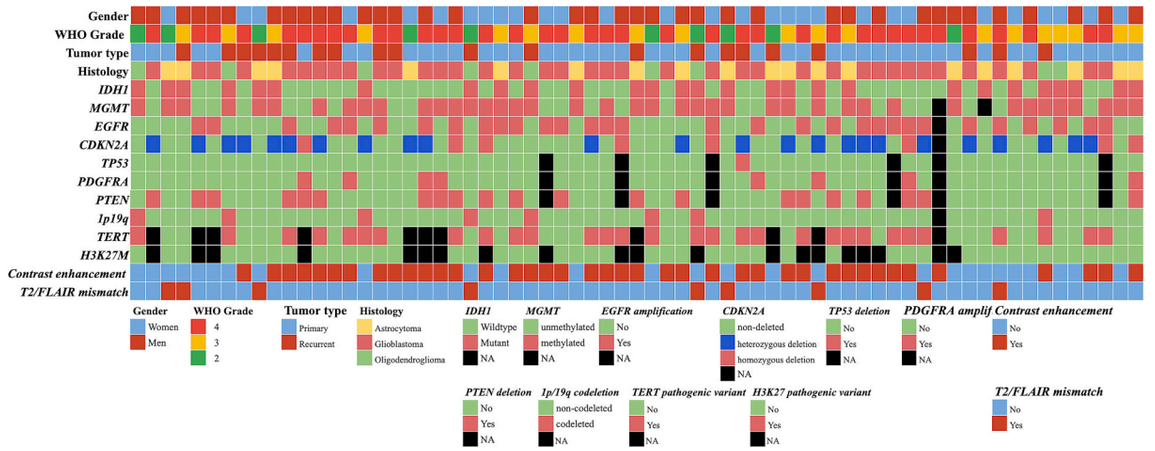

Fig. 2. The genetic landscape of glioma patients. WHO – World Health Organization; *IDH1* – isocitrate dehydrogenase 1; *MGMT* – O^6-methylguanine-DNA methyltransferase; *EGFR* – epidermal growth factor receptor; *CDKN2 A* – loss of cyclin-dependent kinase inhibitor 2 A; *PDGFRA* – platelet-derived growth factor receptor alpha gene; *PTEN* – phosphatase and tensin homolog; *TERT* – telomerase reverse transcriptase; FLAIR – fluid-attenuated inversion recovery.

Table 3
Imaging and perfusion parameters.

		N / Mean	% / Standard Deviation
Contrast Enhancement			
	No	27	40.3
	Yes	40	59.7
T2/FLAIR Mismatch sign			
	No	58	86.6
	Yes	9	13.4
ROIs [mm^2]		79.3	92.4
rCBFROI1		52.2	37.8
rCBFROI2		20	20.8
rCBVROI1		531	630.6
rCBVROI2		133.2	89.6
MTTROI1 [s]		10.2	5.6
MTTROI2 [s]		7.6	3.3
TTPROI1 [s]		46.5	12.6
TTPROI2 [s]		45.6	13.1
T0ROI1 [s]		40.6	11.1
T0ROI2 [s]		41.4	12
rCBF		3.4	2.5
rCBV		4.3	3

Note: ROIs – region of interest surface; rCBF – relative cerebral blood flow; rCBV – relative cerebral blood volume; MTT – mean transit time; TTP – time to peak.

potential role of *CDKN2 A* alterations in influencing these radiological patterns. Furthermore, 1p19q codelated tumors were statistically more likely to fail to contrast enhance on imaging than 1p19q non-codelated tumors ($p = 0.036$). The relationship between the *TERT* pathogenic variant and contrast enhancement was also statistically significant ($p = 0.009$). Tumors with the *TERT* pathogenic variant are significantly more frequently contrast-enhanced than those without the pathogenic variant.

Investigating the T2/FLAIR mismatch sign, we found significant associations with *IDH1* mutation status ($p = 0.019$). Cases with specific *IDH1* mutation status were more likely to exhibit the T2/FLAIR mismatch sign, highlighting the potential relevance of this mutation in shaping distinctive radiological features.

3.3.2. Exploring the relationship between MRI perfusion metrics and genetic markers in primary brain tumors

Our investigation delved into the complex relationship between MRI perfusion parameters and genetic features in patients diagnosed with glioma, offering a deeper understanding of the underlying molecular and radiological intricacies. Table 5 illustrates the associations between perfusion characteristics and key genetic markers.

Examining the mean values of rCBF and rCBV, where similar patterns emerged, across different diagnoses, we observed significant differences. Glioblastoma displayed a markedly higher mean compared to astrocytoma and oligodendroglioma ($p < 0.05$). Analyzing perfusion in the context of tumor recurrence, primary tumors exhibited significantly higher mean rCBF and rCBV compared to recurrent tumors ($p < 0.05$). Considering tumor grade, Grade 4 tumors displayed a substantially higher mean rCBF and rCBV compared to Grade 2 and Grade 3 tumors. The higher the grade the higher the mean rCBF and rCBV. Moving to genetic markers, tumors *IDH1* wildtype exhibited significantly higher mean rCBF and rCBV compared to *IDH1* mutant cases ($p < 0.05$). Similarly, tumors with *EGFR* amplification showed a higher mean rCBF and rCBV compared to those without amplification ($p < 0.05$). These findings emphasize the impact of genetic alterations on perfusion characteristics. Representative examples of the analysis are illustrated in Figs. 3 and 4.

Additionally, tumors with *CDKN2A* homozygous deletion displayed a significantly higher mean rCBV compared to non-deleted and heterozygous deletion cases ($p < 0.05$). This reinforces the association between specific genetic alterations and perfusion patterns. Moreover, tumors with *PDGFRA* amplification present significantly higher rCBV than those without this amplification.

3.4. Optimization of rCBV cut-off values for genetic marker prediction in glioma

Based on our analysis, it was determined that the maximum sensitivity and specificity for accurately predicting the *IDH1* mutation status from rCBV measurements were achieved when the cut-off point exceeded 4. This resulted in a sensitivity of 0.615 and a specificity of 0.821, accompanied by an ROC value of 0.683 ($p < 0.05$; Fig. 5A). The highest sensitivity and specificity for correctly identifying *CDKN2A* deletion status from rCBV measurements were achieved with a cut-off value greater than 5, resulting in a sensitivity of 0.75 and a specificity of 0.746, accompanied by an ROC value of 0.78 ($p < 0.05$; Fig. 5B).

4. Discussion

The comprehensive analysis of advanced MRI perfusion metrics in conjunction with genetic, histopathological, and clinical data has unveiled a multifaceted landscape of brain tumors and represents a pivotal advancement in understanding these malignancies.

Previous research underscores rCBV as a dependable marker for glioma grading [11–14] with high-grade gliomas (HGG, WHO grades 3

Table 4
The relationship between basic radiological and genetic features.

		Contrast enhancement			T2/FLAIR mismatch		
		Absent	Present	p	Absent	Present	p
IDH1 mutation	wildtype	7	32	**0.000***	37	2	**0.019***
	mutant	20	8		21	7	
MGMT methylation	unmethylated	6	18	0.059	22	2	0.325
	methylated	20	21		34	7	
EGFR amplification	No	19	16	**0.019***	28	7	0.109
	Yes	8	23		29	2	
CDKN2A deletion	non-deleted	18	16	**0.038***	28	6	0.586
	heterozygous deletion	9	15		21	3	
	homozygous deletion	0	8		8	0	
	NA	0	1		1	0	
TP53 deletion	No	27	33	0.369	51	9	0.675
	Yes	0	1		1	0	
PDGFRA amplification	No	26	27	0.052	45	8	0.847
	Yes	1	7		7	1	
PTEN deletion	No	23	17	**0.004***	32	8	0.111
	Yes	4	17		20	1	
1p19q codeletion	No	21	37	**0.036***	51	7	0.318
	Yes	6	2		6	2	
TERT pathogenic variant	No	15	11	**0.009***	21	5	0.325
	Yes	7	23		27	3	
H3K27M pathogenic variant	No	20	27		40	7	

Note: * The Chi-square statistic is significant at the 0.05 level. *IDH1* – isocitrate dehydrogenase 1; *MGMT* – O6-methylguanine-DNA methyltransferase; *EGFR* – epidermal growth factor receptor; *CDKN2A* – loss of cyclin-dependent kinase inhibitor 2A; *PDGFRA* – platelet-derived growth factor receptor alpha gene; *PTEN* – phosphatase and tensin homolog; *TERT* – telomerase reverse transcriptase.

Table 5
Relationship between MRI perfusion and genetic features.

		rCBF		rCBV	
		Mean	p	Mean	p < 0.05
Diagnosis	Astrocytoma	2.9		3.5	
	Glioblastoma	3.9		5.2	**p < 0.05**
	Oligodendroglioma	2.2		2.4	
Tumor	Primary	3.9	**p < 0.05**	4.8	**p < 0.05**
	Recurrent	2.2		3.3	
Grade	2	2.6		2.9	
	3	2.7		3.3	
	4	3.9		5.2	
IDH1 mutation	wildtype	3.9	**p < 0.05**	5.2	**p < 0.05**
	mutant	2.7		3.1	
MGMT methylation	unmethylated	3.8		5	
	methylated	3.2		4	
EGFR amplification	No	2.8	**p < 0.05**	4.1	
	Yes	4.1		4.6	
CDKN2A deletion	nondeleted	3.1		3.7	
	heterozygous deletion	3.2		4.3	**p < 0.05**
	homozygous deletion	4.9		7	
TP53 deletion	No	3.3		4.2	
	Yes	3.9		8.3	
PDGFRA amplification	No	3.2		3.9	**p < 0.05**
	Yes	4.2		6.4	
PTEN deletion	No	3.1		3.9	
	Yes	3.7		5.1	
1p19q codeletion	No	3.5		4.6	
	Yes	2.3		2.5	
TERT pathogenic variant	No	2.9		3.8	
	Yes	4.2		4.8	
H3k27 pathogenic variant	No	3.3		4	

Note: Results are based on two-sided tests assuming equal variances. *IDH1* – isocitrate dehydrogenase 1; *MGMT* – O^6-methylguanine-DNA methyltransferase; *EGFR* – epidermal growth factor receptor; *CDKN2A* – loss of cyclin-dependent kinase inhibitor 2A; *PDGFRA* – platelet-derived growth factor receptor alpha gene; *PTEN* – phosphatase and tensin homolog; *TERT* – telomerase reverse transcriptase.

and 4) exhibiting increased rCBV compared to low-grade gliomas (LGG, WHO grades 1 and 2) [15–17], what aligns with our findings that higher tumor grades correlate with elevated rCBV and rCBF. The direct correlation between tumor grade and vascular parameters such as rCBV and rCBF suggests that HGG has increased vascular proliferation. This phenomenon indicates the tumor's aggressive nature, as angiogenesis is essential for supplying the rapidly proliferating tumor cells with nutrients and oxygen. The increase in blood flow and blood volume could be a response to the hypoxic conditions within the tumor microenvironment [18]. Our study also revealed significant variances in mean rCBV and rCBF ratios across different tumor diagnoses, with glioblastomas showing markedly higher means compared to less malignant tumors like astrocytomas or oligodendrogliomas.

Further, our research identified a significant association between primary and recurrent tumors, where primary tumors demonstrated higher rCBF and rCBV ratios, suggesting more pronounced angiogenic activity than recurrent tumors. This difference may reflect a complex interplay of factors, including the impact of treatments like radiation therapy and chemotherapy, which can induce vascular damage and alter the tumor's biological behavior upon recurrence [19,20].

Our findings highlight significant variances in perfusion metrics, particularly rCBV and rCBF, in gliomas with different genetic profiles, revealing a nuanced interplay between tumor genetics and vascular properties. All of these phenomena can be elucidated by their impact on angiogenesis and, as a result, perfusion. We found that *IDH1* wildtype tumors had significantly higher rCBV and rCBF than *IDH1* mutant cases. This is supported by previous literature. A study conducted by Kickingereder et al. reveals that *IDH1* mutant tumors show decreased expression of hypoxia-inducible-factor 1-alpha (HIF1A) targets, leading to strong inhibition of angiogenesis [21]. Our observation that tumors with *EGFR* amplification exhibit higher mean values for rCBF and rCBV also aligns with prior research [22–26]. Collectively, these studies emphasize the critical role of *EGFR* amplification in promoting vascular growth and remodeling within tumors, offering potential targets for therapeutic intervention and non-invasive diagnostic markers through advanced MRI techniques. The relationship between *CDKN2A* homozygous deletion and the increased mean rCBV in tumors was was also observed in a study conducted by Park et al., which found that a higher 95th percentile of rCBV could independently predict the status of

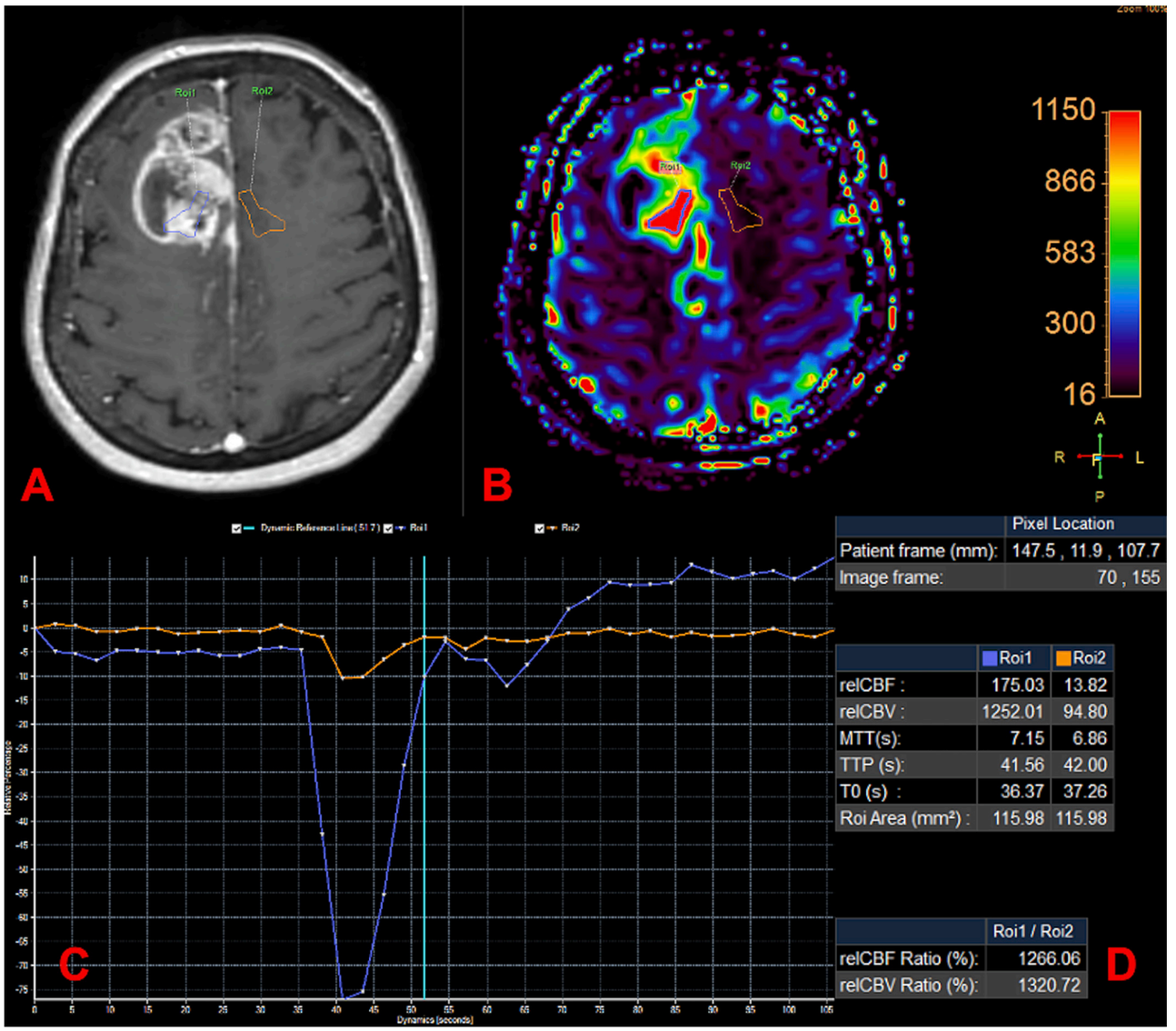

Fig. 3. MRI examination of a patient diagnosed with Glioblastoma (G4). Molecular characteristics: *IHD1*-wt, *MGMT* methylated, *EGFR* amplification, *CDKN2 A* homozygous deletion, 1p19q non-codeleted, *TERT* pathogenic variant. Imaging analysis: rCBV = 13.2; rCBF = 12.7. **A.** T1 post-contrast. **B.** DSC MRI - CBV map. **C.** DSC MRI - histogram. **D.** DSC MRI - perfusion features.

CDKN2A/B homozygous deletion [27]. This correlation is crucial as earlier pathological studies have indicated that *CDKN2A/B* homozygous deletion in gliomas is associated with high proliferative indices, suggesting a more aggressive tumor behavior [28,29]. The elevated rCBV observed in *IDH* mutant astrocytomas with *CDKN2A/B* deletion possibly indicates an increase in angiogenic activity driven by the loss of these tumor suppressor genes [30]. The *CDKN2A/B* locus plays a vital role in mediating anti-angiogenic effects within gliomas, restricting tumor growth by limiting the availability of nutrients and oxygen through inhibiting tumor-induced neovascularization [31]. Moreover, tumors with *PDGFRA* amplification present significantly higher rCBV than those without this amplification. *PDGFRA* is a cell surface tyrosine kinase receptor that, upon activation, triggers various signaling pathways involved in cell proliferation, migration, and angiogenesis. Amplification of *PDGFRA* leads to the overactivation of these pathways, promoting the formation of new blood vessels to supply the growing tumor with necessary nutrients and oxygen [32].

The statistically significant relationship between genetic status and contrast enhancement on MRI images in brain tumors underlines the impact of genetic alterations on the tumor's radiographic appearance, specifically its interaction with the blood-brain barrier. The pronounced contrast enhancement in *IDH1* wildtype tumors points to a higher grade and more aggressive tumor phenotype, often linked with disturbed BBB integrity [33]. Additionally, the association of *TERT* pathogenic variants with higher rates of contrast enhancement reflects the aggressive nature of these tumors, likely due to their enhanced proliferative capacity and potential for rapid growth and invasion. Telomeres extension enables cells to evade the normal limits of cellular replication, which in turn could affect the tumor's vasculature [34]. Moreover, 1p19q codelated tumors were statistically more likely to fail to contrast enhance on imaging than 1p19q non-codelated tumors. The 1p19q codeletion is a well-recognized favorable prognostic marker in oligodendrogliomas and is associated with a better response to chemotherapy and radiotherapy.

The T2/FLAIR mismatch sign, characterized by a lesion's hyperintensity on T2-weighted MRI scans and corresponding hypointensity on FLAIR images, has emerged as a crucial radiogenomic marker. This

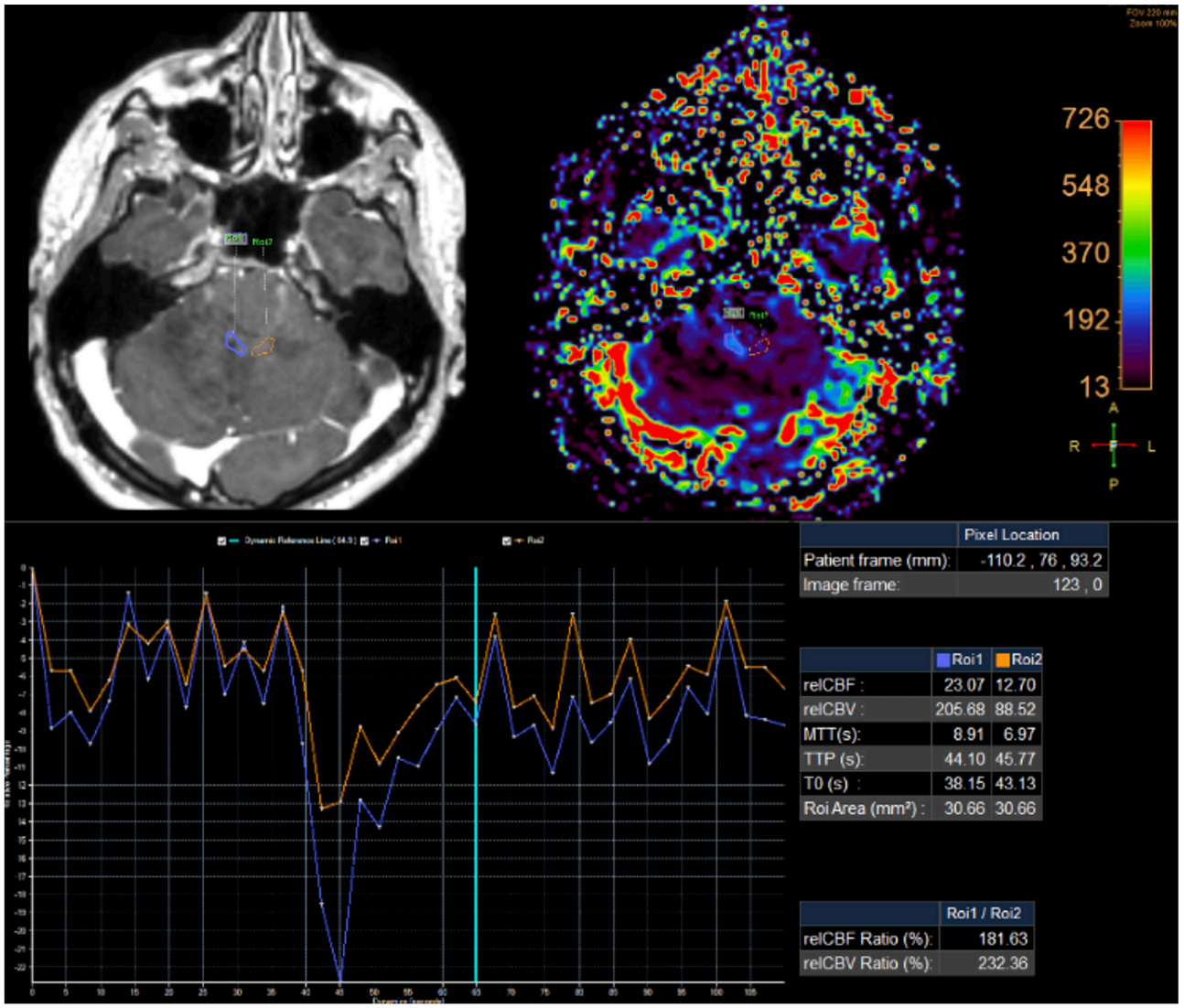

Fig. 4. MRI examination of a patient diagnosed with Astrocytoma (G2). Molecular characteristics: *IHD1*-mt, *MGMT* methylated, *EGFR* non-amplification, *CDKN2 A* non-deleted, 1p19q non-deleted, no *TERT* pathogenic variant. Imaging analysis: rCBV = 2.3; rCBF = 1.8. **A.** T1 post-contrast. **B.** DSC MRI - CBV map. **C.** DSC MRI - histogram. **D.** DSC MRI - perfusion features.

specific imaging phenotype is highly indicative of astrocytomas harboring *IDH* mutations, with an intact 1p19q status, effectively differentiating them from other LGG [35,36]. A meta-analysis conducted in 2021 underscored the diagnostic precision of the T2/FLAIR mismatch sign for identifying tumors with an *IDH* mutant and 1p19q non-codeleted genetic profile, reporting a remarkable pooled specificity of 100 %. However, the sensitivity of this marker was found to be considerably lower, at just 42 % [37]. Our findings revealed that tumors harboring specific *IDH1* mutations were more likely to present with this distinctive imaging feature, underscoring the critical role of the *IDH1* mutation in influencing the tumor's radiological characteristics.

The *IDH1* gene status assessment seems to be a crucial step in the management of a patient with astrocytoma. Based on the *IDH1* genetic analysis and histopathological findings, the direction of further molecular diagnostics should be set [6,38]. Hence, possessing the ability to determine the *IDH1* mutation status during the non-invasive imaging phase of diagnosing might prove advantageous. To date, little effort has been made by researchers to establish threshold values for quantitative parameters acquired during MRI examinations, despite the practical relevance of such data in daily clinical settings. In their study, Xing et al. introduced a threshold value of 2.35 for rCBV in the context of predicting *IDH1* mutation. This threshold value yielded a sensitivity of 100.0 %, specificity of 60.9 %, positive predictive value of 85.6 %, and negative predictive value of 100.0 % [39]. Tan et al. categorized gliomas based on the degree of tumor malignancy and established thresholds for mutations in the *IDH1* gene. Significant variations were seen in the rCBV ratio between the *IDH1* gene mutant and wildtype groups of WHO grade 2, 3, and 4 astrocytomas ($p = 0.005$, 0.045, and 0.005, respectively). The ROC curve for WHO grade 2, 3, and 4 astrocytomas was found to be 0.83, 0.86, and 0.94, respectively. The rCBV ratio was determined to have cutoff values of 2.20, 3.14, and 5.63, respectively [40]. Nevertheless, the clinical use of this technique may be hampered due to the absence of histological confirmation of tumor grade at this diagnostic stage. A cut-off value of 4 was proposed for the *IDH1* mutation, regardless of the other tumor features. While it may have lower sensitivity and specificity, it can be widely employed at the very early phase of tumor diagnosis.

All of the proposed cut-off values, their applicability across different

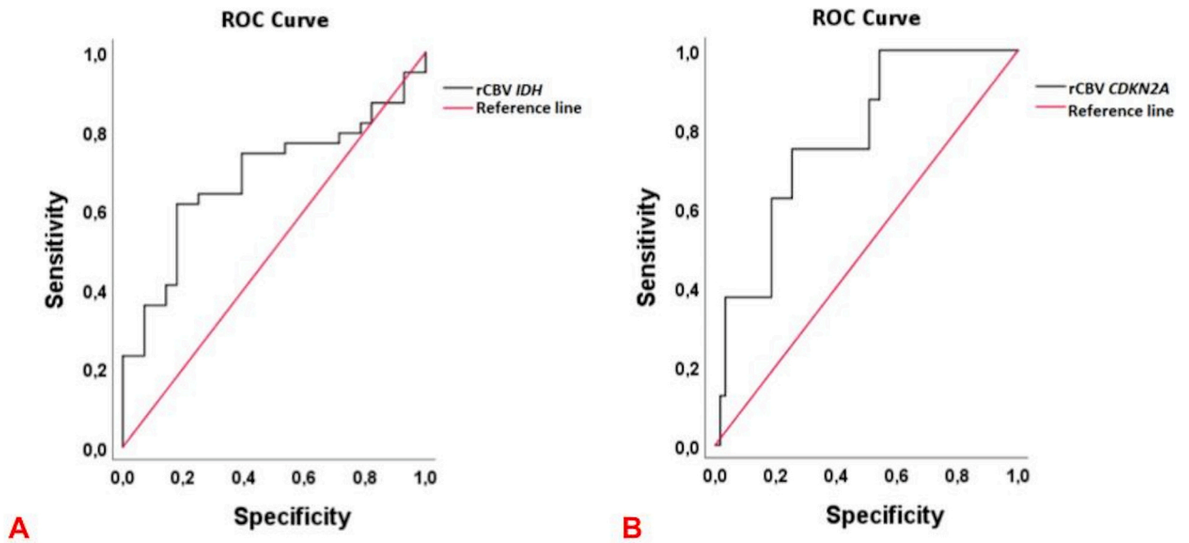

Fig. 5. ROC curves using rCBV ratio values to determine the **A.** *IDH1* gene status (cut-off >4 with a sensitivity of 0.615 and a specificity of 0.821, accompanied by an ROC value of 0.683) and **B.** *CDKN2A* status (with a cut-off value greater than 5, resulting in a sensitivity of 0.75 and a specificity of 0.746, accompanied by an ROC value of 0.78).

institutions and imaging setups warrants careful consideration. Variability in MRI hardware, field strengths (e.g., 1.5 T vs. 3 T), acquisition protocols, and post-processing software can lead to differences in perfusion measurements, potentially affecting the reproducibility of these thresholds. Standardization of imaging protocols is essential for ensuring that the proposed thresholds can be reliably applied in broader clinical contexts. This includes harmonizing DSC imaging techniques, preprocessing pipelines, and normalization methods. Multi-institutional studies with larger and more diverse patient cohorts will also be necessary to validate the robustness of these thresholds and account for inter-site variability. Despite these challenges, the proposed cut-offs serve as a foundation for further exploration and may act as reference points for institutions to adapt based on their specific settings and calibration protocols. Moreover, the integration of machine learning and artificial intelligence could improve the precision and adaptability of these thresholds by identifying complex patterns in perfusion data that are less sensitive to inter-scanner variability. These tools could help refine and validate threshold values in future studies.

4.1. Limitations of the study

This study, while comprehensive, is not without limitations. One potential limitation is the sample size, which may not be large enough to generalize the findings to all brain tumor patients. Another area for improvement is the reliance on data from a single institution, which may not reflect the diversity of patient populations and medical practices elsewhere. Potential biases in MRI scan interpretation must also be acknowledged, as they could influence the study's conclusions. Finally, the complexity of brain tumors and the multifactorial nature of their development mean that not all influencing factors may have been accounted for or measured in this study. Recognizing these limitations is crucial for the accurate interpretation of the study's findings and for guiding future research. Another important limitation is the variability between MRI systems, which may impact the direct application of the proposed CBV and CBF cut-offs across different clinical settings. This variability highlights the importance of standardization and external validation.

4.2. Future research directions

The findings of this study pave the way for several avenues in future research. A primary direction would be to conduct longitudinal studies with larger and more diverse populations to validate and expand upon our findings. Future research should also consider multi-center collaborations to increase the generalizability of the results and to encompass a broader range of genetic and clinical variables. Moreover, incorporating machine learning and artificial intelligence in analyzing complex datasets could provide deeper insights and predictive models in neuro-oncology. Finally, studies focusing on patient-reported outcomes and quality of life post-treatment would add valuable dimensions to the understanding of the holistic impact of brain tumors and their treatments.

5. Conclusions

In conclusion, this study underscores the importance of integrating genetic, clinical, and imaging data to enhance our understanding of brain tumors. When analyzed alongside detailed genetic profiles, the insights gleaned from perfusion MRI offer a window into the genetic influence on tumor phenotype. This integrative approach not only enriches our understanding of tumor biology but also paves the way for more targeted and effective treatment strategies, ultimately contributing to improved patient outcomes.

Funding

The authors received no financial support for the research, authorship, and publication of this article.

Institutional review board statement

The study was conducted in accordance with the Declaration of Helsinki, and The Ethics Committee of the Nicolaus Copernicus University, Collegium Medicum in Bydgoszcz, Poland approved the study protocol.

Informed consent statement

Informed consent was obtained from all subjects involved in the study.

CRediT authorship contribution statement

Paulina Śledzińska-Bebyn: Writing – original draft, Software, Project administration, Methodology, Investigation, Formal analysis, Data curation, Conceptualization. **Jacek Furtak:** Writing – review & editing, Resources, Funding acquisition. **Marek Bebyn:** Writing – review & editing, Visualization, Data curation. **Alicja Bartoszewska-Kubiak:** Resources. **Zbigniew Serafin:** Writing – review & editing, Supervision, Methodology, Funding acquisition.

Declaration of Generative AI and AI-assisted technologies in the writing process

Authors disclose the use of AI and AI-assisted technologies in the writing process.

Declaration of competing interest

The authors declare that they have no known competing financial interests or personal relationships that could have appeared to influence the work reported in this paper.

Data availability

All data relevant to this study are reported within the manuscript.

Appendix A. Supplementary data

Supplementary data to this article can be found online at https://doi.org/10.1016/j.mri.2024.110318.

References

[1] Ostrom QT, Bauchet L, Davis FG, Deltour I, Fisher JL, Langer CE, et al. The epidemiology of glioma in adults: a "state of the science" review. Neuro-Oncol 2014;16:896–913. https://doi.org/10.1093/neuonc/nou087.

[2] Stupp R, Mason WP, van den Bent MJ, Weller M, Fisher B, Taphoorn MJB, et al. Radiotherapy plus concomitant and adjuvant temozolomide for glioblastoma. N Engl J Med 2005;352:987–96. https://doi.org/10.1056/NEJMoa043330.

[3] Molinaro AM, Hervey-Jumper S, Morshed RA, Young J, Han SJ, Chunduru P, et al. Association of maximal extent of resection of contrast-enhanced and non-contrast-enhanced tumor with survival within molecular subgroups of patients with newly diagnosed glioblastoma. JAMA Oncol 2020;6:495–503. https://doi.org/10.1001/jamaoncol.2019.6143.

[4] Gutman DA, Cooper LAD, Hwang SN, Holder CA, Gao J, Aurora TD, et al. MR imaging predictors of molecular profile and survival: multi-institutional study of the TCGA glioblastoma data set. Radiology 2013;267:560–9. https://doi.org/10.1148/radiol.13120118.

[5] Pak E, Choi SH, Park C-K, Kim TM, Park S-H, Won J-K, et al. Added value of contrast leakage information over the CBV value of DSC perfusion MRI to differentiate between pseudoprogression and true progression after concurrent chemoradiotherapy in glioblastoma patients. Investig Magn Reson Imag 2022;26:10. https://doi.org/10.13104/imri.2022.26.1.10.

[6] Louis DN, Perry A, Wesseling P, Brat DJ, Cree IA, Figarella-Branger D, et al. The 2021 WHO classification of tumors of the central nervous system: a summary. Neuro-Oncol 2021. https://doi.org/10.1093/neuonc/noab106. noab106.

[7] Rutman AM, Kuo MD. Radiogenomics: creating a link between molecular diagnostics and diagnostic imaging. Eur J Radiol 2009;70:232–41. https://doi.org/10.1016/j.ejrad.2009.01.050.

[8] Narang S, Lehrer M, Yang D, Lee J, Rao A. Radiomics in glioblastoma: current status, challenges and potential opportunities. Transl Cancer Res 2016:5. https://doi.org/10.21037/tcr.2016.06.31.

[9] Hu LS, Ning S, Eschbacher JM, Baxter LC, Gaw N, Ranjbar S, et al. Radiogenomics to characterize regional genetic heterogeneity in glioblastoma. Neuro-Oncol 2017;19:128–37. https://doi.org/10.1093/neuonc/now135.

[10] Boxerman JL, Quarles CC, Hu LS, Erickson BJ, Gerstner ER, Smits M, et al. Consensus recommendations for a dynamic susceptibility contrast MRI protocol for use in high-grade gliomas. Neuro-Oncol 2020;22:1262–75. https://doi.org/10.1093/neuonc/noaa141.

[11] Donahue KM, Krouwer HG, Rand SD, Pathak AP, Marszalkowski CS, Censky SC, et al. Utility of simultaneously acquired gradient-echo and spin-echo cerebral blood volume and morphology maps in brain tumor patients. Magn Reson Med 2000;43:845–53. https://doi.org/10.1002/1522-2594(200006)43:6<845::aid-mrm10>3.0.co;2-j.

[12] Sugahara T, Korogi Y, Kochi M, Ikushima I, Hirai T, Okuda T, et al. Correlation of MR imaging-determined cerebral blood volume maps with histologic and angiographic determination of vascularity of gliomas. AJR Am J Roentgenol 1998;171:1479–86. https://doi.org/10.2214/ajr.171.6.9843274.

[13] Lev MH, Ozsunar Y, Henson JW, Rasheed AA, Barest GD, Harsh GR, et al. Glial tumor grading and outcome prediction using dynamic spin-echo MR susceptibility mapping compared with conventional contrast-enhanced MR: confounding effect of elevated rCBV of oligodendrogliomas [corrected]. AJNR Am J Neuroradiol 2004;25:214–21.

[14] Schmainda KM, Rand SD, Joseph AM, Lund R, Ward BD, Pathak AP, et al. Characterization of a first-pass gradient-echo spin-echo method to predict brain tumor grade and angiogenesis. AJNR Am J Neuroradiol 2004;25:1524–32.

[15] Park MJ, Kim HS, Jahng G-H, Ryu C-W, Park SM, Kim SY. Semiquantitative assessment of intratumoral susceptibility signals using non-contrast-enhanced high-field high-resolution susceptibility-weighted imaging in patients with gliomas: comparison with MR perfusion imaging. AJNR Am J Neuroradiol 2009;30:1402–8. https://doi.org/10.3174/ajnr.A1593.

[16] Law M, Yang S, Wang H, Babb JS, Johnson G, Cha S, et al. Glioma grading: sensitivity, specificity, and predictive values of perfusion MR imaging and proton MR spectroscopic imaging compared with conventional MR imaging. AJNR Am J Neuroradiol 2003;24:1989–98.

[17] Law M, Young R, Babb J, Rad M, Sasaki T, Zagzag D, et al. Comparing perfusion metrics obtained from a single compartment versus pharmacokinetic modeling methods using dynamic susceptibility contrast-enhanced perfusion MR imaging with glioma grade. AJNR Am J Neuroradiol 2006;27:1975–82.

[18] Latysheva A, Emblem KE, Brandal P, Vik-Mo EO, Pahnke J, Røysland K, et al. Dynamic susceptibility contrast and diffusion MR imaging identify oligodendroglioma as defined by the 2016 WHO classification for brain tumors: histogram analysis approach. Neuroradiology 2019;61:545–55. https://doi.org/10.1007/s00234-019-02173-5.

[19] Park HJ, Griffin RJ, Hui S, Levitt SH, Song CW. Radiation-induced vascular damage in tumors: implications of vascular damage in ablative hypofractionated radiotherapy (SBRT and SRS). Radiat Res 2012;177:311–27. https://doi.org/10.1667/rr2773.1.

[20] Soussain C, Ricard D, Fike JR, Mazeron J-J, Psimaras D, Delattre J-Y. CNS complications of radiotherapy and chemotherapy. Lancet Lond Engl 2009;374:1639–51. https://doi.org/10.1016/S0140-6736(09)61299-X.

[21] Kickingereder P, Sahm F, Radbruch A, Wick W, Heiland S, von Deimling A, et al. IDH mutation status is associated with a distinct hypoxia/angiogenesis transcriptome signature which is non-invasively predictable with rCBV imaging in human glioma. Sci Rep 2015;5:16238. https://doi.org/10.1038/srep16238.

[22] Tykocinski ES, Grant RA, Kapoor GS, Krejza J, Bohman L-E, Gocke TA, et al. Use of magnetic perfusion-weighted imaging to determine epidermal growth factor receptor variant III expression in glioblastoma. Neuro-Oncol 2012;14:613–23. https://doi.org/10.1093/neuonc/nos073.

[23] Gupta A, Young RJ, Shah AD, Schweitzer AD, Graber JJ, Shi W, et al. Pretreatment dynamic susceptibility contrast MRI perfusion in glioblastoma: prediction of EGFR gene amplification. Clin Neuroradiol 2015;25:143–50. https://doi.org/10.1007/s00062-014-0289-3.

[24] Wang Y, Fan X, Zhang C, Zhang T, Peng X, Qian T, et al. Identifying radiographic specificity for phosphatase and tensin homolog and epidermal growth factor receptor changes: a quantitative analysis of glioblastomas. Neuroradiology 2014;56:1113–20. https://doi.org/10.1007/s00234-014-1427-y.

[25] Kickingereder P, Bonekamp D, Nowosielski M, Kratz A, Sill M, Burth S, et al. Radiogenomics of glioblastoma: machine learning-based classification of molecular characteristics by using multiparametric and multiregional MR imaging features. Radiology 2016;281:907–18. https://doi.org/10.1148/radiol.2016161382.

[26] Arevalo-Perez J, Thomas AA, Kaley T, Lyo J, Peck KK, Holodny AI, et al. T1-weighted dynamic contrast-enhanced MRI as a noninvasive biomarker of epidermal growth factor receptor VIII status. AJNR Am J Neuroradiol 2015;36:2256–61. https://doi.org/10.3174/ajnr.A4484.

[27] Park YW, Park KS, Park JE, Ahn SS, Park I, Kim HS, et al. Qualitative and quantitative magnetic resonance imaging phenotypes may predict CDKN2A/B Homozygous Deletion status in isocitrate dehydrogenase-mutant astrocytomas: a multicenter study. Korean J Radiol 2023;24:133–44. https://doi.org/10.3348/kjr.2022.0732.

[28] Ono Y, Tamiya T, Ichikawa T, Kunishio K, Matsumoto K, Furuta T, et al. Malignant astrocytomas with homozygous CDKN2/p16 gene deletions have higher Ki-67 proliferation indices. J Neuropathol Exp Neurol 1996;55:1026–31.

[29] Labuhn M, Jones G, Speel EJ, Maier D, Zweifel C, Gratzl O, et al. Quantitative real-time PCR does not show selective targeting of p14(ARF) but concomitant inactivation of both p16(INK4A) and p14(ARF) in 105 human primary gliomas. Oncogene 2001;20:1103–9. https://doi.org/10.1038/sj.onc.1204197.

[30] Zerrouqi A, Pyrzynska B, Febbraio M, Brat DJ, Van Meir EG. P14ARF inhibits human glioblastoma–induced angiogenesis by upregulating the expression of TIMP3. J Clin Invest 2012;122:1283–95. https://doi.org/10.1172/JCI38596.

[31] Folkman J. Role of angiogenesis in tumor growth and metastasis. Semin Oncol 2002;29:15–8. https://doi.org/10.1053/sonc.2002.37263.

[32] Liu T, Ma W, Xu H, Huang M, Zhang D, He Z, et al. PDGF-mediated mesenchymal transformation renders endothelial resistance to anti-VEGF treatment in

glioblastoma. Nat Commun 2018;9:3439. https://doi.org/10.1038/s41467-018-05982-z.
[33] Liu X, Li Y, Sun Z, Li S, Wang K, Fan X, et al. Molecular profiles of tumor contrast enhancement: a radiogenomic analysis in anaplastic gliomas. Cancer Med 2018;7:4273–83. https://doi.org/10.1002/cam4.1672.
[34] Campa D, Rizzato C, Stolzenberg-Solomon R, Pacetti P, Vodicka P, Cleary SP, et al. TERT gene harbors multiple variants associated with pancreatic cancer susceptibility. Int J Cancer 2015;137:2175–83. https://doi.org/10.1002/ijc.29590.
[35] Deguchi S, Oishi T, Mitsuya K, Kakuda Y, Endo M, Sugino T, et al. Clinicopathological analysis of T2-FLAIR mismatch sign in lower-grade gliomas. Sci Rep 2020;10:10113. https://doi.org/10.1038/s41598-020-67244-7.
[36] Juratli TA, Tummala SS, Riedl A, Daubner D, Hennig S, Penson T, et al. Radiographic assessment of contrast enhancement and T2/FLAIR mismatch sign in lower grade gliomas: correlation with molecular groups. J Neurooncol 2019;141:327–35. https://doi.org/10.1007/s11060-018-03034-6.
[37] Park SI, Suh CH, Guenette JP, Huang RY, Kim HS. The T2-FLAIR mismatch sign as a predictor of IDH-mutant, 1p/19q-noncodeleted lower-grade gliomas: a systematic review and diagnostic meta-analysis. Eur Radiol 2021;31:5289–99. https://doi.org/10.1007/s00330-020-07467-4.
[38] Śledzińska P, Bebyn M, Szczerba E, Furtak J, Harat M, Olszewska N, et al. Glioma 2021 WHO classification: the superiority of NGS over IHC in routine diagnostics. Mol Diagn Ther 2022;26:699–713. https://doi.org/10.1007/s40291-022-00612-3.
[39] Xing Z, Yang X, She D, Lin Y, Zhang Y, Cao D. Noninvasive assessment of IDH mutational status in world health organization grade II and III astrocytomas using DWI and DSC-PWI combined with conventional MR imaging. AJNR Am J Neuroradiol 2017;38:1138–44. https://doi.org/10.3174/ajnr.A5171.
[40] Tan W, Xiong J, Huang W, Wu J, Zhan S, Geng D. Noninvasively detecting Isocitrate dehydrogenase 1 gene status in astrocytoma by dynamic susceptibility contrast MRI. J Magn Reson Imag JMRI 2017;45:492–9. https://doi.org/10.1002/jmri.25358.

Publikacja nr 3

© Pol J Radiol 2025; 90 : e103-e113
DOI: https://doi.org/10.5114/pjr/200967

Received: 05.02.2025
Accepted: 07.02.2025
Published: 20.02.2025

Polish Journal of Radiology

http://www.polradiol.com

Original paper

Diffusion imaging in gliomas: how ADC values forecast glioma genetics

Paulina Śledzińska-Bebyn[1,A,B,C,D,E,F], Jacek Furtak[2,3,D,G], Marek Bebyn[4,C,E], Alicja Bartoszewska-Kubiak[5,B], Zbigniew Serafin[6,A,D,G]

[1]Department of Radiology, 10th Military Research Hospital and Polyclinic, Bydgoszcz, Poland
[2]Department of Clinical Medicine, Faculty of Medicine, University of Science and Technology, Bydgoszcz, Poland
[3]Department of Neurosurgery, 10th Military Research Hospital and Polyclinic, Bydgoszcz, Poland
[4]Department of Internal Diseases, 10th Military Clinical Hospital and Polyclinic, Bydgoszcz, Poland
[5]Laboratory of Clinical Genetics and Molecular Pathology, Department of Medical Analytics, 10th Military Research Hospital and Polyclinic, Bydgoszcz, Poland
[6]Faculty of Medicine, Bydgoszcz University of Science and Technology, Bydgoszcz, Poland

Abstract

Purpose: This study investigates the relationship between diffusion-weighted imaging (DWI) and mean apparent diffusion coefficient (ADC) values in predicting the genetic and molecular features of gliomas. The goal is to enhance non-invasive diagnostic methods and support personalised treatment strategies by clarifying the association between imaging biomarkers and tumour genotypes.

Material and methods: A total of 91 glioma patients treated between August 2023 and March 2024 were included in the analysis. All patients underwent preoperative magnetic resonance imaging (MRI), including DWI, and had available histopathological and genetic test results. Clinical data, tumour characteristics, and genetic markers such as *IDH1* mutation, *MGMT* promoter methylation, *EGFR* amplification, *TERT* pathogenic variant, and *CDKN2A* deletion were collected. Statistical analysis was performed to identify correlations between ADC values, MRI perfusion parameters, and genetic characteristics.

Results: Significant associations were found between lower ADC values and aggressive tumour features, including *IDH1*-wildtype, *MGMT* unmethylated status, *TERT* pathogenic variant, and *EGFR* amplification. Additionally, distinct ADC patterns were observed in gliomas with *CDKN2A*, *TP53*, and *PTEN* gene deletions. These findings were further supported by contrast enhancement and other MRI parameters, indicating their role in tumour characterisation.

Conclusions: DWI and ADC measurements demonstrate strong potential as non-invasive tools for predicting glioma genetics. These imaging biomarkers can aid in tumour characterisation and provide valuable insights for guiding personalised treatment strategies.

Key words: diffusion-weighted imaging, apparent diffusion coefficient, glioma, MRI, tumour characterisation.

Introduction

Gliomas are a diverse group of primary brain tumours distinguished by their different clinical behaviour, histological characteristics, and genetic profiles. Therefore, it is crucial to make precise evaluations and descriptions of these tumours for precise diagnoses to optimise treatment approaches and enhance patient results [1]. Obtaining histopathological specimens for accurate diagnosis might be challenging in clinical situations in which surgery is not possible. To overcome these challenges, it is essential to utilise non-invasive diagnostic technologies to improve the effectiveness and precision of diagnosis.

Correspondence address:
Paulina Śledzińska-Bebyn, Department of Radiology, 10th Military Research Hospital and Polyclinic, 5 Powstańców Warszawy St., 85-681 Bydgoszcz, Poland, e-mail: paula.sledzinska@gmail.com

Authors' contribution:
A Study design · **B** Data collection · **C** Statistical analysis · **D** Data interpretation · **E** Manuscript preparation · **F** Literature search · **G** Funds collection

Although traditional imaging modalities are beneficial, they often lack the information required for a full examination of tumours. This gap has generated curiosity in more sophisticated imaging methods, including diffusion-weighted imaging (DWI) and its derivative – the apparent diffusion coefficient (ADC).

DWI utilises the motion of water molecules in tissue to generate contrast in magnetic resonance images (MRI). The ADC values obtained by DWI yield quantitative assessments of water diffusion, which are inversely correlated with cellular density and the integrity of cellular structures. When studying gliomas, it has been observed that ADC levels are related to the density of tumour cells, their growth rate, and the presence of dead tissue. This method offers a more indirect way of determining the histological and genetic characteristics of the tumour, eliminating the necessity for invasive procedures [2].

Recent research has shown that ADC measures can be used to differentiate between low-grade and high-grade gliomas and to predict certain genetic alterations, such as isocitrate dehydrogenase (*IDH*) status [3,4]. These insights are vital because genetic alterations in glioma have a considerable impact on prognosis and therapy response. For example, gliomas with *IDH* mutations typically correspond to more favourable outcomes and have different metabolic pathways compared to gliomas without *IDH* alterations [5]. Furthermore, evaluating the status of the *IDH1* gene is the initial stage in determining the accurate genetic profile of glioma, serving as an indicator for subsequent genetic analyses [6].

The present study aims to explore the relevance of diffusion imaging, specifically ADC values, in predicting glioma genetics and tumour features. Through the synthesis of current research and clinical data, we seek to clarify how modern imaging techniques might improve our understanding of glioma biology and aid in the development of individualised treatment strategies.

Material and methods

Patient cohort

The research study contains a cohort of 91 individuals who received neurosurgical treatment between August 2023 and March 2024. The inclusion criteria encompassed individuals aged 18 years and above who received preoperative MRI with DWI assessment and had accessible histopathological and genetic test findings. Patients who had incomplete datasets were not included in the study. The study obtained approval from the institutional Bioethics Committee.

Clinical data collection

The clinical data obtained encompassed demographic information, such as age and sex, along with tumour features, including location, laterality, and multiplicity. The recorded additional information included clinical symptoms, history of recurrence, Karnofsky performance status (KPS), handedness, smoking status, particular tumour diagnosis, tumour grade, and body mass index (BMI).

MRI protocol

MRI examinations were conducted using a 1.5 T MRI scanner, using a standardised protocol (Supplementary Table 1) to maintain consistency and reproducibility of imaging data. The sequences comprised pre- and post-gadolinium T1- and T2-weighted images, fluid-attenuated inversion recovery (FLAIR), DWI, and dynamic susceptibility contrast (DSC) imaging. Post-contrast images were acquired after administering a bolus injection of a gadolinium-based contrast agent at a dose of 0.1 mmol/kg body weight, followed by a saline flush.

Radiological variables

The images were examined on the analysis software Philips Intellispace Portal. The radiological characteristics assessed included components from the Vasari classification [7]. The features encompassed multifocal lesions, contrast enhancement characteristics, T2/FLAIR mismatch, intratumoural necrosis, maximal diameter, tumour volume, involvement of the corpus callosum, involvement of the cortex, extension into the ependymal layer, and invasion of the pia mater. In addition, ADC was measured in DWI, while relative cerebral blood volume (rCBV) and relative cerebral blood flow (rCBF) were analysed using DSC imaging the average. The regions of interest (ROIs) were positioned according to the method previously outlined by Xing *et al.* [4]. To accurately position the ROIs on the solid tumour components and avoid areas with cysts, bleeding, necrosis, or swelling around the tumour, the DWI pictures were aligned with conventional MRI scans, including T1-weighted scans before and after the injection of gadolinium and T2-weighted scans. Therefore, the average ADC values were determined by manually positioning between 3 and 5 non-overlapping ROIs positioned within the tumour regions of the visually lowest ADC values.

Histopathological and genetic analysis

The histopathological diagnosis was determined by the most recent WHO CNS5 classification [8]. The genetic indicators that were evaluated were *IDH1* mutation status, O^6-methylguanine-DNA methyltransferase (*MGMT)* methylation, epidermal growth factor receptor (*EGFR)* amplification, cyclin-dependent kinase inhibitor 2A (*CDKN2A)* deletion, *TP53* deletion, platelet-derived growth factor receptor alpha gene (*PDGFRA)* amplification, phosphatase and tensin homologue (*PTEN)* deletion, 1p/19q codeletion, telomerase reverse transcriptase (*TERT)* patho-

genic variants, and *H3F3A* (K27M) pathogenic variants. The markers were chosen based on their well-established significance in brain tumour pathophysiology and prognosis. Standard molecular techniques, such as polymerase chain reaction (PCR), fluorescence in situ hybridisation (FISH), and next-generation sequencing (NGS), were employed for genetic analysis.

Statistical analysis

The normality of the data was evaluated using the Shapiro-Wilk test. The selection of statistical tests, either the Mann-Whitney *U* test or the χ^2 test, depended on whether the data were continuous or categorical. These tests were used to identify any significant differences between the 2 groups of independent variables. Instances with incomplete genetic data were omitted from the statistical analysis to ensure uniformity. The results were presented using 95% confidence intervals (95% CI), and statistical significance was determined by a *p*-value of less than 0.05. The statistical studies were performed using R Studio software.

Results

Demographic and clinical characteristics

Table 1 provides a comprehensive summary of the demographic and clinical characteristics of the 91 patients included in this study.

The cohort comprised a slightly higher proportion of males (52.7%) than females (47.3%), with a mean age of 52 years (SD = 15 years). The malignancies were predominantly found in the temporal (35.2%) and frontal lobes (34.1%). The tumours were evenly distributed across the left and right hemispheres, with each hemisphere accounting for 46.2% of the cases. A minor fraction of tumours (7.7%) affected both hemispheres simultaneously.

The prevalent clinical symptoms were headache (27.5%), epilepsy (26.4%), and paresis (24.2%). Additional symptoms that were documented included speech difficulties (19.8%), vision disturbances (15.4%), memory disorders (11%), ataxia (9.9%), dizziness (4.4%), and paraesthesia (5.5%). A significant proportion of patients, specifically 9.9%, exhibited no symptoms.

The patients' KPS had a mean value of 81 (SD = 12), suggesting that most patients had a relatively high level of functional ability during the examination.

Table 2 provides a comprehensive overview of the diagnosis and molecular characteristics of the study participants.

Among the 91 patients included in the study, 29.7% were diagnosed with astrocytoma, and 70.3% with glioblastoma. The tumours were graded according to the WHO classification, with 9 patients (9.9%) having grade 2 tumours, 17 patients (18.7%) having grade 3 tumours, and 65 patients (71.4%) having grade 4 tumours.

Table 1. Patients' characteristics

Factor	*n*	%
Sex		
Female	43	47.3
Male	48	52.7
Age (Mean; SD)	52	15
Handedness		
Left	2	2.2
Right	72	79.1
Both	2	2.2
NA	15	16.5
Location		
Temporal lobe	32	35.2
Frontal lobe	31	34.1
Parietal lobe	15	16.5
Occipital lobe	4	4.4
Cerebellum	3	3.3
Corpus callosum	3	3.3
Brainstem	2	2.2
Insular	1	1.1
Side		
Left	42	46.2
Right	42	46.2
Both	7	7.7
Paresis	22	24.2
Paraesthesia	5	5.5
Speech disorders	18	19.8
Headache	25	27.5
Dizziness	4	4.4
Epilepsy	24	26.4
Ataxia	9	9.9
Vision disturbance	14	15.4
Memory disorders	10	11
No symptoms	9	9.9
Recurrence	29	31.9
KPS (mean; SD)	81	12
Nicotinism		
No	54	59.3
Yes	11	12.1
NA	26	48.6
BMI (mean; SD)	26.14	4.7

SD – standard deviation, KPS – Karnofsky Performance Scale

The analysis of *IDH1* mutation status revealed that 71.4% of patients had *IDH1*-wildtype tumour, while 28.6% of patients had *IDH1* mutations. Regarding *MGMT*

Table 2. Diagnosis and molecular characteristics

	n	%
Diagnosis		
Astrocytoma	27	29.7
Glioblastoma	64	70.3
Grade		
2	9	9.9
3	17	18.7
4	65	71.4
IDH1 mutation		
Wildtype	65	71.4
Mutant	26	28.6
MGMT methylation		
Unmethylated	33	37.9
Methylated	54	62.1
EGFR amplification		
No	40	46.0
Yes	47	54.0
CDKN2A deletion		
Non-deleted	41	45.1
Heterozygous deletion	28	30.8
Homozygous deletion	17	18.7
NA	5	5.5
TP53 deletion		
Non-deleted	78	85.7
Deleted	3	3.3
NA	10	11.0
PDGFRA amplification		
Non-amplified	67	73.6
Amplified	14	15.4
NA	10	11.0
PTEN deletion		
Non-deleted	45	49.5
Deleted	35	38.5
NA	11	12.1
1p19q codeletion		
Non-codeleted	86	98.9
Codeleted	1	1.1
TERT pathogenic variant		
No	34	37.4
Yes	44	48.4
NA	13	14.3
H3K27M pathogenic variant		
No	68	74.7
NA	23	25.3
Multifocal lesion		
No	68	74.7
Yes	23	25.3

IDH1 – isocitrate dehydrogenase 1, *MGMT* – O^6-methylguanine-DNA methyltransferase; *EGFR* – epidermal growth factor receptor, *CDKN2A* – loss of cyclin-dependent kinase inhibitor 2A, *PDGFRA* – platelet-derived growth factor receptor alpha gene, *PTEN* – phosphatase and tensin homologue, *TERT* – telomerase reverse transcriptase

promoter methylation, 37.9% of patients were found to have *MGMT* promoter unmethylated, whereas 62.1% of patients had *MGMT* promoter methylated. *EGFR* amplification was present in 54% of patients. *CDKN2A* deletion status indicated that 45.1% of patients had non-deleted *CDKN2A*, 30.8% of patients had heterozygous deletions, and 18.7% of patients had homozygous deletions. *TP53* deletion was found in 3.3% of patients. *PDGFRA* amplification was observed in 15.4% of patients. *PTEN* deletion was detected in 38.5% of patients. Only one patient had 1p/19q codeletion, while the vast majority (98.9%) did not have this genetic feature. *TERT* pathogenic variants were identified in 48.4% of patients. Representative patients' examinations are presented in Figures 1–3.

Table 3 outlines the imaging parameters assessed in the study.

Contrast enhancement was observed in 67 patients (73.6%), while 24 patients (26.4%) showed no enhancement. The quality of enhancement was graded as follows: 0 means no enhancement (26.4%), 1 means mild/minimal enhancement (13.2%), and 2 means marked/avid enhancement (62.6%). T2/FLAIR mismatch was present in 9 patients (9.9%). The mean rCBF was 4.1, and the mean rCBV was 5.2. Intratumoural necrosis was noted in 66 patients (72.5%). The maximal diameter of the tumours had a mean of 44.6 mm, and the mean tumour volume was 31.2 cm^3. The mean ADC was 1.36×10^{-3} mm^2/s. Corpus callosum involvement was observed in 25 patients (27.5%), while cortical involvement was noted in 77 patients (84.6%). Ependymal extension was present in 59 patients (64.8%), and pial invasion was seen in 68 patients (74.7%).

Table 4 provides a comprehensive analysis of the relationship between various MRI perfusion parameters and genetic features in gliomas.

Patients with *IDH1*-wildtype gliomas exhibited a significantly lower mean ADC value compared to those with *IDH1* mutations ($p < 0.05$). Contrast enhancement was significantly more frequent in *IDH1*-wildtype gliomas compared to *IDH1* mutant gliomas ($p < 0.05$). Enhancement quality, T2/FLAIR mismatch, and other variables also varied significantly between these 2 groups ($p < 0.05$).

Gliomas without *MGMT* promoter methylation had a significantly lower mean ADC value compared to *MGMT* promoter methylated gliomas ($p < 0.05$). Contrast enhancement was observed more frequently in gliomas

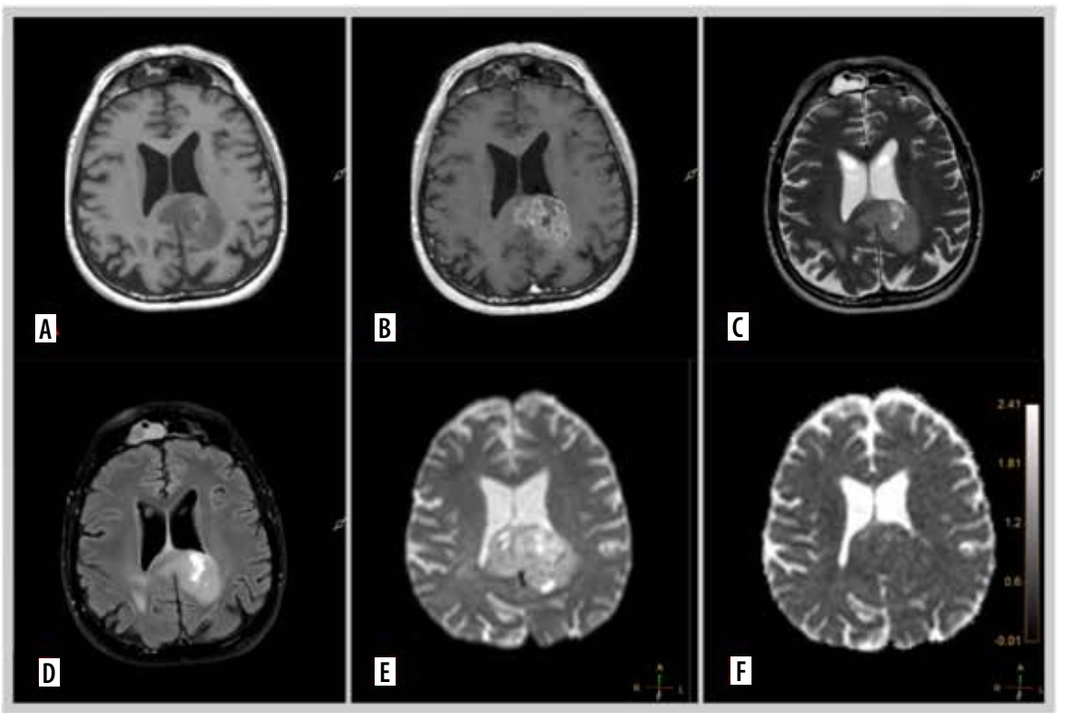

Figure 1. Representative magnetic resonance images of examined patient. A 68-year-old man with glioblastoma G4. Molecular characteristics: *IDH1*-wild-type, present *TERT* promoter pathogenic variant, *CDKN2A* homozygous deletion, *EGFR* amplification, *MGMT* promoter unmethylated. **A)** Pre-contrast T1. **B)** Contrast enhanced tumour on T1 post gadolinium. **C)** T2-weighted scan. **D)** Fluid-attenuated inversion recovery (FLAIR). **E)** Diffusion-weighted imaging (DWI). **F)** Reduced diffusion on apparent diffusion coefficient (ADC) map

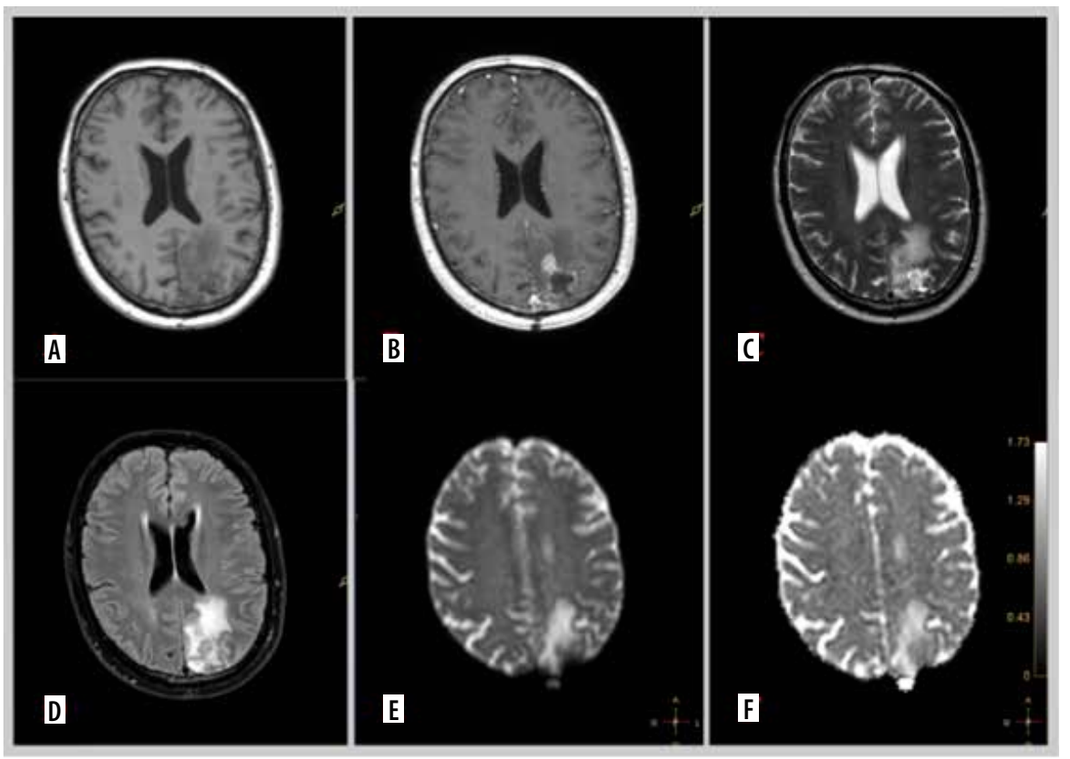

Figure 2. Representative magnetic resonance images of examined patient. A 67-year-old man with glioblastoma G4. Molecular characteristics: *IDH1*-wild-type, present *TERT* promoter pathogenic variant, *CDKN2A* homozygous deletion, *EGFR* amplification, *MGMT* promoter unmethylated. **A)** Pre-contrast T1. **B)** Contrast enhanced tumour on T1 post gadolinium. **C)** T2-weighted scan. **D)** Fluid-attenuated inversion recovery (FLAIR). **E)** Diffusion-weighted imaging (DWI). **F)** Apparent diffusion coefficient (ADC) map

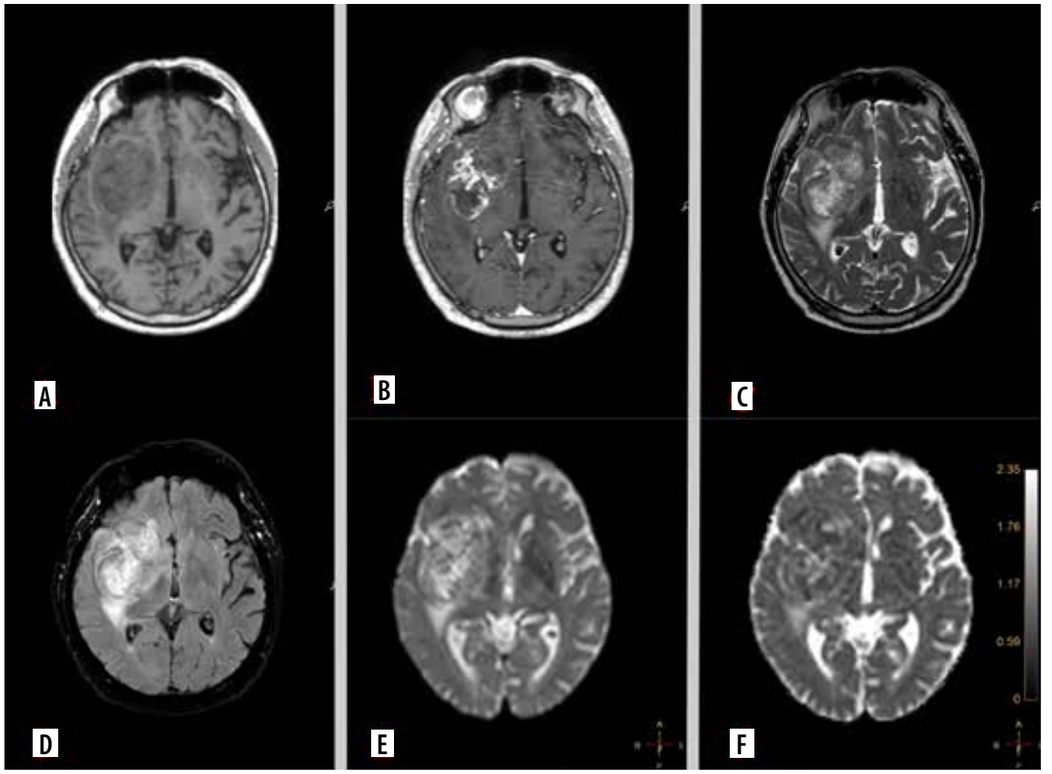

Figure 3. Representative magnetic resonance images of examined patient. A 52-year-old man with glioblastoma G4. Molecular characteristics: *IDH1*-wild-type, present *TERT* promoter pathogenic variant, *CDKN2A* non-deleted, *EGFR* non-amplification, *MGMT* promoter unmethylated. **A**) Pre-contrast T1. **B)** Contrast enhanced tumour on T1 post gadolinium. **C)** T2-weighted scan. **D)** Fluid-attenuated inversion recovery (FLAIR). **E)** Diffusion-weighted imaging (DWI).. **F)** ADC map

Table 3. Imaging parameters

	n	%
Contrast enhancement		
No	24	26.4
Yes	67	73.6
Enhancement quality		
0	24	26.4
1	12	13.2
2	55	62.6
T2/FLAIR mismatch		
No	82	90.1
Yes	9	9.9
rCBF (Mean; SD)	4.1	
rCBV (Mean; SD)	5.2	
Intratumoural necrosis		
No	25	27.5
Yes	66	72.5
Maximal diameter (mm) (mean; SD)	44.6	374.7
Volume (cm^3) (mean; SD)	31.12	429.5
Mean ADC ($\times 10^3$ mm^3s) (mean; SD)	1.36	

	n	%
Corpus callosum involvement		
No	66	72.5
Yes	25	27.5
Cortical involvement		
0	14	15.4
1	77	84.6
Ependymal extension		
0	32	35.2
1	59	64.8
Pial invasion		
No	23	25.3
Yes	68	74.7

rCBF – regional cerebral blood flow, rCBV – relative cerebral blood volume, ADC – apparent diffusion coefficient

Table 4. Relationship between magnetic resonance imaging perfusion and genetic features

		Mean ADC [x10-3mm²/s]		Contrast enhancement			Enhancement quality				T2/FLAIR mismatch			Intratumoural necrosis >5%			Corpus callosum involvement			Ependymal extension			Pial invasion			Cortical involvement		
		Mean	*p*	Absent	Present	*p*	0	1	2	*p*	Absent	Present	*p*	Absent	Present	*p*	Absent	Present	*p*	Absent	Present	*p*	Absent	Present	*p*	Absent	Present	*p*
IDH1 mutation	Wildtype	1.3	< 0.05	6	59	< 0.05	6	11	49	< 0.05	63	2	< 0.05	18	47		45	20		21	44		16	49		7	58	
	Mutant	1.52		18	8		18	1	7		19	7		7	19		21	5		11	15		7	19		7	19	
MGMT methylation	Unmethylated	1.21	< 0.05	3	30	< 0.05	3	3	27	< 0.05	31	2		11	22		27	6		13	20		7	26		4	29	
	Methylated	1.46		20	34		20	8	26		47	7		14	40		37	17		19	35		14	40		10	44	
EGFR amplification	No	1.47	< 0.05	17	23	< 0.05	17	3	20	< 0.05	34	6		12	28		33	7		17	23		8	32		9	31	
	Yes	1.26		6	41		6	8	33		45	2		13	34		32	15		15	32		12	35		5	42	
CDKN2A deletion	Non-deleted	1.51	< 0.05	17	24	< 0.05	17	3	21	< 0.05	37	4		9	32		35	6		19	22		12	29		9	32	
	Heterozygous deletion	1.21		3	25		3	3	22		26	2		11	17		21	7		8	20		4	24		3	25	
	Homozygous deletion	1.26		3	14		3	4	10		15	2		5	12		9	8		5	12		4	13		2	15	
TP53 deletion	No	1.36	< 0.05	23	55		23	9	46		70	8		23	55		59	19		30	48		19	59		12	66	
	Yes	1.95		0	3		0	0	3		3	0		0	3		3	0		0	3		0	3		1	2	
PDGFRA amplification	No	1.4		22	45		22	8	37		60	7		18	49		51	16		26	41		17	50		12	55	
	Yes	1.29		1	13		1	1	12		13	1		5	9		11	3		4	10		2	12		1	13	
PTEN deletion	No	1.42		21	24	< 0.05	21	1	23	< 0.05	38	7		10	35		37	8		20	25		6	39	< 0.05	11	34	< 0.05
	Yes	1.31		2	33		2	8	25		34	1		13	22		24	11		10	25		13	22		2	33	
1p19q codeletion	No	1.37		22	64		22	11	53		77	9		24	62		64	22		31	55		21	65		14	72	
	Yes	1.8		1	0		1	0	0		1	0		1	0		0	1		0	1		0	1		0	1	
TERT pathogenic variant	No	1.54	< 0.05	16	18	< 0.05	16	1	17	< 0.05	28	6		8	26		26	8		13	21		9	25		6	28	
	Yes	1.3		5	39		5	9	30		42	2		10	34		32	12		15	29		11	33		6	38	
H3k27 pathogenic variant	No	1.41		19	49		18	8	41		0	1		16	52		53	15		26	42		17	51		11	57	

Results are based on two-sided tests assuming equal variances.

IDH1 – isocitrate dehydrogenase 1, *MGMT* – O^6-methylguanine-DNA methyltransferase, *EGFR* – epidermal growth factor receptor, *CDKN2A* – loss of cyclin-dependent kinase inhibitor 2A, *PDGFRA* – platelet-derived growth factor receptor alpha gene, *PTEN* – phosphatase and tensin homologue, *TERT* – telomerase reverse transcriptase

with *MGMT* promoter methylation compared to unmethylated cases ($p < 0.05$). Similar trends were observed across other MRI parameters.

Gliomas without *EGFR* amplification had a higher mean ADC value compared to those with amplification ($p < 0.05$). Contrast enhancement was more common in *EGFR*-amplified gliomas compared to non-amplified cases ($p < 0.05$).

Gliomas with non-deleted *CDKN2A* exhibited a higher mean ADC value compared to heterozygous deletions and homozygous deletions ($p < 0.05$). Contrast enhancement was less frequent in gliomas with homozygous deletions compared to non-deleted gliomas ($p < 0.05$).

The mean ADC value was significantly higher in gliomas with *TP53* deletion compared to non-deleted *TP53* gliomas ($p < 0.05$).

Gliomas without *PDGFRA* amplification showed a higher mean ADC value compared to those with amplification, but this difference was not statistically significant.

Gliomas without *PTEN* deletion had a higher mean ADC value compared to those with *PTEN* deletion. This difference was statistically significant ($p < 0.05$). Contrast enhancement was more common in gliomas with *PTEN* deletion compared to non-deleted *PTEN* gliomas ($p < 0.05$).

Gliomas with *TERT* pathogenic variants exhibited a lower mean ADC value compared to those without the variant ($p < 0.05$). Contrast enhancement was more frequent in gliomas with *TERT* variants compared to those without ($p < 0.05$).

Discussion

The present study examines the significant relationship between DWI measures, particularly mean ADC values, and various genetic and molecular features of gliomas. The results of our research show that DWI and ADC values can be used as non-invasive indicators to predict genetic changes and tumour features. This is particularly significant in the setting of tumours where biopsy is challenging or unfeasible, providing a vital alternative for acquiring diagnostic and prognostic information without intrusive treatments.

IDH1 mutation status

Our results indicate that *IDH1*-wildtype gliomas exhibit significantly lower mean ADC values compared to *IDH1*-mutant gliomas. Mounting evidence suggests that mutations in the *IDH* gene family can decrease the production of α-ketoglutarate, resulting in the formation of the oncometabolite (R)-2-hydroxyglutarate. This, in turn, leads to an increase in cell proliferation or cellularity. Therefore, our findings align with previous studies suggesting that *IDH1* wildtype gliomas are typically more aggressive and have higher cellularity, resulting in lower ADC values [4,9-12]. The significant association between lower ADC values and the presence of contrast enhancement further supports the aggressive nature of *IDH1*-wildtype gliomas. Prompt determination of the *IDH1* gene status is crucial, particularly during the initial non-invasive diagnostic phase. The significance of the *IDH1* gene status determines the subsequent genetic tests necessary for a comprehensive diagnosis (layered report structure) and accurate classification of the tumour, as required by the current CNS5 classification [8].

MGMT methylation

The study reveals that gliomas with unmethylated promoter of *MGMT* have lower mean ADC values compared to methylated *MGMT* gliomas. This observation corroborates existing literature indicating that *MGMT* methylation is associated with better prognosis and lower cellular density, reflected in higher ADC values [5]. However, it is important to note that the relationship between ADC values and *MGMT* status has been strongly debated in the literature. Some studies, such as those by Romano *et al.* [13] and Moon *et al.* [14], report higher ADC values in methylated *MGMT* tumours, supporting the notion of lower cellular density in these tumours. Conversely, Pope *et al.* [15] and others have found lower ADC values in unmethylated tumours, suggesting that these results may not be consistent across all cases and may vary depending on the tumour region analysed (e.g. enhancing versus peritumoral tissue). The higher frequency of contrast enhancement in methylated *MGMT* gliomas suggest enhanced tumour permeability and angiogenesis, characteristics often observed in these tumours [16]. Early assessment of *MGMT* promoter methylation is vital for optimising treatment strategies and improving prognostication in glioma patients. Specifically, patients with methylated promoters respond better to temozolomide [17]. It also aids in risk stratification, guiding clinical decision-making, and enhancing clinical trial design by selecting appropriate patient cohorts [18]. Thus, integrating *MGMT* methylation assessment early in the diagnostic process is crucial for effective glioma patient management.

According to the recent CNS5 and cIMPACT-NOW, specific genetic alterations change the final diagnosis. Confirming the presence of certain genetic alterations in glioma can reclassify the tumour as "molecularly" high-grade, resulting in a considerably lower survival rate compared to gliomas without mutations [19]. *IDH1*-wildtype lower-grade gliomas that exhibit one of three particular genetic markers (*EGFR* amplification, +7/–10 abnormality, or *TERT* promoter alterations) are classified as the most malignant type of tumour, known as WHO grade 4 [20]. In *IDH1*-mutant lower-grade gliomas, the mutation of the highest malignancy is *CDKN2A* homozygous deletion. Hence, identifying these indicators during the initial phase of diagnosis potentially influences subsequent treat-

ment. Noninvasive assessment of molecular characteristics is primarily employed in patients for whom acquiring histopathology material is highly hazardous or unfeasible. For these patients, MRI and acquired ADC are advantageous because DWI is the typical sequence performed during initial diagnosis.

EGFR amplification

Gliomas without *EGFR* amplification showed higher mean ADC values compared to those with *EGFR* amplification. This is consistent with the notion that *EGFR* amplification is related to increased tumour aggressiveness and cellularity, resulting in lower ADC values [21]. The higher prevalence of contrast enhancement in *EGFR* amplified gliomas further underscores their aggressive phenotype.

CDKN2A deletion

In the presented study non-deleted *CDKN2A* gliomas exhibited higher mean ADC values compared to those with heterozygous or homozygous deletions. *CDKN2A* deletions are known to contribute to tumour progression and malignancy, which could be reflected in lower ADC values [22]. The relationship between *CDKN2A* gene status and ADC value has been investigated in several studies, which have shown contradictory findings. Indeed, certain research has shown a substantial correlation between ADC and *CDKN2A*, although in other studies the correlation is not statistically significant [23,24].

TERT pathogenic variants

TERT is an enzyme responsible for maintaining telomeres that safeguard genomic integrity during cell division. *TERT* is highly expressed in stem cells and cancer cells, playing a crucial role in cellular immortality. Mutations in promoter of *TERT* are a hallmark of various cancers, including glioblastoma, and they are commonly used as diagnostic and prognostic markers. Suppression of *TERT* by promotion mutation expression has been shown to increase cellular sensitivity to DNA damage, making *TERT* a promising target for novel therapeutic approaches in GBM. In our study, gliomas with *TERT* pathogenic variants exhibited lower mean ADC values, indicative of higher tumour cellularity and increased aggressiveness, which is in line with previous research [25]. This finding aligns with the established role of *TERT* mutations in promoting tumour proliferation and malignancy. Additionally, the significant association between *TERT* promoter mutations and increased contrast enhancement on MRI further underscores the aggressive nature of these tumours. Contrast enhancement reflects the disruption of the blood-brain barrier and neovascularisation, which are characteristic of high-grade, rapidly growing tumours. The combined observation of lower ADC values and greater contrast enhancement in *TERT*-mutant gliomas provides robust non-invasive indicators of tumour aggressiveness and highlights the potential utility of advanced imaging techniques in the characterisation and management of these malignancies.

In summary, this study highlights the utility of DWI and ADC values in non-invasively predicting the genetic and molecular landscape of gliomas. The significant correlations between imaging biomarkers and genetic features underscore the potential of advanced MRI techniques in guiding personalised treatment approaches.

Limitations of the study

Despite the promising findings and significant insights provided by this study, several limitations should be acknowledged to contextualise the results and guide future research.

Firstly, the study cohort, although comprehensive, was relatively small and drawn from a single institution. This limits the generalisability of the findings across broader populations and different clinical settings. Larger, multicentre studies are necessary to validate these results and account for potential variations in imaging protocols, genetic testing methods, and patient demographics. Secondly, the study's retrospective design inherently introduces certain biases, including selection bias and information bias. The study also relied heavily on mean ADC values, which, while informative, may not capture the full complexity of tumour diffusion characteristics. ADC values can be influenced by various factors, including tumour heterogeneity, necrosis, and surrounding oedema. Advanced diffusion imaging techniques, such as diffusion tensor imaging (DTI) and diffusion kurtosis imaging (DKI), might provide more detailed insights into the microstructural properties of gliomas.

Future directions

This study reveals the potential of DWI and ADC values in glioma characterisation and treatment planning. To validate these associations, larger, multicentre cohorts are needed to account for variations in imaging protocols, genetic testing methods, and patient demographics. Longitudinal studies tracking changes in ADC values during and after treatment can provide insights into tumour response and resistance mechanisms. Moreover, further research is needed to understand the biological mechanisms driving the observed correlations between ADC values and genetic alterations. Automated analysis tools leveraging artificial intelligence and machine learning can facilitate the processing of large imaging datasets and aid in real-time clinical decision-making. Expanding research to include paediatric populations and rare glioma subtypes will ensure the benefits of advanced imaging techniques are realised across diverse patient groups.

Conclusions

This study underscores the significant potential of DWI and mean ADC values as non-invasive biomarkers for predicting genetic and molecular characteristics of gliomas. Our findings demonstrate that lower ADC values are generally associated with more aggressive tumour phenotypes and specific genetic alterations, such as *IDH1*-wildtype, *MGMT* unmethylated status, *EGFR* amplification, and *CDKN2A* homozygous deletion.

In conclusion, DWI and ADC metrics provide critical insights into the genetic and molecular landscape of gliomas, offering a non-invasive and effective tool for enhancing diagnostic precision and tailoring therapeutic interventions. This study highlights the transformative potential of advanced imaging in the era of personalised oncology, ultimately aiming to improve patient outcomes through more targeted and informed treatment strategies.

Disclosures

1. Institutional review board statement: The study was conducted in accordance with the Declaration of Helsinki, and the Ethics Committee of the Nicolaus Copernicus University, Collegium Medicum in Bydgoszcz, Poland approved the study protocol.
2. Assistance with the article: None.
3. Financial support and sponsorship: None.
4. Conflicts of interest: None.

References

1. Weller M, Wick W, Aldape K, Brada M, Berger M, Pfister SM, et al. Glioma. Nat Rev Dis Primer 2015; 1: 15017. DOI: https://doi.org/10.1038/nrdp.2015.17.
2. Hagmann P, Jonasson L, Maeder P, Thiran JP, Wedeen VJ, Meuli R. Understanding diffusion MR imaging techniques: from scalar diffusion-weighted imaging to diffusion tensor imaging and beyond. Radiogr Rev Publ Radiol Soc N Am Inc 2006; 26 Suppl 1: S205-S223. DOI: https://doi.org/10.1148/rg.26si065510.
3. Zhang L, Min Z, Tang M, Chen S, Lei X, Zhang X. The utility of diffusion MRI with quantitative ADC measurements for differentiating high-grade from low-grade cerebral gliomas: evidence from a meta-analysis. J Neurol Sci 2017; 373: 9-15.
4. Xing Z, Yang X, She D, Lin Y, Zhang Y, Cao D. Noninvasive assessment of IDH mutational status in World Health Organization grade II and III astrocytomas using DWI and DSC-PWI combined with conventional MR imaging. Am J Neuroradiol 2017; 38: 1138-1144.
5. Śledzińska P, Bebyn MG, Furtak J, Kowalewski J, Lewandowska MA. Prognostic and predictive biomarkers in gliomas. Int J Mol Sci 2021; 22: 10373. DOI: https://doi.org/10.3390/ijms221910373.
6. Śledzińska P, Bebyn M, Szczerba E, Furtak J, Harat M, Olszewska N, et al. Glioma 2021 WHO classification: the superiority of NGS over IHC in routine diagnostics. Mol Diagn Ther 2022; 26: 699-713.
7. VASARI Research Project – The Cancer Imaging Archive (TCIA) Public Access – Cancer Imaging Archive Wiki n.d. Available at: https://wiki.cancerimagingarchive.net/display/Public/VASARI+Research+Project (Accessed: 10.08.2024).
8. Louis DN, Perry A, Wesseling P, Brat DJ, Cree IA, Figarella-Branger D, et al. The 2021 WHO classification of tumors of the central nervous system: a summary. Neuro Oncol 2021; 23: 1231-1251.
9. Leu K, Ott GA, Lai A, Nghiemphu PL, Pope WB, Yong WH, et al. Perfusion and diffusion MRI signatures in histologic and genetic subtypes of WHO grade II-III diffuse gliomas. J Neurooncol 2017; 134: 177-188.
10. Thust SC, Hassanein S, Bisdas S, Rees JH, Hyare H, Maynard JA, et al. Apparent diffusion coefficient for molecular subtyping of non-gadolinium-enhancing WHO grade II/III glioma: volumetric segmentation versus two-dimensional region of interest analysis. Eur Radiol 2018; 28: 3779-3788.
11. Maynard J, Okuchi S, Wastling S, Busaidi AA, Almossawi O, Mbatha W, et al. World Health Organization grade II/III glioma molecular status: prediction by MRI morphologic features and apparent diffusion coefficient. Radiology 2020; 296: 111-121.
12. Kim M, Jung SY, Park JE, Jo Y, Park SY, Nam SJ, et al. Diffusion- and perfusion-weighted MRI radiomics model may predict isocitrate dehydrogenase (IDH) mutation and tumor aggressiveness in diffuse lower grade glioma. Eur Radiol 2020; 30: 2142-2151.
13. Romano A, Calabria LF, Tavanti F, Minniti G, Rossi-Espagnet MC, Coppola V, et al. Apparent diffusion coefficient obtained by magnetic resonance imaging as a prognostic marker in glioblastomas: correlation with MGMT promoter methylation status. Eur Radiol 2013; 23: 513-520.
14. Moon WJ, Choi JW, Roh HG, Lim SD, Koh YC. Imaging parameters of high grade gliomas in relation to the MGMT promoter methylation status: the CT, diffusion tensor imaging, and perfusion MR imaging. Neuroradiology 2012; 54: 555-563.
15. Pope WB, Lai A, Mehta R, Kim HJ, Qiao J, Young JR, et al. Apparent diffusion coefficient histogram analysis stratifies progression-free survival in newly diagnosed bevacizumab-treated glioblastoma. AJNR Am J Neuroradiol 2011; 32: 882-889.
16. Ellingson BM. Radiogenomics and imaging phenotypes in glioblastoma: novel observations and correlation with molecular characteristics. Curr Neurol Neurosci Rep 2015; 15: 506. DOI: https://doi.org/10.1007/s11910-014-0506-0.
17. Hegi ME, Diserens AC, Gorlia T, Hamou MF, de Tribolet N, Weller M, et al. MGMT gene silencing and benefit from temozolomide in glioblastoma. N Engl J Med 2005; 352: 997-1003.
18. Weller M, Stupp R, Reifenberger G, Brandes AA, van den Bent MJ, Wick W, et al. MGMT promoter methylation in malignant gliomas: ready for personalized medicine? Nat Rev Neurol 2010; 6: 39-51.
19. Aibaidula A, Chan AKY, Shi Z, Li Y, Zhang R, Yang R, et al. Adult IDH wild-type lower-grade gliomas should be further stratified. Neuro Oncol 2017; 19: 1327-1337.

20. Brat DJ, Aldape K, Colman H, Holland EC, Louis DN, Jenkins RB, et al. cIMPACT-NOW update 3: recommended diagnostic criteria for "Diffuse astrocytic glioma, IDH-wildtype, with molecular features of glioblastoma, WHO grade IV." Acta Neuropathol (Berl) 2018; 136: 805-810.
21. Park YW, Park JE, Ahn SS, Kim EH, Kang SG, Chang JH, et al. Magnetic resonance imaging parameters for noninvasive prediction of epidermal growth factor receptor amplification in isocitrate dehydrogenase-wild-type lower-grade gliomas: a multicenter study. Neurosurgery 2021; 89: 257-265.
22. Appay R, Dehais C, Maurage CA, Alentorn A, Carpentier C, Colin C, et al. CDKN2A homozygous deletion is a strong adverse prognosis factor in diffuse malignant IDH-mutant gliomas. Neuro Oncol 2019; 21: 1519-1528.
23. Park YW, Park KS, Park JE, Ahn SS, Park I, Kim HS, et al. Qualitative and quantitative magnetic resonance imaging phenotypes may predict CDKN2A/B homozygous deletion status in isocitrate dehydrogenase-mutant astrocytomas: a multicenter study. Korean J Radiol 2023; 24: 133-144.
24. Chiang GC, Pisapia DJ, Liechty B, Magge R, Ramakrishna R, Knisely J, et al. The prognostic value of MRI subventricular zone involvement and tumor genetics in lower grade gliomas. J Neuroimaging 2020; 30: 901-909.
25. Chen L, Chen R, Li T, Huang L, Tang C, Li Y, et al. MRI radiomics model for predicting TERT promoter mutation status in glioblastoma. Brain Behav 2023; 13: e3324. DOI: https://doi.org/10.1002/brb3.3324.

Zgoda Komisji Bioetycznej

Uniwersytet Mikołaja Kopernika w Toruniu
Collegium Medicum im L. Rydygiera w Bydgoszczy
KOMISJA BIOETYCZNA
Ul. M. Skłodowskiej-Curie 9, 85-094 Bydgoszcz, tel.(052) 585-35-63, fax.(052) 585-38-11

KB 467/2022 Bydgoszcz, 27.09.2022 r.

Działając na podstawie art. 29 ustawy z dnia 5.12.1996 r. o zawodach lekarza i lekarza dentysty Dz.U. z 1997 r. Nr 28 poz. 152 (wraz z późniejszymi zmianami), rozporządzenia Ministra Zdrowia i Opieki Społecznej z dnia 11.05.1999 r. w sprawie szczegółowych zasad powoływania i finansowania oraz trybu działania komisji bioetycznych (Dz.U. Nr 47 poz.480) oraz Zarządzenia Nr 21 Rektora UMK z dnia 4.03.2009 r. z późn. zm. w sprawie powołania oraz zasad działania Komisji Bioetycznej Uniwersytetu Mikołaja Kopernika w Toruniu przy Collegium Medicum im Ludwika Rydygiera w Bydgoszczy oraz zgodnie z zasadami zawartymi w DH i GCP

Komisja Bioetyczna przy UMK w Toruniu, Collegium Medicum w Bydgoszczy

(skład podano w załączeniu), na posiedzeniu w dniu **27.09.2022 r.** przeanalizowała wniosek, który złożył kierownik badania:

dr n. med. Jacek Furtak
10 Wojskowy Szpital Kliniczny z Poliklinika w Bydgoszczy
ul. Powstańców Warszawy 5
85-681 Bydgoszcz

z zespołem w składzie:

dr n. med. Jacek Furtak, lek. Marek Bebyn, lek. Paulina Śledzińska, prof. dr hab. Marek Harat

w sprawie badania:

„Badanie potencjalnych biomarkerów nowotworowych oraz ocena danych klinicznych w celu znalezienia prognostycznych i predykcyjnych markerów w nowotworach układu nerwowego."

Po zapoznaniu się ze złożonym wnioskiem i w wyniku przeprowadzonej dyskusji oraz głosowania Komisja podjęła

Uchwałę o pozytywnym zaopiniowaniu wniosku

w sprawie przeprowadzenia badań, w zakresie określonym we wniosku pod warunkiem:

- w odniesieniu do części retrospektywnej badania:

- posiadania zgody osób badanych na przetwarzanie danych osobowych w celach naukowych, a w przypadku braku takiej zgody, analizowania jedynie danych zanonimizowanych, pozbawionych danych personalnych (zgodnie z RODO). Zgoda obejmuje tylko dane z dokumentacji uczestników badania z okresu od 01.01.2015r. do 26.09.2022 r.

- w odniesieniu do części prospektywnej badania:

- poinformowania na piśmie uczestników badania o celu oraz zakresie badań i uzyskania od każdego z nich osobnej, pisemnej, świadomej zgody na udział w badaniu, zgodnie z obowiązującymi przepisami, datowanej najpóźniej na moment rozpoczęcia badania, a nie wcześniej niż data uzyskania z Komisji Bioetycznej pozytywnej opinii o badaniu;

- zachowania tajemnicy wszystkich danych, w tym danych osobowych uczestników badania, umożliwiających ich identyfikację w ewentualnych publikacjach
- zapewnienia, że osoby uczestniczące w eksperymencie badawczym nie są ubezwłasnowolnione, nie są żołnierzami służby zasadniczej, nie są osobami pozbawionymi wolności, nie pozostają w zależności służbowej, dydaktycznej lub innej z prowadzącym badanie;
- zawarcia obowiązkowego ubezpieczenia odpowiedzialności cywilnej podmiotu przeprowadzającego eksperyment medyczny.
- sugerujemy uzyskanie podpisu uczestnika badania pod informacją o badaniu, lub sporządzenie formularza informacji i świadomej zgody na udział w badaniu w ramach jednego dokumentu.

Jednocześnie informujemy, iż „Zgoda na udział w badaniu" winna zawierać m.in.: imię i nazwisko badanej osoby; adres zamieszkania lub PESEL lub nr historii choroby pacjenta (L.ks.gł. Oddziału/Poradni) oraz datę i podpis badanej osoby, a także klauzule, że uczestnik badania wyraża zgodę na przetwarzanie danych osobowych dotyczących realizacji tematu badawczego, zgodnie z obowiązującym prawem (RODO).

Kierownik badania zobowiązany jest do przechowywania wszystkich dokumentów dotyczących badania przez okres dwudziestu lat.jest do przechowywania wszystkich dokumentów dotyczących badania przez okres dwudziestu lat.

Zgoda obowiązuje od daty podjęcia uchwały (27.09.2022 r.) do końca 2027 r.

Wydana opinia dotyczy tylko rozpatrywanego wniosku z uwzględnieniem przedstawionego projektu; każda zmiana i modyfikacja wymaga uzyskania odrębnej opinii. Wnioskodawca zobowiązany jest do informowania o wszelkich poprawkach, które mogłyby mieć wpływ na opinię Komisji oraz poinformowania o zakończeniu badania.

Od niniejszej uchwały podmiot zamierzający przeprowadzić eksperyment medyczny, kierownik zakładu opieki zdrowotnej, w której eksperyment medyczny ma być przeprowadzony, mogą wnieść odwołanie do Odwoławczej Komisji Bioetycznej przy Ministrze Zdrowia, za pośrednictwem Komisji Bioetycznej przy Collegium Medicum im. L. Rydygiera w Bydgoszczy, w terminie 14 dni od daty otrzymania niniejszej Uchwały.

Prof. dr hab. med. Karol Śliwka

Przewodniczący Komisji Bioetycznej

Otrzymuje:
dr n. med. Jacek Furtak
10 Wojskowy Szpital Kliniczny z Poliklinika w Bydgoszczy
ul. Powstańców Warszawy 5
85-681 Bydgoszcz

Lista obecności

na posiedzeniu Komisji Bioetycznej

w dniu 27.09.2022 r.

Lp.	Imię i nazwisko	Funkcja/ Specjalizacja	Podpis
1.	Prof. dr hab. med. Karol Śliwka	*medycyna sądowa*	
2.	Mgr prawa Joanna Połetek-Żygas	*prawniczka*	
3.	Prof. dr hab. med. Mieczysława Czerwionka-Szaflarska	*pediatra, alergologia i gastroenterologia dziecięca*	
4.	Prof. dr hab. med. Marek Grabiec	*położnictwo, ginekologia onkologiczna*	
5.	Prof. dr hab. n med. Maria Kłopocka	*choroby wewnętrzne, gastroenterologia*	
6.	Prof. dr hab. med. Zbigniew Włodarczyk	*chirurgia ogólna, transplantologia kliniczna*	
7.	Dr hab. n. med. Maciej Słupski, prof. UMK	*chirurgia ogólna, transplantologia kliniczna*	
8.	Dr hab. n. med. Katarzyna Sierakowska, prof. UMK	*anestezjologia i intensywna terapia*	
9.	Ks. dr hab. Wojciech Szukalski, prof. UAM	*duchowny*	
10.	Dr n. med. Radosława Staszak-Kowalska	*pediatria, choroby płuc*	
11.	Mgr prawa Patrycja Brzezicka	*prawniczka*	
12.	Mgr farm. Aleksandra Adamczyk	*farmaceutka*	
13.	Mgr Lidia Iwińska-Tarczykowska	*pielęgniarka*	

Oświadczenia współautorów

Załącznik nr 5 do uchwały Nr 38 Senatu UMK z dnia 26 września 2023 r.

w sprawie postępowania o nadanie stopnia doktora na Uniwersytecie Mikołaja Kopernika w Toruniu

Toruń, dnia 01.03.2025 r.

lek. Paulina Śledzińska-Bebyn
(tytul, stopień, imię i nazwisko kandydata/współautora)

Kliniczny Zakład Radiologii Lekarskiej
10 Wojskowy Szpital Kliniczny z Poliklinika w Bydgoszczy.
(jednostka zatrudniająca kandydata/współautora)

Rada Dyscypliny Nauki Medyczne
Uniwersytetu Mikołaja Kopernika
w Toruniu

Oświadczenie o współautorstwie

Niniejszym oświadczam, że w pracy *Śledzińska-Bebyn P, Furtak J, Bebyn M, Serafin Z.* ***Beyond conventional imaging: Advancements in MRI for glioma malignancy prediction and molecular profiling.*** *Magn Reson Imaging 2024;112:63–81. https://doi.org/10.1016/j.mri.2024.06.004.* mój udział polegał na opracowaniu pierwotnego szkicu publikacji, przygotowaniu wizualizacji, przeglądzie literaturowym, pozyskaniu zasobów, zarządzaniu projektem, planowaniu koncepcyjnym oraz przeglądzie i edycji treści.
Mój udział w powstaniu pracy wynosi 80%.

Niniejszym oświadczam, że w pracy *Śledzińska-Bebyn P, Furtak J, Bebyn M, Bartoszewska-Kubiak A, Serafin Z.* ***Investigating glioma genetics through perfusion MRI: rCBV and rCBF as predictive biomarkers.*** *Magn Reson Imaging 2024:110318. https://doi.org/10.1016/j.mri.2024.110318.* mój udział polegał na opracowaniu koncepcji badania, stworzeniu metodologii, opracowaniu i wykorzystaniu oprogramowania, przeprowadzeniu analizy formalnej, prowadzeniu badań, analizie statystycznej danych, przygotowaniu pierwotnego szkicu manuskryptu oraz wizualizacji.
Mój udział w powstaniu pracy wynosi 75%.

Niniejszym oświadczam, że w pracy *Śledzińska-Bebyn P, Furtak J, Bebyn M, Bartoszewska-Kubiak A, Serafin Z.* ***Diffusion imaging in gliomas: how ADC values forecast glioma genetics.*** *Polish Journal of Radiology. 2025;90:103-113. doi:10.5114/pjr/200967.* mój udział polegał na współtworzeniu koncepcji, zbieraniu danych, analizie statystycznej, interpretacji uzyskanych wyników, przygotowaniu manuskryptu.
Mój udział w powstaniu pracy wynosi 75%.

Śledzińska-Bebyn Paulina
(podpis)

PAULINA ŚLEDZIŃSKA-BEBYN
LEKARZ
4215014

Informacja o przetwarzaniu danych osobowych

Na podstawie Rozporządzenia Parlamentu Europejskiego i Rady (UE) 2016/679 z dnia 27 kwietnia 2016 r. w sprawie ochrony osób fizycznych w związku z przetwarzaniem danych osobowych i w sprawie swobodnego przepływu takich danych oraz uchylenia dyrektywy 95/46/WE, zwanego dalej „RODO", informujemy, że:

1. Administratorem Pana/Pani danych osobowych będzie Uniwersytet Mikołaja Kopernika w Toruniu z siedzibą przy ul. Gagarina 11, 87-100 Toruń (dalej: Uczelnia, ADO).
2. Pana/Pani dane osobowe w związku w związku z postępowaniem o nadanie stopnia naukowego będą przetwarzane:
   a. na podstawie art. 6 ust. 1 lit. c) RODO – obowiązek prawny wynikający z przepisów ustawy z dnia 20 lipca 2018 r. Prawo o szkolnictwie wyższym i nauce (Dz. U. z 2020, poz. 85);
   b. na podstawie art. 6 ust. 1 lit. f) RODO – prawnie uzasadniony interes ADO:
      - do ustalenia, obrony lub dochodzenia roszczeń – przez okres do przedawnienia roszczeń, lub przez okres prowadzenia postępowania przez właściwe organy lub sądy w przypadku dochodzenia roszczeń,
      - na potrzeby wewnętrzne tworzenia zestawień, analiz i statystyk – przez okres obowiązywania umowy,
      - na potrzeby prowadzenia ewidencji korespondencji przychodzącej i wychodzącej – wieczyście,
      - na potrzeby marketingu produktów i usług ADO.
3. Z zastrzeżeniem przepisów powszechnie obowiązującego prawa przysługują Panu/Pani prawa, które zrealizujemy na wniosek o:
   a. Żądanie dostępu do danych osobowych oraz prawo ich sprostowania,
   b. Żądanie usunięcia lub ograniczenia przetwarzania.
4. Przysługuje Panu/Pani również prawo wniesienia sprzeciwu na przetwarzanie danych osobowych.
5. Podanie przez Pana/Panią danych osobowych jest niezbędne do wykonania celu wymienionego w pkt 2 lit. a i b., a brak ich podania uniemożliwi otwarcie i przeprowadzenie postępowania.
6. Przysługuje Panu/Pani prawo wniesienia skargi do Prezesa Urzędu Ochrony Danych Osobowych.
7. Pana/Pani dane osobowe mogą być udostępnione recenzentom lub organom administracji publicznej, sądom, komornikom w zakresie sytuacji przewidzianych w przepisach prawa.
8. Na dzień zbierania Pana/Pani danych osobowych nie planujemy przekazywać ich poza EOG (obejmujący Unię Europejską, Norwegię, Lichtenstein i Islandię), nie wykluczając tego w przyszłości, o czym zostanie Pan/Pani poinformowania ze stosownym wyprzedzeniem.
9. W stosunku do Pana/Pani nie będą prowadzone działania polegające na podejmowaniu decyzji w sposób zautomatyzowany, nie będą one również podlegały zautomatyzowanemu profilowaniu.
10. Jeżeli chce Pan/Pani skontaktować się z Uczelnią w sprawach związanych z przetwarzaniem danych osobowych, w szczególności w związku z wniesieniem wniosku o realizację przysługujących praw prosimy o kontakt pod adresem e-mail: iod@umk.pl lub adresem korespondencyjnym: UMK w Toruniu, ul. Gagarina 11, 87-100 Toruń, z dopiskiem „IOD", dostępny jest również kontakt telefoniczny: 56 611 27 42.

Załącznik nr 5 do uchwały Nr 38 Senatu UMK z dnia 26 września 2023 r. w sprawie postępowania o nadanie stopnia doktora na Uniwersytecie Mikołaja Kopernika w Toruniu

Toruń, dnia 05.03.2025 r.

lek. Marek Bebyn
(tytuł, stopień, imię i nazwisko kandydata/współautora)

10 Wojskowy Szpital Kliniczny z Poliklinika w Bydgoszczy
(jednostka zatrudniająca kandydata/współautora)

Rada Dyscypliny Nauki Medyczne
Uniwersytetu Mikołaja Kopernika
w Toruniu

Oświadczenie o współautorstwie

Niniejszym oświadczam, że w pracy *Śledzińska-Bebyn P, Furtak J, Bebyn M, Serafin Z.* ***Beyond conventional imaging: Advancements in MRI for glioma malignancy prediction and molecular profiling.*** *Magn Reson Imaging 2024;112:63–81. https://doi.org/10.1016/j.mri.2024.06.004.* mój udział polegał na przygotowaniu elementów wizualnych publikacji oraz współtworzeniu pierwotnego szkicu manuskryptu.
Mój udział w powstaniu pracy wynosi 5%.

Niniejszym oświadczam, że w pracy *Śledzińska-Bebyn P, Furtak J, Bebyn M, Bartoszewska-Kubiak A, Serafin Z.* ***Investigating glioma genetics through perfusion MRI: rCBV and rCBF as predictive biomarkers.*** *Magn Reson Imaging 2024:110318. https://doi.org/10.1016/j.mri.2024.110318.* mój udział polegał na przygotowaniu wizualizacji oraz przeglądzie i edycji treści manuskryptu.
Mój udział w powstaniu pracy wynosi 5%.

Niniejszym oświadczam, że w pracy *Śledzińska-Bebyn P, Furtak J, Bebyn M, Bartoszewska-Kubiak A, Serafin Z.* ***Diffusion imaging in gliomas: how ADC values forecast glioma genetics.*** *Polish Journal of Radiology. 2025;90:103-113. doi:10.5114/pjr/200967.* mój udział polegał na przygotowaniu wizualizacji oraz przeglądzie i edycji treści manuskryptu.
Mój udział w powstaniu pracy wynosi 5%.

Marek Bebyn
(podpis)

Informacja o przetwarzaniu danych osobowych

Na podstawie Rozporządzenia Parlamentu Europejskiego i Rady (UE) 2016/679 z dnia 27 kwietnia 2016 r. w sprawie ochrony osób fizycznych w związku z przetwarzaniem danych osobowych i w sprawie swobodnego przepływu takich danych oraz uchylenia dyrektywy 95/46/WE, zwanego dalej „RODO", informujemy, że:

1. Administratorem Pana/Pani danych osobowych będzie Uniwersytet Mikołaja Kopernika w Toruniu z siedzibą przy ul. Gagarina 11, 87-100 Toruń (dalej: Uczelnia, ADO).
2. Pana/Pani dane osobowe w związku w związku z postępowaniem o nadanie stopnia naukowego będą przetwarzane:
   a. na podstawie art. 6 ust. 1 lit. c) RODO – obowiązek prawny wynikający z przepisów ustawy z dnia 20 lipca 2018 r. Prawo o szkolnictwie wyższym i nauce (Dz. U. z 2020, poz. 85);
   b. na podstawie art. 6 ust. 1 lit. f) RODO – prawnie uzasadniony interes ADO:
      - do ustalenia, obrony lub dochodzenia roszczeń – przez okres do przedawnienia roszczeń, lub przez okres prowadzenia postępowania przez właściwe organy lub sądy w przypadku dochodzenia roszczeń,
      - na potrzeby wewnętrzne tworzenia zestawień, analiz i statystyk – przez okres obowiązywania umowy,
      - na potrzeby prowadzenia ewidencji korespondencji przychodzącej i wychodzącej – wieczyście,
      - na potrzeby marketingu produktów i usług ADO.
3. Z zastrzeżeniem przepisów powszechnie obowiązującego prawa przysługują Panu/Pani prawa, które zrealizujemy na wniosek o:
   a. Żądanie dostępu do danych osobowych oraz prawo ich sprostowania,
   b. Żądanie usunięcia lub ograniczenia przetwarzania.
4. Przysługuje Panu/Pani również prawo wniesienia sprzeciwu na przetwarzanie danych osobowych.
5. Podanie przez Pana/Panią danych osobowych jest niezbędne do wykonania celu wymienionego w pkt 2 lit. a i b., a brak ich podania uniemożliwi otwarcie i przeprowadzenie postępowania.
6. Przysługuje Panu/Pani prawo wniesienia skargi do Prezesa Urzędu Ochrony Danych Osobowych.
7. Pana/Pani dane osobowe mogą być udostępnione recenzentom lub organom administracji publicznej, sądom, komornikom w zakresie sytuacji przewidzianych w przepisach prawa.
8. Na dzień zbierania Pana/Pani danych osobowych nie planujemy przekazywać ich poza EOG (obejmujący Unię Europejską, Norwegię, Lichtenstein i Islandię), nie wykluczając tego w przyszłości, o czym zostanie Pan/Pani poinformowania ze stosownym wyprzedzeniem.
9. W stosunku do Pana/Pani nie będą prowadzone działania polegające na podejmowaniu decyzji w sposób zautomatyzowany, nie będą one również podlegały zautomatyzowanemu profilowaniu.
10. Jeżeli chce Pan/Pani skontaktować się z Uczelnią w sprawach związanych z przetwarzaniem danych osobowych, w szczególności w związku z wniesieniem wniosku o realizację przysługujących praw prosimy o kontakt pod adresem e-mail: iod@umk.pl lub adresem korespondencyjnym: UMK w Toruniu, ul. Gagarina 11, 87-100 Toruń, z dopiskiem „IOD", dostępny jest również kontakt telefoniczny: 56 611 27 42.

Załącznik nr 5 do uchwały Nr 38 Senatu UMK z dnia 26 września 2023 r. w sprawie postępowania o nadanie stopnia doktora na Uniwersytecie Mikołaja Kopernika w Toruniu

Toruń, dnia ...06.03.2025

dr hab. n o zdr. Jacek Furtak, prof. PBŚ
(tytuł, stopień, imię i nazwisko kandydata/współautora)

Politechnika Bydgoska im. Jana i Jędrzeja Śniadeckich,
Wydział Medyczny
10 Wojskowy Szpital Kliniczny z Polikliniką w Bydgoszczy
(jednostka zatrudniająca kandydata/współautora)

Rada Dyscypliny Nauki Medyczne
Uniwersytetu Mikołaja Kopernika
w Toruniu

Oświadczenie o współautorstwie

Niniejszym oświadczam, że w pracy *Śledzińska-Bebyn P, Furtak J, Bebyn M, Serafin Z.* ***Beyond conventional imaging: Advancements in MRI for glioma malignancy prediction and molecular profiling.*** *Magn Reson Imaging 2024;112:63–81. https://doi.org/10.1016/j.mri.2024.06.004.* mój udział polegał na przeglądzie i edycji tekstu.
Mój udział w powstaniu pracy wynosi 5%.

Niniejszym oświadczam, że w pracy *Śledzińska-Bebyn P, Furtak J, Bebyn M, Bartoszewska-Kubiak A, Serafin Z.* ***Investigating glioma genetics through perfusion MRI: rCBV and rCBF as predictive biomarkers.*** *Magn Reson Imaging 2024:110318. https://doi.org/10.1016/j.mri.2024.110318.* mój udział polegał na kierowaniu pacjentów na badania MRI przed operacją lub biopsją guza mózgu i analizie formalnej uzyskanych wyników.
Mój udział w powstaniu pracy wynosi 5%.

Niniejszym oświadczam, że w pracy *Śledzińska-Bebyn P, Furtak J, Bebyn M, Bartoszewska-Kubiak A, Serafin Z.* ***Diffusion imaging in gliomas: how ADC values forecast glioma genetics.*** *Polish Journal of Radiology. 2025;90:103-113. doi:10.5114/pjr/200967.* mój udział polegał na pomocy w interpretacji danych.
Mój udział w powstaniu pracy wynosi 5%.

Dr hab. Jacek Furtak
SPECJALISTA NEUROCHIRURG
Prof. P.B.Ś.
9173253
tel. kom. 604 104 065

.....
(podpis)

Informacja o przetwarzaniu danych osobowych

Na podstawie Rozporządzenia Parlamentu Europejskiego i Rady (UE) 2016/679 z dnia 27 kwietnia 2016 r. w sprawie ochrony osób fizycznych w związku z przetwarzaniem danych osobowych i w sprawie swobodnego przepływu takich danych oraz uchylenia dyrektywy 95/46/WE, zwanego dalej „RODO", informujemy, że:

1. Administratorem Pana/Pani danych osobowych będzie Uniwersytet Mikołaja Kopernika w Toruniu z siedzibą przy ul. Gagarina 11, 87-100 Toruń (dalej: Uczelnia, ADO).
2. Pana/Pani dane osobowe w związku w związku z postępowaniem o nadanie stopnia naukowego będą przetwarzane:
   a. na podstawie art. 6 ust. 1 lit. c) RODO – obowiązek prawny wynikający z przepisów ustawy z dnia 20 lipca 2018 r. Prawo o szkolnictwie wyższym i nauce (Dz. U. z 2020, poz. 85);
   b. na podstawie art. 6 ust. 1 lit. f) RODO – prawnie uzasadniony interes ADO:
      - do ustalenia, obrony lub dochodzenia roszczeń – przez okres do przedawnienia roszczeń, lub przez okres prowadzenia postępowania przez właściwe organy lub sądy w przypadku dochodzenia roszczeń,
      - na potrzeby wewnętrzne tworzenia zestawień, analiz i statystyk – przez okres obowiązywania umowy,
      - na potrzeby prowadzenia ewidencji korespondencji przychodzącej i wychodzącej – wieczyście,
      - na potrzeby marketingu produktów i usług ADO.
3. Z zastrzeżeniem przepisów powszechnie obowiązującego prawa przysługują Panu/Pani prawa, które zrealizujemy na wniosek o:
   a. Żądanie dostępu do danych osobowych oraz prawo ich sprostowania,
   b. Żądanie usunięcia lub ograniczenia przetwarzania.
4. Przysługuje Panu/Pani również prawo wniesienia sprzeciwu na przetwarzanie danych osobowych.
5. Podanie przez Pana/Panią danych osobowych jest niezbędne do wykonania celu wymienionego w pkt 2 lit. a i b., a brak ich podania uniemożliwi otwarcie i przeprowadzenie postępowania.
6. Przysługuje Panu/Pani prawo wniesienia skargi do Prezesa Urzędu Ochrony Danych Osobowych.
7. Pana/Pani dane osobowe mogą być udostępnione recenzentom lub organom administracji publicznej, sądom, komornikom w zakresie sytuacji przewidzianych w przepisach prawa.
8. Na dzień zbierania Pana/Pani danych osobowych nie planujemy przekazywać ich poza EOG (obejmujący Unię Europejską, Norwegię, Lichtenstein i Islandię), nie wykluczając tego w przyszłości, o czym zostanie Pan/Pani poinformowania ze stosownym wyprzedzeniem.
9. W stosunku do Pana/Pani nie będą prowadzone działania polegające na podejmowaniu decyzji w sposób zautomatyzowany, nie będą one również podlegały zautomatyzowanemu profilowaniu.
10. Jeżeli chce Pan/Pani skontaktować się z Uczelnią w sprawach związanych z przetwarzaniem danych osobowych, w szczególności w związku z wniesieniem wniosku o realizację przysługujących praw prosimy o kontakt pod adresem e-mail: iod@umk.pl lub adresem korespondencyjnym: UMK w Toruniu, ul. Gagarina 11, 87-100 Toruń, z dopiskiem „IOD", dostępny jest również kontakt telefoniczny: 56 611 27 42.

Załącznik nr 5 do uchwały Nr 38 Senatu UMK z dnia 26 września 2023 r.

w sprawie postępowania o nadanie stopnia doktora na Uniwersytecie Mikołaja Kopernika w Toruniu

Toruń, dnia 12.03.2025 r.

dr n. med. inż. Alicja Bartoszewska-Kubiak
(tytul, stopień, imię i nazwisko kandydata/współautora)

10 Wojskowy Szpital Kliniczny z Poliklinika w Bydgoszczy.
(jednostka zatrudniająca kandydata/współautora)

Rada Dyscypliny Nauki Medyczne
Uniwersytetu Mikołaja Kopernika
w Toruniu

Oświadczenie o współautorstwie

Niniejszym oświadczam, że w pracy *Śledzińska-Bebyn P, Furtak J, Bebyn M, Bartoszewska-Kubiak A, Serafin Z.* ***Investigating glioma genetics through perfusion MRI: rCBV and rCBF as predictive biomarkers.*** *Magn Reson Imaging 2024:110318. https://doi.org/10.1016/j.mri.2024.110318.* mój udział polegał na wykonaniu badań genetycznych niezbędnych do realizacji projektu.
Mój udział w powstaniu pracy wynosi 5%.

Niniejszym oświadczam, że w pracy *Śledzińska-Bebyn P, Furtak J, Bebyn M, Bartoszewska-Kubiak A, Serafin Z.* ***Diffusion imaging in gliomas: how ADC values forecast glioma genetics.*** *Polish Journal of Radiology. 2025;90:103-113. doi:10.5114/pjr/200967.* mój udział polegał na wykonaniu badań genetycznych niezbędnych do realizacji projektu.
Mój udział w powstaniu pracy wynosi 5%.

Alicja Bartoszewska-Kubiak
(podpis)

Informacja o przetwarzaniu danych osobowych

Na podstawie Rozporządzenia Parlamentu Europejskiego i Rady (UE) 2016/679 z dnia 27 kwietnia 2016 r. w sprawie ochrony osób fizycznych w związku z przetwarzaniem danych osobowych i w sprawie swobodnego przepływu takich danych oraz uchylenia dyrektywy 95/46/WE, zwanego dalej „RODO", informujemy, że:

1. Administratorem Pana/Pani danych osobowych będzie Uniwersytet Mikołaja Kopernika w Toruniu z siedzibą przy ul. Gagarina 11, 87-100 Toruń (dalej: Uczelnia, ADO).
2. Pana/Pani dane osobowe w związku w związku z postępowaniem o nadanie stopnia naukowego będą przetwarzane:
   a. na podstawie art. 6 ust. 1 lit. c) RODO – obowiązek prawny wynikający z przepisów ustawy z dnia 20 lipca 2018 r. Prawo o szkolnictwie wyższym i nauce (Dz. U. z 2020, poz. 85);
   b. na podstawie art. 6 ust. 1 lit. f) RODO – prawnie uzasadniony interes ADO:
      - do ustalenia, obrony lub dochodzenia roszczeń – przez okres do przedawnienia roszczeń, lub przez okres prowadzenia postępowania przez właściwe organy lub sądy w przypadku dochodzenia roszczeń,
      - na potrzeby wewnętrzne tworzenia zestawień, analiz i statystyk – przez okres obowiązywania umowy,
      - na potrzeby prowadzenia ewidencji korespondencji przychodzącej i wychodzącej – wieczyście,
      - na potrzeby marketingu produktów i usług ADO.
3. Z zastrzeżeniem przepisów powszechnie obowiązującego prawa przysługują Panu/Pani prawa, które zrealizujemy na wniosek o:
   a. Żądanie dostępu do danych osobowych oraz prawo ich sprostowania,
   b. Żądanie usunięcia lub ograniczenia przetwarzania.
4. Przysługuje Panu/Pani również prawo wniesienia sprzeciwu na przetwarzanie danych osobowych.
5. Podanie przez Pana/Panią danych osobowych jest niezbędne do wykonania celu wymienionego w pkt 2 lit. a i b., a brak ich podania uniemożliwi otwarcie i przeprowadzenie postępowania.
6. Przysługuje Panu/Pani prawo wniesienia skargi do Prezesa Urzędu Ochrony Danych Osobowych.
7. Pana/Pani dane osobowe mogą być udostępnione recenzentom lub organom administracji publicznej, sądom, komornikom w zakresie sytuacji przewidzianych w przepisach prawa.
8. Na dzień zbierania Pana/Pani danych osobowych nie planujemy przekazywać ich poza EOG (obejmujący Unię Europejską, Norwegię, Lichtenstein i Islandię), nie wykluczając tego w przyszłości, o czym zostanie Pan/Pani poinformowania ze stosownym wyprzedzeniem.
9. W stosunku do Pana/Pani nie będą prowadzone działania polegające na podejmowaniu decyzji w sposób zautomatyzowany, nie będą one również podlegały zautomatyzowanemu profilowaniu.
10. Jeżeli chce Pan/Pani skontaktować się z Uczelnią w sprawach związanych z przetwarzaniem danych osobowych, w szczególności w związku z wniesieniem wniosku o realizację przysługujących praw prosimy o kontakt pod adresem e-mail: iod@umk.pl lub adresem korespondencyjnym: UMK w Toruniu, ul. Gagarina 11, 87-100 Toruń, z dopiskiem „IOD", dostępny jest również kontakt telefoniczny: 56 611 27 42.

Załącznik nr 5 do uchwały Nr 38 Senatu UMK z dnia 26 września 2023 r.

sprawie postępowania o nadanie stopnia

Toruń, dnia 14. Marca 2025r.

prof. dr hab. n med. Zbigniew Serafin
(tytuł, stopień, imię i nazwisko kandydata/współautora)

Zakład Diagnostyki Obrazowej, Szpital Kliniczny im. E.Warmińskiego Politechniki Bydgoskiej

Politechnika Bydgoska im. Jana i Jędrzeja Śniadeckich, Wydział Medyczny
(jednostka zatrudniająca kandydata/współautora)

Rada Dyscypliny Nauki Medyczne
Uniwersytetu Mikołaja Kopernika
w Toruniu

Oświadczenie o współautorstwie

Niniejszym oświadczam, że w pracy *Śledzińska-Bebyn P, Furtak J, Bebyn M, Serafin Z.* ***Beyond conventional imaging: Advancements in MRI for glioma malignancy prediction and molecular profiling.*** *Magn Reson Imaging 2024;112:63–81. https://doi.org/10.1016/j.mri.2024.06.004.* mój udział polegał na nadzorze merytorycznym nad publikacją, planowaniu koncepcji pracy oraz przeglądzie i edycji treści.
Mój udział w powstaniu pracy wynosi 10%.

Niniejszym oświadczam, że w pracy *Śledzińska-Bebyn P, Furtak J, Bebyn M, Bartoszewska-Kubiak A, Serafin Z.* ***Investigating glioma genetics through perfusion MRI: rCBV and rCBF as predictive biomarkers.*** *Magn Reson Imaging 2024:110318. https://doi.org/10.1016/j.mri.2024.110318.* mój udział polegał na współtworzeniu metodologii, nadzorze merytorycznym nad projektem oraz przeglądzie i edycji treści manuskryptu.
Mój udział w powstaniu pracy wynosi 10%.

Niniejszym oświadczam, że w pracy *Śledzińska-Bebyn P, Furtak J, Bebyn M, Bartoszewska-Kubiak A, Serafin Z.* ***Diffusion imaging in gliomas: how ADC values forecast glioma genetics.*** *Polish Journal of Radiology. 2025;90:103-113. doi:10.5114/pjr/200967.* mój udział polegał na a współtworzeniu koncepcji badawczej, nadzorze merytorycznym nad projektem oraz pozyskaniu finansowania.
Mój udział w powstaniu pracy wynosi 10%.

.....
(podpis)

Informacja o przetwarzaniu danych osobowych

Na podstawie Rozporządzenia Parlamentu Europejskiego i Rady (UE) 2016/679 z dnia 27 kwietnia 2016 r. w sprawie ochrony osób fizycznych w związku z przetwarzaniem danych osobowych i w sprawie swobodnego przepływu takich danych oraz uchylenia dyrektywy 95/46/WE, zwanego dalej „RODO", informujemy, że:

1. Administratorem Pana/Pani danych osobowych będzie Uniwersytet Mikołaja Kopernika w Toruniu z siedzibą przy ul. Gagarina 11, 87-100 Toruń (dalej: Uczelnia, ADO).
2. Pana/Pani dane osobowe w związku w związku z postępowaniem o nadanie stopnia naukowego będą przetwarzane:
   a. na podstawie art. 6 ust. 1 lit. c) RODO – obowiązek prawny wynikający z przepisów ustawy z dnia 20 lipca 2018 r. Prawo o szkolnictwie wyższym i nauce (Dz. U. z 2020, poz. 85);
   b. na podstawie art. 6 ust. 1 lit. f) RODO – prawnie uzasadniony interes ADO:
      - do ustalenia, obrony lub dochodzenia roszczeń – przez okres do przedawnienia roszczeń, lub przez okres prowadzenia postępowania przez właściwe organy lub sądy w przypadku dochodzenia roszczeń,
      - na potrzeby wewnętrzne tworzenia zestawień, analiz i statystyk – przez okres obowiązywania umowy,
      - na potrzeby prowadzenia ewidencji korespondencji przychodzącej i wychodzącej – wieczyście,
      - na potrzeby marketingu produktów i usług ADO.
3. Z zastrzeżeniem przepisów powszechnie obowiązującego prawa przysługują Panu/Pani prawa, które zrealizujemy na wniosek o:
   a. Żądanie dostępu do danych osobowych oraz prawo ich sprostowania,
   b. Żądanie usunięcia lub ograniczenia przetwarzania.
4. Przysługuje Panu/Pani również prawo wniesienia sprzeciwu na przetwarzanie danych osobowych.
5. Podanie przez Pana/Panią danych osobowych jest niezbędne do wykonania celu wymienionego w pkt 2 lit. a i b., a brak ich podania uniemożliwi otwarcie i przeprowadzenie postępowania.
6. Przysługuje Panu/Pani prawo wniesienia skargi do Prezesa Urzędu Ochrony Danych Osobowych.
7. Pana/Pani dane osobowe mogą być udostępnione recenzentom lub organom administracji publicznej, sądom, komornikom w zakresie sytuacji przewidzianych w przepisach prawa.
8. Na dzień zbierania Pana/Pani danych osobowych nie planujemy przekazywać ich poza EOG (obejmujący Unię Europejską, Norwegię, Lichtenstein i Islandię), nie wykluczając tego w przyszłości, o czym zostanie Pan/Pani poinformowania ze stosownym wyprzedzeniem.
9. W stosunku do Pana/Pani nie będą prowadzone działania polegające na podejmowaniu decyzji w sposób zautomatyzowany, nie będą one również podlegały zautomatyzowanemu profilowaniu.
10. Jeżeli chce Pan/Pani skontaktować się z Uczelnią w sprawach związanych z przetwarzaniem danych osobowych, w szczególności w związku z wniesieniem wniosku o realizację przysługujących praw prosimy o kontakt pod adresem e-mail: iod@umk.pl lub adresem korespondencyjnym: UMK w Toruniu, ul. Gagarina 11, 87-100 Toruń, z dopiskiem „IOD", dostępny jest również kontakt telefoniczny: 56 611 27 42.